AEROSOL MEASUREMENT

Principles, Techniques, and Applications

Third Edition

Edited by

PRAMOD KULKARNI, D.Sc. and PAUL A. BARON, Ph.D.

Centers for Disease Control and Prevention, National Institute for Occupational Safety and Health, Cincinnati, Ohio

KLAUS WILLEKE, Ph.D.

Department of Environmental Health, University of Cincinnati, Cincinnati, Ohio

WILEY

A JOHN WILEY & SONS. INC. PUBLICATION

AEROSOL MEASUREMENT

AEROSOL MEASUREMENT

Principles, Techniques, and Applications

Third Edition

Edited by

PRAMOD KULKARNI, D.Sc. and PAUL A. BARON, Ph.D.

Centers for Disease Control and Prevention, National Institute for Occupational Safety and Health, Cincinnati, Ohio

KLAUS WILLEKE, Ph.D.

Department of Environmental Health, University of Cincinnati, Cincinnati, Ohio

WILEY

A JOHN WILEY & SONS. INC. PUBLICATION

Published by John Wiley & Sons, Inc., Hoboken, New Jersey
Published simultaneously in Canada

Library of Congress Cataloging-in-Publication Data:

Aerosol measurement : principles, techniques, and applications / edited by Paul A. Baron, Pramod Kulkarni, Klaus Willeke. — 3rd ed.
p. cm.
Includes bibliographical references and index.
ISBN 978-0-470-38741-2 (cloth)
1. Aerosols–Measurement. 2. Air–Pollution–Measurement. I. Baron, Paul A., 1944- II. Kulkarni, Pramod. III. Willeke, Klaus.
TD884.5.A33 2011
628.5′30287—dc22

2010036839

Printed in the United States of America
10 9 8 7 6 5 4 3 2 1

In Memoriam

Paul A. Baron (1944–2009)

CONTENTS

PREFACE

We would like to dedicate this edition to our late colleague and coeditor Paul Baron. Paul passed away on May 20, 2009, after a long battle with cancer. He was actively involved with the preparation of this edition until his last days. A passionate champion of aerosol science, he made many significant contributions to the field of aerosol measurement. His modesty, energy, and wisdom were a source of inspiration to his colleagues and friends who miss him greatly.

The science of aerosol measurement has significantly advanced over the past several decades. From simple gravimetric measurements of airborne dusts in the early 1900s to the state-of-the-art instruments that can perform near-instantaneous size and chemical composition measurements, the advances are indeed exciting and promising with wide implications for public health and environmental protection, climate research, medicine, and industrial technology. Until the late 1980s, the development of new measurement methods was primarily driven by the need to evaluate particulate pollution control devices and to find better means of monitoring "undesirable" indoor and outdoor aerosols. In later years, many monitoring methods and instruments were developed to address newly promulgated environmental and occupational safety regulations. More recently, aerosol instrumentation has been developed to further our understanding of atmospheric aerosol processes, particularly in the context of atmospheric and climate research. Industrial or technological applications of aerosol measurement to characterize "desirable" aerosols have also grown substantially. With the advent of nanotechnology, aerosol measurement techniques are not only needed to help produce functional nanomaterials, but also to minimize risks from their environmental or occupational exposure. Aerosol measurement has assumed critical importance in a variety of fields including industrial hygiene, air pollution, epidemiology, atmospheric science, material science, powder technology, nanotechnology, filtration, particle toxicology, and drug delivery. As a consequence, the number of undergraduate and graduate students taking courses in aerosol science and measurement has increased dramatically in recent years. The increased importance of this field is also evident from the rapid growth of aerosol research societies in the United States, Europe, and Asia.

This book represents a comprehensive reference text on the basic principles, techniques, and applications of aerosol measurement instrumentation and methods. Historically, development of most *techniques* for measurement of aerosols have been motivated by a variety of *applications*, ranging from public health and air pollution, climate research, to industrial technology. In turn, most measurement techniques derive from various *principles* from physical sciences such as Stokes' law, Millikan's experiments, or Einstein's theory of the Brownian motion. Accordingly, the book is structured into three parts: *Principles, Techniques*, and *Applications*. Fundamental physical concepts, as they relate to aerosol measurement, are presented in Part I of the book, and are essential to comprehend various types of instrumentation. Part II expands on a variety of measurement tools by devoting a chapter to each principal measurement technique or group of techniques. Part III discusses different applications of aerosol instrumentation presented in Part II, ranging from ambient air and workplace monitoring, bioaerosols, aircraft-based measurements, material synthesis, to pharmaceutical aerosols. Each application requires a specific set of aerosol properties to be measured, thus dictating the type of measurement technique or group of techniques that can be applied. The book attempts to bridge the science and the applications of aerosol measurement.

We have made many changes to the third edition by dropping or combining a few chapters to make room for new topics. The chapter on historical aspects of aerosol measurement has been dropped, as dedicated texts on this topic are now available. Other omissions include chapters on fugitive dust emissions, mine aerosol measurement, and radon; some key, relevant content from the omitted topics has been absorbed in appropriate chapters. The two chapters on optical instrumentation were combined into a single chapter in this edition. Other minor reductions were achieved for chapters describing instruments no longer used or commercially available. All chapters have been updated to reflect

advances since the second edition. Many new chapters have been added to cover topics that are emerging, lacked coverage elsewhere, or just deserved a place in this book. These include chapters on electrospray, satellite-based aerosol measurement, new particle formation, sub-5 nm aerosol measurement, atmospheric large particle (>10 μm) measurement, electrical-sensing aerosol instruments, satellite-based aerosol measurement, and finally a chapter on health effects of inhaled particles. The chapter on health effects, though not directly related to aerosol measurement, we believe, should be helpful in providing a broader perspective to scientists and engineers interested in making measurement of aerosols to study their health effects.

Striking the right balance between the theoretical and applied aspects of aerosol measurement in a limited space can be challenging for a book of this nature. The contributing authors indeed deserve praise for attempting to meet this formidable challenge while ensuring the high quality of the chapters. Needless to say, we appreciate their patience in undertaking requested revisions, which were often numerous and tedious. During the editing process we have tried to ensure that the content and presentation are of interest to a wide readership including graduate students, professionals new to aerosol measurement, as well as practicing aerosol scientists and engineers. We have also tried to ensure consistent use of terminology, nomenclature, and definitions across different chapters to the extent possible. Lists of symbols have been included at the end of chapters where needed. Numerical examples are included in many chapters to illustrate key concepts. We have made use of extensive cross-referencing between chapters to allow readers to quickly locate relevant topics spread across different chapters. Various appendices included at the end of the book should serve as useful, quick reference.

We extend our heartfelt thanks to many colleagues and peers from the aerosol community who have assisted in the preparation of this edition. More than 100 peer reviewers have helped us review book chapters; we are very grateful to them for providing their time and expertise. We would like to thank Prasoon Diwakar, Chaolong Qi, and Greg Deye for their help during the final days of manuscript preparation. Thanks are also due to Bob Esposito, Michael Leventhal, and Christine Punzo at John Wiley for their help during the preparation of this edition. Excellent copy-editing by Mary Safford Curioli and efficient coordination of proofs by Nick Barber is greatly appreciated. P.K. would like to thank his wife Debjani for her support and encouragement during this rather long project. K.W., who now lives in Orinda, California, since his retirement from the University of Cincinnati in 2003, wishes to extend his appreciation to his wife Audrone for her support.

PRAMOD KULKARNI
Cincinnati, Ohio

KLAUS WILLEKE
Orinda, California

CONTRIBUTORS

Ian M. Anderson, National Institute of Standards and Technology, Gaithersburg, Maryland

Paul A. Baron, Centers for Disease Control and Prevention, National Institute for Occupational Safety and Health, Cincinnati, Ohio

Pratim Biswas, Department of Energy, Environmental and Chemical Engineering, Washington University in Saint Louis, Saint Louis, Missouri

John E. Brockmann, Sandia National Laboratories, Albuquerque, New Mexico

Heinz Burtscher, Fachhochschule Aargau, University of Applied Sciences, Windisch, Switzerland

Vincent Castranova, Centers for Disease Control and Prevention, National Institute for Occupational Safety and Health, Morgantown, West Virginia

Bean T. Chen, Centers for Disease Control and Prevention, National Institute for Occupational Safety and Health, Morgantown, West Virginia

Yung-Sung Cheng, Inhalation Toxicology Research Institute, Albuquerque, New Mexico

Judith C. Chow, Desert Research Institute, Nevada System of Higher Education, Reno, Nevada

E. James Davis, Department of Chemical Engineering, University of Washington, Seattle, Washington

Juan Fernandez de la Mora, Department of Mechanical Engineering, Yale University, New Haven, Connecticut

Weiwei Deng, Department of Mechanical, Materials and Aerospace Engineering, University of Central Florida, Orlando, Florida

Suresh Dhaniyala, Department of Mechanical and Aeronautical Engineering, Clarkson University, Potsdam, New York

Anne Marie Dixon, Cleanroom Management Associates, Carson City, Nevada

Kensei Ehara, National Institute of Advanced Industrial Science and Technology, Tsukuba, Japan

Fred Eisele, Atmospheric Chemistry Division, National Center for Atmospheric Research, Boulder, Colorado

David S. Ensor, RTI International, Research Triangle Park, North Carolina

Martin Fierz, Institut für Aerosol- und Sensortechnologie, Fachhochschule Nordwestschweiz, Windisch, Switzerland

Richard C. Flagan, California Institute of Technology, Pasadena, California

Robert A. Fletcher, National Institute of Standards and Technology, Gaithersburg, Maryland

Matthew P. Fraser, Global Institute of Sustainability, Arizona State University, Tempe, Arizona

Alessandro Gomez, Department of Mechanical Engineering, Yale University, New Haven, Connecticut

Sergey Grinshpun, Department of Environmental Health, University of Cincinnati, Cincinnati, Ohio

Martin Harper, Centers for Disease Control and Prevention, National Institute for Occupational Safety and Health, Morgantown, West Virginia

Pierre Herckes, Department of Chemistry and Biochemistry, Arizona State University, Tempe, Arizona

Anthony J. Hickey, Eshelman School of Pharmacy, University of North Carolina, Chapel Hill, North Carolina

William C. Hinds, Department of Environmental Health Sciences, University of California, Los Angeles School of Public Health, Los Angeles, California

Mark D. Hoover, Centers for Disease Control and Prevention, National Institute for Occupational Safety and Health, Morgantown, West Virginia

Christoph Hüglin, Empa, Laboratory for Air Pollution/ Environmental Technology, Dübendorf, Switzerland

Rudolf B. Husar, Department of Energy, Environment and Chemical Engineering, Washington University, Saint Louis, MO, USA

Walter John, Walnut Creek, California

Murray V. Johnston, Department of Chemistry and Biochemistry, University of Delaware, Newark, Delaware

Haflidi Jonsson, Naval Postgraduate School, Marina, California

Jorma Keskinen, Department of Physics, Tampere University of Technology, Tampere, Finland

Toivo T. Kodas, Cabot Corporation, Boston, Massachusetts

Chongai Kuang, Atmospheric Sciences Division, Brookhaven National Laboratory, Upton, New York

Pramod Kulkarni, Centers for Disease Control and Prevention, National Institute for Occupational Safety and Health, Cincinnati, Ohio

David Leith, Department of Environmental Sciences and Engineering, University of North Carolina at Chapel Hill, School of Public Health, Chapel Hill, North Carolina

Arkadi Maisels, Evonik Degussa GmbH, Hanau, Germany

Marko Marjamäki, Department of Physics, Tampere University of Technology, Tampere, Finland

Virgil A. Marple, Mechanical Engineering Department, University of Minnesota, Minneapolis, Minnesota

Andrew D. Maynard, University of Michigan School of Public Health, Ann Arbor, Michigan

Malay K. Mazumder, Department of Electrical and Computer Engineering, Boston University, Boston, Massachusetts

Peter H. McMurry, Particle Technology Laboratory, Department of Mechanical Engineering, University of Minnesota, Minneapolis, Minnesota

Owen R. Moss, POK Research, Apex, North Carolina

Aino Nevalainen, National Institute for Health and Welfare, Kuopio, Finland

Kenneth E. Noll, Department of Civil, Architecture and Environmental Engineering, Illinois Institute of Technology, Chicago, Illinois

Bernard A. Olson, Mechanical Engineering Department, University of Minnesota, Minneapolis, Minnesota

Thomas M. Peters, Department of Occupational and Environmental Health, University of Iowa, Iowa City, Iowa

Sotiris E. Pratsinis, Institut für Verfahrenstechnik, Zürich, Switzerland

Gurumurthy Ramachandran, Division of Environmental Health Sciences, School of Public Health, University of Minnesota, Minneapolis, Minnesota

Peter C. Raynor, Division of Environmental Health Sciences, School of Public Health, University of Minnesota, Minneapolis, Minnesota

Tiina Reponen, Department of Environmental Health, University of Cincinnati, Cincinnati, Ohio

Nicholas W.M. Ritchie, National Institute of Standards and Technology, Gaithersburg, Maryland

Charles E. Rodes, Aerosol Exposure, RTI International, Research Triangle Park, North Carolina

George Skillas, Evonik Degussa GmbH, Hanau, Germany

John A. Small, National Institute of Standards and Technology, Gaithersburg, Maryland

James N. Smith, Atmospheric Chemistry Division, National Center for Atmospheric Research, Boulder, Colorado

Paul A. Solomon, National Exposure Laboratory, U.S. Environmental Protection Agency, Las Vegas, Nevada

Christopher M. Sorensen, Department of Physics, Kansas State University, Manhattan, Kansas

Elijah Thimsen, Argonne National Laboratory, Argonne, Illinois

Dhesikan Venkatesan, Department of Civil, Architecture and Environmental Engineering, Illinois Institute of Technology, Chicago, Illinois

Jon C. Volkwein, Centers for Disease Control and Prevention, National Institute for Occupational Safety and Health, Pittsburgh, Pennsylvania

John G. Watson, Desert Research Institute, Nevada System of Higher Education, Reno, Nevada

Ernest Weingartner, Laboratory of Atmospheric Chemistry, Paul Scherrer Institut, Villigen, Switzerland

Anthony S. Wexler, Departments of Mechanical and Aeronautical Engineering, Civil and Environmental Engineering, and Land, Air and Water Resources, University of California, Davis, California

Klaus Willeke, Department of Environmental Health, University of Cincinnati, Cincinnati, Ohio

James C. Wilson, Department of Engineering, University of Denver, Denver, Colorado

Jun Zhao, Atmospheric Chemistry Division, National Center for Atmospheric Research, Boulder, Colorado

PART I

PRINCIPLES

1

INTRODUCTION TO AEROSOL CHARACTERIZATION

PRAMOD KULKARNI AND PAUL A. BARON

Centers for Disease Control and Prevention,[1] *National Institute for Occupational Safety and Health, Cincinnati, Ohio*

KLAUS WILLEKE

Department of Environmental Health, University of Cincinnati, Cincinnati, Ohio

1.1 INTRODUCTION

The term *aerosol* refers to suspension of liquid or solid particles in a gaseous medium. The term originated as the gas-phase analogue to *hydrosols* (meaning "water particle" in Greek) and refers to suspension of particles in a liquid. Aerosols are two-phase systems, consisting of the suspended solid or liquid phase, and the surrounding gas phase. Aerosols are formed by the conversion of gases to particles or by the disintegration of liquids or solids into finer constituents. Aerosols are quite ubiquitous; airborne particles from resuspended soil, atmospheric cloud droplets, welding fumes, smoke from power generation, airborne particles from volcanic eruptions, cigarette smoke, and salt particles formed from ocean spray are all examples of aerosols. Many commonly known phenomena such as dust, suspended particulate matter, fume, smoke, mist, fog, haze, clouds, or smog can be described as aerosols.

The need to measure aerosols has increased dramatically over the last few decades in various fields including air pollution, public health, atmospheric science, nanotechnology, chemical manufacturing, pharmaceuticals, and medicine. For instance, environmental engineers and industrial hygienists perform aerosol measurements in order to ensure that the public and the industrial work force are not exposed to hazardous aerosols at undesirable concentration levels, while atmospheric scientists measure aerosols to understand their influence on the earth's climate. Increasingly complex and demanding regulations to mitigate particulate matter pollution mean that aerosol measurements are becoming more and more time- and resource-intensive. These measurements may often require more than elementary knowledge to conduct and interpret the measurements. Devising a cost-effective mitigation strategy depends on reliable measurement of physical and chemical characteristics of aerosols.

In contrast to the abovementioned "undesirable" effects of aerosols on health and the environment, aerosol methods that produce "desirable" specialty materials are increasingly being used by material scientists and engineers. For instance, large quantities of powders and pigments can be produced

[1]The findings and conclusions in this chapter are those of the authors and do not necessarily represent the views of the Centers for Disease Control and Prevention.

Aerosol Measurement: Principles, Techniques, and Applications, Third Edition. Edited by P. Kulkarni, P. A. Baron, and K. Willeke

by flowing precursor feed materials into flame, plasma, laser, or furnace reactors where aerosol particles with desired chemical and physical characteristics are formed. In these technological applications, aerosol measurement plays a vital role. In recent years, the emergence of nanotechnology has sparked a renewed interest in aerosol measurement. Aerosol methods are being increasingly employed to develop novel functional nanomaterials. On the other hand, there is also a growing concern over the health risks posed by potential exposure to such nanomaterials when they are aerosolized. This has led to renewed interest in measurement tools and methods for characterizing nanomaterial exposures.

The research efforts focused on characterizing "desirable" and "undesirable" aerosols have served as a continual driver for rapid development of sophisticated and sensitive aerosol instruments. The fast-evolving nature of aerosol measurement technology makes it necessary for novices and experienced practitioners alike to become familiar with the new techniques and the applications of aerosol measurements. This book attempts to address these aspects in three parts. Part I on "Principles" is devoted to the basic concepts of aerosol mechanics, which describe the behavior of particles suspended in gas. Because the characteristic dimensions of the particulate phase of an aerosol are typically in the range of 10^{-9} to 10^{-4} m [1 nm to 100 μm], one must adopt a "microscopic" view to understand the dynamics of individual particles. In this context, it is fortunate that many early advances in the development of fundamental physical concepts related to Stokes' law, Millikan's measurements of the electronic charge, Einstein's theory of Brownian motion, and C.T.R. Wilson's nucleation experiments have formed the foundation for understanding aerosol behavior. Some of these concepts, as they relate to aerosol measurement, are presented in the "Principles" part of the book and are essential for comprehension of the various types of instrumentation described in this book. The "Principles" section ends with a chapter that combines these basic concepts with real-world situations where measurements must be made by taking into account the characteristics of measurement environment, desired aerosol properties, and the available measurement tools. Part II on "Techniques" expands on various measurement tools by devoting a chapter to each principal measurement technique or group of techniques. Part III on "Applications" begins with a chapter on nonspherical particle measurements, followed by chapters that discuss a wide range of applications of the aerosol instrumentation presented in Part II. Each application requires a specific set of aerosol properties to be measured, thus dictating the type of measurement technique or group of techniques that can be applied. As such, the book bridges the science and applications of aerosol measurement.

There are a number of tools available for understanding the basic concepts of aerosol measurement. The scientific literature provides a wealth of information to aid in selecting instrumentation and understanding aerosol behavior. A summary of general references consisting of useful publications, books, journals, and other key resources is presented at the end of this chapter.

1.2 UNITS AND USE OF EQUATIONS

Most equations and calculations in the book are shown in Système Internationale (SI) units. Whenever deemed appropriate, calculations in centimeter-gram-second (cgs) units are shown subsequently in square brackets. Because aerosol particles range in diameter from about 10^{-9} m to about 10^{-4} m, the unit of *micrometer* (1 μm = 10^{-6} m) is generally used when discussing particle dimensions. The term "micron" has been used in older aerosol literature as a colloquial version of micrometer, but is no longer accepted as a SI unit. Another unit, called *nanometer* (1 nm = 10^{-9} m), has been widely used to refer to much smaller particles, typically in the range 0.001–0.1 μm. In this book, unless specified otherwise, particle size refers to particle diameter.

The SI unit for aerosol mass concentration, that is, the mass of particulate matter in a unit volume of gas, is expressed in kg/m^3. Because the amount of aerosol mass is generally very low, the aerosol mass concentration is usually expressed in g/m^3, mg/m^3, $\mu g/m^3$, or ng/m^3. Particle velocity, for example, under the influence of gravity or an electric field, is expressed in m/s [shown also in cm/s in square brackets]. Volume is frequently indicated in liters ($L = 10^{-3}\ m^3$) because sampling volumes are often on the order of liters. Aerosol number concentrations are expressed in number/m^3 [number/cm^3]. Tables in Appendix B give the conversion factors for the major units used in aerosol research.

The SI unit for pressure is expressed in Pascal units ($1\ Pa = 1\ N/m^2$). Atmospheric pressure ($101\ kPa = 1.01 \times 10^6\ dyne/cm^3$) may also be referred to as 1 atm (= 14.7 psig = 760 mm Hg = 1040 cm H_2O = 408 inch H_2O). Gas and particle properties are listed at normal temperature and pressure (NTP), which refers to 101 kPa and 293 K [1 atmosphere and 20 °C = 68 °F]. Many handbooks list values at 100 kPa and 273 K [1 atmosphere and 0 °C] (standard temperature and pressure = STP), which are less useful because most aerosol measurements in the environment are at temperatures close to 293 K [20 °C].

Calculations occasionally will also be performed in both these systems to facilitate conversion, because each system has its advantages. Calculations of electrostatic systems in the SI system have an advantage in that they use the familiar units of volts and amperes. The elementary unit of charge, *e*, is equal to 1.6×10^{-19} coulomb. However, there is some convenience in using the cgs units because the proportionality constant in Coulomb's law is unity. In this system, all electrical units are defined having the prefix "stat." The

elementary unit of charge, e, is equal to 4.8×10^{-10} statcoulomb. The electric field is expressed in statvolts/cm. One statvolt equals 300 volts in SI units. Also, particle motions expressed in centimeters per second (cm/s) reflect convenient magnitudes of particle velocity in an electric field.

1.3 TERMINOLOGY

Various terminologies have been used to describe airborne particulate matter. The term *particle* refers to a single unit of matter, generally having a density approaching the intrinsic density of the bulk material. Individual particles may be chemically homogeneous or contain a variety of chemical species as well as consist of solid or liquid materials or both. Particle shapes could range from simple spherical shapes to nonspherical geometries such as cylinders or cubes to highly irregular, complex shapes not describable by Euclidean geometry. Table 1-1 lists some common terminology used to describe aerosol systems. Many of these terms do not have strict scientific definitions; some have been derived from popular or colloquial use referring to the appearance or source of particles (e.g., smoke, fog) while some are based on arbitrary or expedient conventions (e.g., nanoparticles). A number of terms describing the shape, structure, origin, and other characteristics of particles in an aerosol are listed in Table 1-2.

Appendix A gives additional definitions of terminologies used to describe aerosol systems.

TABLE 1-1 Terminology Used to Describe Common Aerosol Systems

Bioaerosol	An aerosol of biological origin, including airborne suspension of viruses, pollen, bacteria, and fungal spores, and their fragments.
Cloud	A very dense or concentrated suspension of particles in air, often with a well-defined boundary at a macroscopic length scale.
Dust	Solid particles formed by crushing or other mechanical action resulting in physical disintegration of a parent material. These particles generally have irregular shapes and are larger than about 0.5 μm.
Fog or mist	Suspension of liquid droplets. These can be formed by condensation of supersaturated vapors or by nebulization, spraying, or bubbling.
Fume	Particles resulting from condensed vapor with subsequent agglomeration. Solid fume particles typically consist of complex chains of submicrometer-sized particles (usually <0.05 μm) of similar dimension. Fumes are often the result of combustion and other high temperature processes. Note that the common usage of "fume" also refers to noxious vapor components.
Haze	A visibility-reducing aerosol.
Nanoparticle	A particle in the size range of 1–100 nm.
Particle	A small, discrete object.
Particulate	An adjective indicating that the material in question has particle-like properties (e.g., particulate matter). Sometimes used incorrectly as a noun to represent particles.
Smog	An aerosol consisting of solid and liquid particles created, at least in part, by the action of sunlight on vapors. The term smog is a combination of the words "smoke" and "fog" and often refers to the entire range of such pollutants, including the gaseous constituents.
Smoke	A solid or liquid aerosol, the result of incomplete combustion or condensation of supersaturated vapor. Most smoke particles are submicrometer in size.
Spray	Droplet aerosol formed by mechanical or electrostatic breakup of a liquid.

TABLE 1-2 Terms Used to Describe Physical Shape, Structure, or Origin of Aerosol Particles

Agglomerate	A loosely linked group of small particles often held together by van der Waals forces or surface tension. Often formed in the gas phase by collision of particles with each other due to Brownian motion or external force or flow fields.
Primary particle	The individual particles that make up the agglomerate.
Aggregate	Particle formed by a group of smaller particles linking together strongly, often through a process of coalescence and sintering at high temperatures. Strong necking between the smaller particles makes the aggregate difficult to break apart. It is often difficult to define a primary particle due to strong necking. Aggregates are sometimes referred to as hard agglomerates.
Flocculate	A group of particles very loosely held together, usually by electrostatic forces. Flocculates can easily be broken apart by shear forces in the airflow.
Primary aerosol	An aerosol resulting from the direct introduction of particles from a source into the atmosphere.
Secondary aerosol	In contrast to the primary aerosols, secondary aerosols are formed by condensation of gas phase chemical species. This term is sometimes used to describe agglomerated or redispersed or resuspended particles.
Monodisperse	Monodisperse aerosol has particles of the same size and is often used for calibration of instruments.
Polydisperse	Polydisperse aerosol has particles with a wide range of size.

1.4 PARAMETERS AFFECTING AEROSOL BEHAVIOR

1.4.1 Particle Size and Shape

Particle size is perhaps the most important property that determines its behavior in a gas; particles of different sizes behave differently and can be governed by different physical laws. For example, on the earth's surface, particles only slightly larger than gas molecules are governed primarily by Brownian motion, while large particles in the order of few micrometers are affected primarily by gravitational and inertial forces.

For spherical particles, the diameter is an unequivocal, and usually a universal, measure of particle size. Many atmospheric particles from air pollution sources tend be somewhat spherical due to their growth by condensation of liquid from the gas phase. For nonspherical particles such as fibers and agglomerates, a universal characteristic size is more difficult to define. For such particles, there are numerous definitions of particle size and shape depending upon what measurement technique is employed or what particle property is relevant in a given application.

The concept of *equivalent diameter* is most often used in aerosol science to "assign" a size to a particle that represents its specific property or behavior of interest in a given system. An equivalent diameter is reported as the diameter of a sphere having the same value of a specific physical property as the particle under consideration (Fig. 1-1). For instance, *aerodynamic equivalent diameter* (equivalent is often left out or implied for simplicity) is the diameter of a standard-density ($1000\,kg/m^3$ or $1\,g/cm^3$) sphere having the same terminal velocity when settling under gravity as the particle under consideration. The aerodynamic diameter is useful for describing the behavior of particles (typically larger than 0.3-0.5 μm) in the respiratory tract and in engineered devices such as filters, cyclones, or impactors, where inertial behavior dominates. The motion of extremely small particles, in the order of a few nanometers, is dominated less by inertia (under typical atmospheric conditions) and more by Brownian motion. For such particles, the aerodynamic diameter may not be relevant, instead, a *mobility equivalent diameter* is used. Mobility equivalent diameter is the diameter of a spherical particle with the same mobility (defined as the particle velocity produced by a unit external force) as the particle in question.

Equivalent diameters based on a particle's mass, volume, or surface area have also been defined, which can be useful in describing particles with complex shapes, structures, or internal voids. The *volume equivalent diameter* is defined as the diameter of a spherical particle of the same volume as the particle under consideration. For an irregular particle, volume equivalent diameter is the sphere diameter that the particle would acquire if it were liquefied to form a droplet while preserving any internal void volume (i.e., internal pockets of voids isolated from the gas surrounding the particle). Some aggregates from combustion processes can have internal void volumes. The *mass equivalent diameter* of a particle is the diameter of a nonporous sphere composed of a bulk particle material that has the same mass as the particle in question. Another diameter called the *envelope equivalent diameter* has also been used; it is defined as the diameter of a sphere that is composed of a bulk particle material and includes the same internal volume of voids, and has the same mass as the particle in question. The diameter of a circle having the same area as that of particle's cross-sectional area projected on a plane gives the *projected area-equivalent diameter*. Spray aerosol droplets used as fuel in combustion processes burn or react at their surfaces. Therefore, to capture the critical role of surface area, *Sauter mean diameter* has been used; this is the diameter of a sphere with the same surface area-to-volume ratio as the particle under consideration. In addition to the various equivalent diameters mentioned above, any other particle property, such as behavior in a magnetic or electric field, external surface area, radioactivity, optical property, or chemical concentration can be used to define an equivalent diameter. Chapters 2 and 23 of this book discuss these definitions in a greater detail.

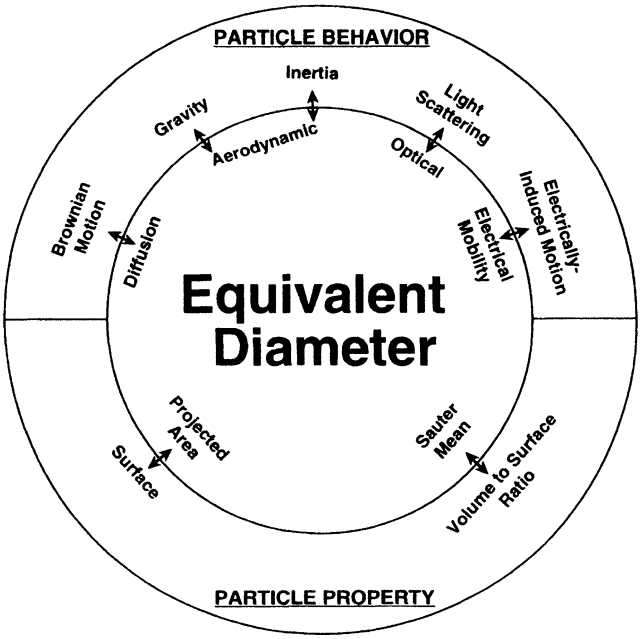

Figure 1-1 Particle size definitions that depend on observations of particle properties or behavior.

Most theories describing aerosol behavior assume that the particles are spherical. Use of equivalent diameters and other correction factors allows application of these theories to nonspherical particles. For example, a *dynamic shape factor* is a correction term used in Stokes' law that allows its application to nonspherical particles. Where only approximate analysis is desired, shape can usually be ignored, as it rarely leads to a

property change of more than a factor of two. Particles with very high aspect ratios, such as long, thin fibers, can be treated using idealized geometries such as long cylinders or prolate or oblate spheroids. The complex shape of some agglomerate particles can be described using fractal geometry. Chapter 23 discusses these aspects of particle characterization in a greater detail.

Although air consists of nitrogen, oxygen, and other gases, a representative "air molecule" can be considered for most calculations as having an average diameter of 3.7×10^{-10} m (0.37 nm or 0.00037 μm). In comparison, the particle diameters that exhibit aerosol behavior range from molecular clusters as small as 10^{-9} m (1 nm) to dust particles or cloud droplets as large as 100 μm. Particles larger than 100 μm generally settle too quickly to form a stable suspension over the timescales of interest. The lower size limit for aerosol behavior is not well-defined, partly because the size at which there is a clear transition from molecular (or atomic) to aerosol behavior can not often be well defined. A conventional limit of 1 nm is used which approximately corresponds to the lower measurement limit of aerosol instruments such as electrical mobility classifiers (see Chapters 15 and 32) or condensation particle counters (see Chapters 17 and 32).

1.4.2 Particle Concentration

Particle concentration is used to describe spatial distribution of a particular aerosol property and is defined as the specific property of the particle suspension per unit volume of gas. Depending on the application, aerosol concentrations are described in different ways. The most commonly used types of particle concentration are number, mass, surface area, and volume concentration. Particle number concentrations are used to characterize cleanrooms and atmospheric cloud condensation nuclei. Federal air pollution and workplace exposure standards are usually stated in terms of aerosol mass per unit volume of gas. Surface area concentrations can be important in many particle toxicology studies. Volume fraction, that is, volume of particulate matter per unit volume of gas, is often used as a measure of particle concentration in some engineering applications where the overall viscosity of the suspension is of interest.

Particle number concentration is defined analogous to gas density, that is, the number of particles per unit volume of gas. The units of number concentration are m^{-3} (or cm^{-3}; often denoted as particles/cm^3). The total number concentration, including all sizes, in a polluted urban atmosphere is generally on the order of 10^5 cm^{-3} or higher, while concentrations in less polluted regions are likely to be around 10^4 cm^{-3}. Number concentrations near emission sources, such as engine exhaust, or in many industrial atmospheres can easily approach 10^7 cm^{-3} or higher. Cleanrooms used in the manufacturing of microelectronic components are rated according to the number concentration of particles in a specific size range. For example, for a Class 1 cleanroom, number concentration of particles with 0.1 μm diameter particles must be kept below 10^3 m^{-3} (Chapter 36). Depending on the particle size, different instruments are employed to measure particle number concentrations such as optical particle counters (Chapter 13) and condensation particle counters (Chapters 17 and 32).

Particle mass concentration is usually determined by filtering a known volume of aerosol and weighing the collected particles. The average mass concentration over the measurement time is obtained by dividing the measured particulate mass by the volume of gas filtered. The most common units for mass concentration are $\mu g/m^3$ and mg/m^3. Atmospheric aerosol mass concentrations range from about 20 $\mu g/m^3$ for unpolluted air to 200 $\mu g/m^3$ for polluted air; mass concentrations in polluted industrial environments can be in the range of several mg/m^3, and those in the industrial aerosol reactors can be as high as several g/m^3.

For monodisperse aerosols one type of concentration can be easily converted to the other, whereas for polydisperse aerosols more detailed characterization may be necessary.

1.4.3 Particle Size Distribution

One of the most of important characteristics of polydisperse aerosol is its particle size distribution, which represents the distribution of a specific aerosol property over the particle size range of interest. To construct a particle size distribution, the particle size is "weighted" by either number, mass, surface area, volume, or other aerosol property of interest. Aerosol instruments not only differ in what equivalent size they measure, but also in how they "weigh" the particle size when they construct a size distribution. Size distributions with different weighting factors can differ substantially. A grocery store analogy can help elucidate. If ten large apples and one hundred small raisins are purchased, the median size of the total "population" will be only slightly larger than the average size of raisins, if the median is based on the *number count*. This is because the median size divides the "population" in two groups of equal number, and in this case, most of the "population" consists of small raisins. Instead of number count, if each piece of fruit is weighed on a scale and the *weight* of the apples (or mass in the case of particles) is used to calculate the median, then the median size will be much larger than the one based on number count. Thus, particle size distribution weighted by "mass" results in a larger median size than that weighted by "count" for a given population of particles. Therefore, any size distribution measurement is accompanied by a description of the *weighting factor*, or the *weighting* as it is commonly called.

If aerosol particles in a population are "sized" and "counted," and particles are then grouped into discrete, contiguous size bins, the size distribution can be represented by

plotting particle number on y-axis versus size on x-axis. The lower and upper particle diameter limits, d_l and d_u, of each size bin must be chosen with some care in order to get a useful description of the overall size distribution. The number of particles in each bin will depend on the size of the bin, that is, $d_u - d_l$. To remove this dependence on the bin width, the number of particles in each bin is usually normalized by the bin width. Size distribution properties of aerosols are discussed in more detail in Chapters 4, 5, and 22.

Often a representative size of a population of particles is reported as the *mean size* (arithmetic average of all sizes), *median size* (equal number of particles above and below this size), or the *mode* (size corresponding to the highest frequency). The spread of the particle size distribution is characterized by an *arithmetic* or *geometric* (logarithmic) *standard deviation*. Typically, the particle size distribution is *lognormal*, that is, the particle concentration versus particle size curve looks *normal* (also referred to as a Gaussian or bell-shaped curve) when the particle size is plotted on a logarithmic scale (see Chapters 5 and 22).

The reason for the use of logarithmic or geometric size scale can be illustrated by considering an example of successive disintegration of a piece of blackboard chalk. For example, a 64 mm-long piece of chalk would break up into two pieces of 32 mm length each. Subsequent breakups yield pieces with lengths 16, 8, 4, 2, 1 mm, and so on, until one reaches molecular length scales. The ratio of adjacent sizes is always two, thus appearing at the same linear distance on a logarithmic or geometric size scale. Because with each breakage step, more and more particles are produced, the distribution is skewed, so that there are many more smaller particles than larger ones. This exercise of successive disintegration of a piece of chalk mimics the way particles are produced in many natural as well as industrial systems. Therefore, aerosol particle size is generally plotted on a logarithmic size scale.

Many aerosols measured in ambient or industrial environments or in industrial process streams are a mixture of aerosols, resulting in more than one particle mode over a wide size range. This may make the measurement and analysis of the aerosol size distribution considerably more complex.

1.4.4 Particle Adhesion and Detachment

Understanding forces that affect attachment and detachment of particles to wall surfaces, briefly described below, is important for conducting reliable aerosol measurements.

1.4.4.1 Adhesion Forces In contrast to gas molecules, aerosol particles that contact one another generally adhere to each other and form agglomerates. This is one of the most important characteristics that distinguishes aerosols from atoms and molecules, as well as from much larger, millimeter-sized particles. If an aerosol particle contacts a wall surface, such as those in a filter or any other particle collection device, it is most likely to remain adhered.

The London–van der Waals forces, attractive forces responsible for adhesion in most systems, are short-range forces, meaning they act over very short distances relative to the particle dimensions. According to the theory of their origin, random motion of the electrons in an electrically neutral material creates instantaneous dipoles that may induce complementary dipoles in neighboring material and thus attract the surfaces to each other.

Many particles 0.1 μm or larger carry some small net charge that exerts an attractive force in the presence of a particle with an opposite charge (Hinds 1999, p. 143). For two charged particles (point charges), this Coulomb force is inversely proportional to the square of the separation distance. After two surfaces have made contact with each other, the surfaces may deform with time, thereby increasing the contact area, further decreasing the separation distance, and thus increasing the force of adhesion. A charged particle in the vicinity of an electrically neutral surface can also induce an equal and opposite charge on the surface, resulting in an attractive electrostatic force between the particle and the surface.

Figure 1-2a illustrates how air humidity may affect particle adhesion. At high humidity, liquid molecules are adsorbed on the particle surface and fill the capillary spaces at and near the point of contact. The surface tension of this adsorbed liquid layer increases the adhesion between the two surfaces.

1.4.4.2 Detachment Forces and Particle Bounce Figure 1-2b illustrates the detachment of a particle from a rotating body. The centrifugal force is proportional to the particle's mass or volume, that is, particle diameter cubed (d^3). Detachment by other types of motion, such as vibration, is similarly proportional to d^3, while detachment by air currents is proportional to d^2. In contrast, most adhesion forces are linearly dependent on particle diameter. Consequently, large particles are more readily detached than small ones. While individual

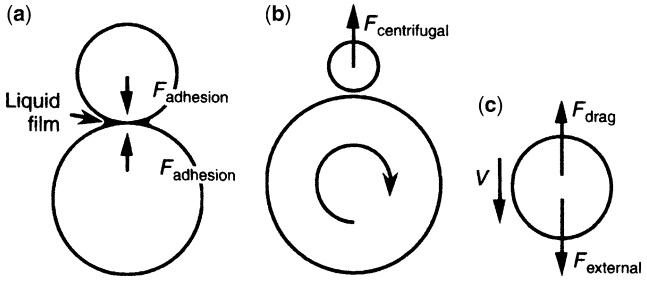

Figure 1-2 Examples of interparticle and external forces acting on the particle. **(a)** Adhesion due to liquid film. **(b)** Detachment due to centrifugal force. **(c)** Particle motion at velocity V due to balance between drag force and an external force.

particles less than 10 μm are not likely to be easily removed, for example, by vibration, a thick layer of such particles may be easily dislodged in large (0.1–10 mm) chunks (Hinds 1999, p. 144). This has implications for most aerosol instruments, which involve deposition of particles in various regions. Re-entrainment of deposited particles from wall surfaces into an aerosol flow may interfere with the measurements.

If an aerosol flow is directed toward a surface, for example in filters and impactors, particles with sufficient inertia will deviate from the flow streamlines and move toward the surface. Liquid and "sticky" small particles will deposit on the surface. Upon contact, a solid particle and the surface may deform. If the rebound energy is greater than the adhesion energy—which can happen when impact velocity is very high—a solid particle may "bounce", that is, move away after contact with the surface. Upon surface contact, some or all of the particle's kinetic energy is converted to thermal energy, resulting in reduced kinetic energy on rebound or heating of the particle/surface interface on sticking. Grease or oil on the surface will generally increase the likelihood of adhesion, but after a layer of particles has been deposited, the incoming particles may bounce from the top surface of the previously deposited particles. Particle adhesion on impact is an especially critical factor in inertial collection devices and is discussed in Chapter 8.

1.4.5 Applied External Forces

When particles are subjected to an external force, such as gravity or an electrical force, the particles will move in the force field. The migration velocity in the force field is particle-size dependent, a fact that is exploited by most aerosol size spectrometers for particle-size discrimination.

When an airborne particle is subjected to an external applied force, for example gravity, the particle will migrate under the influence of that force. Opposing this external force is the aerodynamic drag force, as shown in Figure 1-2c. When the two forces are in equilibrium, which happens almost instantaneously (there is a very short relaxation time), the particle moves in the force field with migration velocity V. Knowledge of the two opposing forces allows determination of this velocity. Particle velocity is important for estimating collection on surfaces as well as for separating particles by size.

In space, astronauts must pay special attention to the dust generated by their clothing and the activities they engage in. Otherwise, their living space quickly becomes polluted with aerosols. On earth, gravity has a major cleaning effect on ambient and industrial aerosols. Larger particles tend to settle out more rapidly due to gravity. This is the basis for the definition of aerodynamic diameter, and for many instruments that exploit this behavior to measure particle aerodynamic size (see Chapter 8). Inertial forces can be applied to particles by forcing the suspending air to change direction. Size-dependent inertial effects are used for particle separation, collection, and measurement in such devices as impactors, cyclones, centrifuges, aerodynamic lenses, and acceleration nozzles (Chapters 8, 11, and 14).

We are familiar with the attraction of lint particles to clothing. This is due to electrostatic attraction between the lint and the clothing. Similarly, charged aerosol particles can be attracted to or repelled from charged surfaces or other charged particles. Particles that are freshly emitted from a source, particularly those resulting from mechanical friction or shear, tend to carry greater charge levels than particles that have been airborne for hours or longer. This aging effect is due to the attraction of oppositely charged airborne ions produced by natural radiation. For smaller particles, the electric force on charged particles may easily exceed the gravitational force by several orders of magnitude. This fact is exploited by carefully controlling the electrical force on a particle and its migration to achieve particle-size separation and measurement in electrical mobility analyzers, as discussed in Chapter 15. The same electrical force is also used to "levitate" large particles by balancing the gravitational and the electrical force in electrodynamic balance, as described in Chapter 19. Similarly, the aerosol particle mass analyzer, described in Chapter 12, uses the balance between electrical and centrifugal force to separate particles based on their mass-to-charge ratio.

If there is a spatial gradient in the concentration of particles present in the air, Brownian diffusion can lead to particles moving from high concentration to low concentration region. It is often the dominant mechanism for particles smaller than about 0.2 μm in diameter. This is exploited in a diffusion battery, which is commonly used for measuring submicrometer particles. Diffusion is also important for understanding the particle deposition properties in the human lung. If the suspending gas is a nonuniform mixture of gases, the particle transport may also be affected by diffusiophoretic forces caused by the concentration gradient of the gas components.

If there is a temperature gradient in the aerosol-containing space between two surfaces, the higher activity of the air molecules near the hot surface pushes the particles toward the colder surface (thermophoretic force). This property is exploited in the thermal precipitator, which is used to collect particles onto a desired surface (Chapter 8). A special case of thermophoresis, but generally not very useful for measurement purposes, is produced by light. Illumination of a particle heats up one side of the particle as well as gas molecules nearby, which push the particle toward the colder side. Illumination can also produce radiation pressure, whereby the stream of photons exerts a force on the particle (photophoresis). A focused laser beam can be used as optical "tweezers" to move small particles, for example, bacteria, in a liquid.

1.5 AEROSOL INSTRUMENTATION CONSIDERATIONS

Most aerosol measurement techniques fall in two categories: the first relies on collection of aerosol particles on a substrate, such as a filter, for subsequent laboratory measurement (usually at a remote location), and the second allows *in situ*, near-real-time[2] measurement of aerosols. Traditionally, collection followed by measurement has been used widely as it can utilize many powerful analytical techniques available in the laboratory (Chapters 7 to 10 and 12). However, this approach has a disadvantage in that the particles may be modified by the transport and collection processes, measurements are time-averaged, and the measurement result is not immediately available. Real-time techniques, on the other hand, can provide much quicker measurements *in situ*; however, they may provide a more limited degree of particle characterization (Chapters 11 to 15 and 18).

In situ, real-time techniques can be subdivided further into *extractive* and *external sensing* techniques. Extractive techniques require the aerosol to be brought to the instrument sensor, while the external sensing techniques allow noninvasive measurement of the aerosol in its undisturbed native state. For example, Chapter 13 describes many instruments that detect light scattered from particles brought into an instrument (e.g., optical particle counters) as well as optical systems that detect particles immediately outside the instrument, without the need to extract any sample (e.g., forward-scattering spectrometer probe).

In general, one cannot obtain particle size information on the entire five-decade size range of 0.001 μm to 100 μm with a single instrument. On a macroscopic scale, this would be equivalent to measuring a 1 mm distance with a small scale and then using the same scale for measuring a 1 km distance (which is six orders of magnitude larger than 1 mm). Optical techniques that use visible wavelengths of light (from 400 to 700 nm) cannot probe particles smaller than the wavelength. Inertial techniques become inefficient below about 0.5 μm at normal temperature and pressure. In an electron microscope, the probing tool is electrons, which have a much smaller wavelength that can "see" much smaller particles. Therefore, one may have to resort to using a variety of instrumentation, each employing different measurement techniques and measuring different equivalent size to obtain a broader picture of distribution of particles sizes over the range of interest.

[2]The term *real-time* has been loosely applied in the literature to denote *in situ*, short-time measurement capability of the instruments compared to methods that involve aerosol collection followed by laboratory analysis, which can take from a few hours to days to obtain measurement results. However, what is real-time in one application may not be so in another. The term "direct-reading" has also been used to refer to real-time instruments. Real-time has been used in this book to generally refer to instruments that can provide *in situ*, short-time measurements on the order of a few seconds to few minutes. The term *semi-continuous* has also been used to refer to *in situ* techniques with slightly longer measurement times.

1.6 REFERENCES

Hinds, W.C. 1999. *Aerosol Technology*. New York: John Wiley & Sons.

General Aerosol-Related Works

Abraham, F.F. 1974. *Homogeneous Nucleation Theory: The Pretransition Theory of Vapor Condensation, Supplement I: Advances in Theoretical Chemistry*. New York: Academic.

Bailey, A.G. 1988. *Electrostatic Spraying of Liquids*. New York: John Wiley & Sons.

Beddow, J.K. 1980. *Particulate Science and Technology*. New York: Chemical Publishing.

Bohren, C.F., and D.R. Huffman. 1983. *Absorption and Scattering of Light by Small Particles*. New York: John Wiley & Sons.

Clift, R., J.R. Grace, and M.E. Weber. 1978. *Bubbles, Drops, and Particles*. Boston: Academic.

Colbeck, I. (ed.). 1997. *Physical and Chemical Properties of Aerosols*. Dordrecht, The Netherlands: Kluwer Academic.

Davies, C.N. (ed.). 1966. *Aerosol Science*. New York: John Wiley & Sons.

Dennis, R. 1976. *Handbook on Aerosols*. Publication TID-26608. Springfield, VA: National Technical Information Service, U.S. Department of Commerce.

Einstein, A. 1956. *Investigations on the Theory of Brownian Motion*. New York: Dover.

Friedlander, S.K. 2000. *Smoke, Dust, and Haze: Fundamentals of Aerosol Dynamics*, 2 ed, New York: Oxford University Press.

Fuchs, N.A. 1989. *The Mechanics of Aerosols*. New York: John Wiley & Sons.

Fuchs, N.A., and A.G. Sutugin. 1970. *Highly Dispersed Aerosols*. Ann Arbor, MI: Ann Arbor Science Publishers.

Green, H.L., and W.R. Lane. 1964. *Particulate Clouds, Dust, Smokes and Mists*, 2 ed. Princeton, NJ: Van Nostrand.

Happel, J., and H. Brenner. 1973. *Low Reynolds Number Hydrodynamics with Special Applications to Particulate Media*, 2 rev. ed. Leyden: Noordhoff International.

Hesketh, H.E. 1977. *Fine Particles in Gaseous Media*. Ann Arbor, MI: Ann Arbor Science Publishers.

Hidy, G.M. 1972. *Aerosols and Atmospheric Chemistry*. New York: Academic.

Hidy, G.M., and J.R. Brock. 1970. *The Dynamics of Aerocolloidal Systems*. New York: Pergamon.

Hidy, G.M., and J.R. Brock (eds.). 1971. *Topics in Recent Aerosol Research*, Part 1. New York: Pergamon.

Hidy, G.M., and J.R. Brock (eds.). 1972. *Topics in Current Aerosol Research*, Part 2. New York: Pergamon.

Hinds, W.C. 1999. *Aerosol Technology*. New York: John Wiley & Sons.

Kerker, M. 1969. *The Scattering of Light and Other Electromagnetic Radiation*. New York: Academic.

Lefebvre, A.H. 1989. *Atomization and Sprays*. New York: Hemisphere.

Liu, B.Y.H. (ed.). 1976. *Fine Particles*. New York: Academic.

Marlow, W.H. (ed.). 1982. *Aerosol Microphysics I, Chemical Physics of Microparticles*. Berlin: Springer-Verlag.

Marlow, W.H. (ed.). 1982. *Aerosol Microphysics II, Chemical Physics of Microparticles*. Berlin: Springer-Verlag.

Mason, B.J. 1971. *The Physics of Clouds*. Oxford: Clarendon.

McCrone, W.C., et al. 1980. *The Particle Atlas,* vols. I–VII. Ann Arbor, MI: Ann Arbor Science Publishers.

Mednikov, E.P. 1980. *Turbulent Transport of Aerosols* [in Russian]. Moscow: Science Publishers.

Orr, C., Jr. 1966. *Particulate Technology*. New York: Macmillan.

Reist, P.C. 1984. *Aerosol Science and Technology*. New York: McGraw-Hill.

Ruzer, L.S., and N.H. Harley. 2004. *Aerosols Handbook: Measurement, Dosimetry, and Health Effects*. Boca Raton, FL: CRC.

Seinfeld, J.H., and S.N. Pandis. 2006. *Atmospheric Chemistry and Physics: From Air Pollution To Climate Change*. New York: John Wiley & Sons.

Sanders, P.A. 1979. *Handbook of Aerosol Technology*. Melbourne, FL: Krieger.

Sedunov, Y.S. 1974. *Physics of Drop Formation in the Atmosphere* [translated from Russian]. New York: John Wiley & Sons.

Twomey, S. 1977. *Atmospheric Aerosols*. Amsterdam: Elsevier Science.

Van de Hulst, H.C. 1957. *Light Scattering by Small Particles*. New York: John Wiley & Sons. Republished unabridged and corrected. 1981. New York: Dover.

Vohnsen, M.A. 1982. *Aerosol Handbook*, 2 ed. Mendham, NJ: Dorland Publishing.

Wen, C.S. 1996. *The Fundamentals of Aerosol Dynamics*. Hackensack, NJ: World Scientific.

Whytlaw-Grey, R.W., and H.S. Patterson. 1932. *Smoke: A Study of Aerial Disperse Systems*. London: E. Arnold.

Withers, R.S. 1979. *Transport of Charged Aerosols*. New York: Garland.

Willeke, K. (ed.). 1980. *Generation of Aerosols and Facilities for Exposure Experiments*. Ann Arbor, MI: Ann Arbor Science Publishers.

Williams, M.M.R., and S.K. Loyalka. 1991. *Aerosol Science Theory and Practice: With Special Application to the Nuclear Industry*. Oxford: Pergamon.

Yoshida, T., Y. Kousaka, and K. Okuyama. 1979. *Aerosol Science for Engineers*. Tokyo: Tokyo Power Company.

Zimon, A.D. 1969. *Adhesion of Dust and Powders*, 2 ed. New York: Plenum.

Zimon, A.D. 1976. *Adhesion of Dust and Powders*, 2 ed. [in Russian]. Moscow: Khimia.

Measurement Techniques

Allen, T. 1968. *Particle Size Measurement*. London: Chapman and Hall.

Allen, T. 1981. *Particle Size Measurement*, 3 ed. New York: Methuen.

Barth, H.G. (ed.). 1984. *Modern Methods of Particle Size Analysis*. New York: John Wiley & Sons.

Beddow, J.K. 1980. *Testing and Characterization of Powders and Fine Particles*. New York: John Wiley & Sons.

Beddow, J.K. 1984. *Particle Characterization in Technology*. Boca Raton, FL: CRC.

Cadle, R.D. 1965. *Particle Size: Theory and Industrial Applications*. New York: Reinhold.

Cadle, R.D. 1975. *The Measurement of Airborne Particles*. New York: John Wiley & Sons.

Cheremisinoff, P.N. (ed.). 1981. *Air Particulate Instrumentation and Analysis*. Ann Arbor, MI: Ann Arbor Science Publishers.

Dallavalle, J.M. 1948. *Micromeritics*, 2 ed. New York: Pitman.

Dzubay, T.G. 1977. *X-Ray Fluorescence Analysis of Environmental Samples*. Ann Arbor, MI: Ann Arbor Science Publishers.

Herdan, G. 1953. *Small Particle Statistics*. New York: Elsevier Science.

Jelinek, Z.K. [translated by W. A. Bryce]. 1974. *Particle Size Analysis*. New York: Halstead.

Lodge, J.P., Jr., and T.L. Chan (eds.). 1986. *Cascade Impactor, Sampling and Data Analysis*. Akron, OH: American Industrial Hygiene Association.

Malissa, H. (ed.). 1978. *Analysis of Airborne Particles by Physical Methods*. Boca Raton, FL: CRC.

Nichols, A.L. 1998. *Aerosol Particle Size Analysis: Good Calibration Practices*. Cambridge: Royal Society of Chemistry.

Orr, C., and J.M. Dallavalle. 1959. *Fine Particle Measurement*. New York: Macmillan.

Rahjans, G.S., and J. Sullivan. 1981. *Asbestos Sampling and Analysis*. Ann Arbor, MI: Ann Arbor Science Publishers.

Silverman, L., C. Billings, and M. First. 1971. *Particle Size Analysis in Industrial Hygiene*. New York: Academic.

Stockham, J.D., and E.G. Fochtman. 1977. *Particle Size Analysis*. Ann Arbor, MI: Ann Arbor Science Publishers.

Vincent, J.H. (ed.). 1998. *Particle Size: Selective Sampling for Particulate Air Contaminants*, Cincinnati, OH: American Conference of Governmental Industrial Hyienists.

Vincent, J.H. 2007. *Aerosol Sampling: Science, Standards, Instrumentation, and Applications*. New York: John Wiley & Sons.

Gas Cleaning

Clayton, P. 1981. *The Filtration Efficiency of a Range of Filter Media for Submicrometer Aerosols*. New York: State Mutual Book and Periodical Service.

Davies, C.N. 1973. *Air Filtration*. London: Academic.

Dorman, R.G. 1974. *Dust Control and Air Cleaning*. New York: Pergamon.

Mednikov, E.P. 1965. *Acoustic Coagulation and Precipitation of Aerosols*. New York: Consultants Bureau.

Ogawa, A. 1984. *Separation of Particles from Air and Gases*, vols. I and II. Boca Raton, FL: CRC.

Spurny, K. 1998. *Advances in Aerosol Filtration*. Boca Raton, FL: Lewis.

White, H.J. 1963. *Industrial Electrostatic Precipitation*. Reading, MA: Addison-Wesley.

Environmental Aerosols/Health Aspects

American Conference of Governmental Industrial Hygienists. 2001. *Air Sampling Instruments*, 9 ed. Cincinnati, OH: Author.

Brenchly, D.L., C.D. Turley, and R.F. Yarmae. 1973. *Industrial Source Sampling*. Ann Arbor, MI: Ann Arbor Science Publishers.

Cadle, R.D. 1966. *Particles in the Atmosphere and Space*. New York: Reinhold.

Cox, C.S., and C.M. Wathes. 1995. *Bioaerosols Handbook*. Boca Raton: David Lewis Publishing.

Drinker, P., and T. Hatch. 1954. *Industrial Dust*. New York: McGraw-Hill.

Flagan, R.C., and J.H. Seinfeld. 1988. *Fundamentals of Air Pollution Engineering*. New York: Prentice Hall.

Hickey, A. J. 1996. *Inhalation Aerosols*. New York: Marcel Dekker.

Hidy, G.M. 1972. *Aerosols and Atmospheric Chemistry*. New York: Academic.

Junge, C. 1963. *Air Chemistry and Radioactivity*. New York: Academic.

Lighthart, B., and A.J. Mohr. 1994. *Atmospheric Microbial Aerosols: Theory and Applications*. London: Chapman and Hall.

McCartney, E.J. 1976. *Optics of the Atmosphere*. New York: John Wiley & Sons.

Mercer, T.T. 1973. *Aerosol Technology in Hazard Evaluation*. New York: Academic.

Middleton, W.E.K. 1952. *Vision Through the Atmosphere*. Toronto: University of Toronto Press.

Moren, F., M.B. Dolovich, M.T. Newhouse, and S.P. Newman. 1993. *Aerosols in Medicine: Principles, Diagnosis, and Therapy*. Amsterdam: Elsevier Science.

Muir, D.C.F. (ed.). 1972. *Clinical Aspects of Inhaled Particles*. London: Heinemann.

National Research Council, Subcommittee on Airborne Particles. 1979. *Airborne Particles*. Baltimore, MD: University Park Press.

National Research Council. 1996. *A Plan for a Research Program on Aerosol Radiative Forcing and Climate Changes*. Washington, D.C.: National Academy Press.

Perera, F., and A.K. Ahmen. 1979. *Respirable Particles: Impact of Airborne Fine Particles on Health and Environment*. Cambridge, MA: Ballinger.

Seinfeld, J.H., and Pandis, S. 1998. *Atmospheric Chemistry and Physics*. New York: John Wiley & Sons.

Spurny, K. 1999. *Aerosol Chemical Processes in Polluted Atmospheres*. Boca Raton, FL: Lewis.

Spurny, K. 1999. *Analytical Chemistry of Aerosols*. Boca Raton, FL: Lewis.

Vincent, J.H. 1995. *Aerosol Science for Industrial Hygienists*. Tarrytown, NY: Elsevier.

Whitten, R.C. (ed.). 1982. *The Stratospheric Aerosol Layer*. Berlin: Springer-Verlag.

Industrial Applications and Processes

Andonyev, S., and O. Filipyev. 1977. *Dust and Fume Generation in the Iron and Steel Industry*. Chicago: Imported Publications.

Austin, P.R., and S.W. Timmerman. 1965. *Design and Operation of Clean Rooms*. Detroit, MI: Business News Publishing.

Boothroyd, R.G. 1971. *Flowing Gas-Solids Suspensions*. London: Chapman and Hall.

Donnet, J.B., and A. Voet. 1976. *Carbon Black*. New York: Marcel Dekker.

Kodas, T.T., and M.J. Hampden-Smith. 1999. *Aerosol Processing of Materials*. New York: John Wiley & Sons.

Marshall, W.R., Jr. 1954. *Atomization and Spray Drying*. Chemical Engineering Progress Monograph Series, vol. 50, no. 23. New York: American Institute of Chemical Engineers.

Proceedings of Meetings

Advances in Air Sampling. 1988. Papers from the American Conference of Governmental Industrial Hygienists Symposium. Ann Arbor, MI: Lewis.

American Society for Testing Materials. 1959. *ASTM Symposium on Particle Size Measurement*. ASTM Special Technical Publication No. 234. Philadelphia, PA: Author.

Barber, D.W., and R.K. Chang. 1988. *Optical Effects Associated with Small Particles*. Singapore: World Scientific.

Beard, M.E., and H.L. Rook (eds.). 2000. *Advances in Environmental Measurement Methods for Asbestos*. Special Technical Publication No. 1342. Philadelphia: American Society for Testing Materials.

Beddow, J.K., and T.P. Meloy (eds.). 1980. *Advanced Particulate Morphology*. Boca Raton, FL: CRC.

Davies, C.N. 1964. *Recent Advances in Aerosol Research*. New York: Macmillan.

Dodgson, J., R.I. McCallum, M.R. Bailey, and D.R. Fisher (eds.). 1989. *Inhaled Particles VI*. Oxford: Pergamon.

Fedoseev, V.A. 1971. *Advances in Aerosol Physics* [translation of *Fizika Aerodispersnykh Sistem*]. New York: Halsted.

Gerber, H.E., and E.E. Hindman (eds.). 1982. *Light Absorption by Aerosol Particles*. Hampton, VA: Spectrum.

Hobbs, P. V. 1993. *Aerosol-Cloud-Climate Interactions*. New York: Academic Press.

Israel, G. 1986. *Aerosol Formation and Reactivity. Proceedings of the Second International Aerosol Conference, 22–26 September 1986, Berlin (West)*. Oxford: Pergamon.

Kuhn, W.E., H. Lamprey, and C. Sheer (eds.). 1963. *Ultrafine Particles*. New York: John Wiley & Sons.

Lee, S.D., T. Schneider, L.D. Grant, and P.J. Verkerk (eds.). 1986. *Aerosols: Research, Risk Assessment and Control Strategies*. Proceedings of the Second U.S. – Dutch International Symposium, Williamsburg, Virginia May 19–25, 1985. Chelsea, MI: Lewis Publishers.

Liu, B.Y.H., D.Y.H. Pui, and H.J. Fissan. 1984. *Aerosols: Science, Technology and Industrial Applications of Airborne Particles*. 300 Extended Abstracts from the First International Aerosol Conference, Minneapolis, Minnesota, September 17–21, 1984. New York: Elsevier Science.

Lundgren, D.A., Harris, F.S., Marlow, W.H., Lippmann, M., Clark, W.E. and Durham, M.D. (eds.). 1979. *Aerosol Measurement*. Gainesville, FL: University Press of Florida.

Marple, V.A., and B.H.Y. Liu (eds.). 1983. *Aerosols in the Mining and Industrial Work Environments*. Ann Arbor, MI: Ann Arbor Science Publishers.

Mathai, C.V. (ed.). 1989. *Visibility and Fine Particles*. Proceedings of the 1989 AWMA/EPA International Specialty Conference. Pittsburgh, PA: Air and Waste Management Association.

Mercer, T.T., P.E. Morrow, and W. Stober (eds.). 1972. *Assessment of Airborne Particles*. Springfield, IL: C.C. Thomas.

Mittal, K.L. (ed.). 1988. *Particles on Surfaces 1: Detection, Adhesion, and Removal*. Proceedings of a Symposium held at the Seventeenth Annual Meeting of the Fine Particle Society, July 28–August 2, 1986. New York: Plenum.

Mittal, K.L. (ed.). 1990. *Particles on Surfaces 2: Detection, Adhesion, and Removal*. Proceedings of a Symposium held at the Seventeenth Annual Meeting of the Fine Particle Society, July 28–August 2, 1986. New York: Plenum.

Preining, O., and E.J. Davis (eds.). 2000. History of Aerosol Science. Proceedings of the History of Aerosol Science, August 31–September 2, 1999. Vienna: Austrian Academy of Science.

Richardson, E.G. (ed.). 1960. *Aerodynamic Capture of Particles*. New York: Pergamon.

Shaw, D.T. (ed.). 1978. *Fundamentals of Aerosol Science*. New York: John Wiley & Sons.

Shaw, D.T. (ed.). 1978. *Recent Developments in Aerosol Technology*. New York: John Wiley & Sons.

Siegla, P.C., and G.W. Smith (eds.). 1981. *Particle Carbon: Formation During Combustion*. New York: Plenum.

Spurny, K. 1965. *Aerosols: Physical Chemistry and Applications*. Proceedings of the First National Conference on Aerosols, October 8–13, 1962. Prague: Publishing House of the Czechoslovak Academy of Sciences.

Walton, W.H. (ed.). 1971. *Inhaled Particles III*. Surrey: Unwin Brothers.

Walton, W.H. (ed.). 1977. *Inhaled Particles IV*. Oxford: Pergamon.

Walton, W.H. (ed.). 1982. *Inhaled Particles V*. Oxford: Pergamon Press.

SELECTED JOURNALS ON AEROSOL SCIENCE AND APPLICATIONS

Aerosol Science and Technology
American Industrial Hygiene Association Journal
Annals of Occupational Hygiene
Atomization and Sprays
Atmospheric Environment
Environmental Science and Technology
International Journal of Multiphase Flow
Journal of Aerosol Medicine
Journal of Aerosol Research, Japan
Journal of Aerosol Science
Journal of the Air and Waste Management Association (formerly *Journal of the Air Pollution Control Association*)
Journal of Colloid and Interface Science
Journal of Geophysical Research-Atmospheres
Journal of Nanoparticle Research
Langmuir
Particle & Particle Systems Characterization
Particulate Science and Technology
Powder Technology

2

FUNDAMENTALS OF SINGLE PARTICLE TRANSPORT

PRAMOD KULKARNI AND PAUL A. BARON

Centers for Disease Control and Prevention,[1] *National Institute for Occupational Health and Safety, Cincinnati, Ohio*

KLAUS WILLEKE

Department of Environmental Health, University of Cincinnati, Cincinnati, Ohio

2.1 INTRODUCTION

Understanding aerosol transport, that is, how the aerosol particles move in space, is of fundamental interest in design of all aerosol instruments and devices. Virtually every measurement technique described in this book exploits a certain characteristic transport property of particles to alter their behavior to achieve a measurement objective. The aerosol consists of two components: the particles and the gas (usually air) in which they are suspended. At a microscopic level, each particle modifies the gas flow over and around it through its own physical properties which, in turn, affects the drag force acting on it. On the other hand, at a

[1]The findings and conclusions in this chapter are those of the authors and do not necessarily represent the views of the Centers for Disease Control and Prevention.

Aerosol Measurement: Principles, Techniques, and Applications, Third Edition. Edited by P. Kulkarni, P. A. Baron, and K. Willeke

macroscopic level, it is the gas flow characteristics that may determine how the particle is transported from one point to the other or how it deposits on a surface. To understand aerosol transport, it is essential to understand the basic physical concepts of fluid flow in which the particle is suspended, the interaction of a single particle with the gas surrounding it, and how the particle behaves in response to various external forces acting on it. This chapter introduces the basic framework to describe gas and particle motion.

2.2 CONTINUUM FLOW DESCRIPTION

Gas in which the particles are suspended is made up of molecules that collide with each other or an object in the vicinity. The continuum description of the fluid (gas and fluid are used interchangeably in this chapter) neglects the fact that it is made up of discrete molecules. Properties such as density, pressure, temperature, and velocity are taken to be well-defined at infinitely small points, and are assumed to vary "continuously" from one point to another.

Governing equations for continuum fluid flow are derived using Newton's second law, resulting in the following well-known Navier–Stokes equations for incompressible flow, expressed as,

$$\underbrace{\rho_g\left[\frac{\partial \mathbf{u}}{\partial t}+\mathbf{u}\cdot\nabla\mathbf{u}\right]}_{\text{Inertial forces}} = \underbrace{-\nabla p}_{\text{Forces from pressure gradient}} + \underbrace{\eta\nabla^2\mathbf{u}}_{\text{Viscous shear forces}} \qquad \text{(Eq. 2-1)}$$

and,

$$\nabla\cdot\mathbf{u}=0 \qquad \text{(Eq. 2-2)}$$

where $\mathbf{u}$ is the local flow velocity vector, ρ_g is the gas density, p is the pressure, and η is the dynamic viscosity of the gas. Equation 2-1 can be nondimensionalized by using various reference quantities to get,

$$Re\left[\frac{1}{Str}\frac{\partial \mathbf{u}^*}{\partial t^*}+\mathbf{u}^*\cdot\nabla'\mathbf{u}^*\right]=-\nabla' p^*+\nabla'^2\mathbf{u}^* \qquad \text{(Eq. 2-3)}$$

where $\mathbf{u}^*=\mathbf{u}/U$, $p^*=p/(\eta U/l_c)$, $t^*=t/t_c$, and $\nabla'=l_c\nabla$ are nondimensional parameters obtained using dimensional characteristic quantities U, l_c, t_c for velocity, length, and time, respectively. *Str* in the above equation is a nondimensional number called Strouhal number ($=t_cU/l_c$) and *Re* is a dimensionless number called *Reynolds number* defined as,

$$Re=\frac{\rho_g U d}{\eta}=\frac{Ud}{\nu} \qquad \text{(Eq. 2-4)}$$

where U is the characteristic velocity of the gas representing the whole system, η is the dynamic gas viscosity, ν is the kinematic viscosity ($=\eta/\rho_g$) and d is a characteristic dimension of the object, which, in the case of particles, is generally their diameter. Equation 2-3 shows that for steady flows Reynolds number determines the relative magnitudes of the acceleration terms on the left and the viscous and pressure gradient terms on the right.

2.2.1 Reynolds Number

Reynolds number defined in Equation 2-4 gives the measure of ratio of inertial forces to viscous forces in a fluid flow and is often used to describe flow conditions in aerosol systems. The flow pattern, whether it is "smooth" or turbulent, is governed by this ratio *Re*. Since this dimensionless number characterizes the flow, it is a function of gas density, ρ_g, and not particle density. At normal temperature and pressure (NTP), that is, 293 K [20 °C] and 101 kPa [1 atm], $\rho_g=1.192\,\text{kg/m}^3$ [$1.192\times10^{-3}\,\text{g/cm}^3$] and $\eta=1.833\times10^{-5}\,\text{Pa}\cdot\text{s}$ [1.833×10^{-4} dyne-s/cm^2], which reduces Equation 2-4 to

$$\begin{aligned} Re &= 65{,}000\ Ud \ (\text{for } U \text{ in m/s, and } d \text{ in m}) \\ [Re &= 6.5\ Ud \ (\text{for } U \text{ in cm/s, and } d \text{ in cm})] \end{aligned} \qquad \text{(Eq. 2-5)}$$

In the above equation, the characteristic dimension d depends on the fluid flow under consideration. For instance, in the case of an aerosol flowing in a circular tube, if the flow in a tube is of interest, then the cross-sectional diameter of the tube would be used as the characteristic dimension to calculate *flow Reynolds number, Re*$_f$. If the flow around a particle inside the tube is of interest, the diameter of the particle, and the particle's relative velocity would be used to calculate the *particle Reynolds number*, *Re*$_p$. Thus it is important to make distinction between the *Re*$_p$ and *Re*$_f$.

2.2.2 Streamlines

The solution of Navier–Stokes equations in Equations 2-1 and 2-2 gives the velocity vector field in three-dimensional space. *Streamlines* are field lines resulting from this vector field description of the flow. A streamline is tangential to the instantaneous velocity direction and shows the direction of an infinitesimally small packet of fluid traveling at any point in time. The streamline pattern is therefore an instructive way of visualizing the nature of fluid flow and is similar to what one would observe in a flow visualization using a suitable visible tracer such as smoke. By definition, in a steady flow the streamlines do not intersect, because a fluid particle cannot have two different velocities at the same point. Streamline analysis is often employed in representing flows fields in aerosol instruments and samplers.

2.2.3 Mach Number

Equations 2-1 and 2-2 describing the fluid flow are applicable for incompressible flow, that is, the density ρ_f of the fluid is constant over space and time. However, when the gas velocity, U, is high relative to the sound velocity, U_{sonic}, in that gas, the flow becomes compressible. The degree of compression depends on the *Mach number*, *Ma*, defined as,

$$Ma = \frac{U}{U_{sonic}} \qquad \text{(Eq. 2-6)}$$

When $Ma \ll 1$, the flow is considered incompressible. This is the case in most aerosol instruments and samplers. In air, the sonic or sound velocity at ambient temperature is about 340 m/s (1100 ft/s).

2.2.4 Laminar and Turbulent Flow

Continuum gas flow is described either as laminar or turbulent, depending on the relative importance of viscous and inertial forces. When friction forces dominate the flow, that is, at low Reynolds numbers, the flow is said to be *laminar* and is "smooth." The gas flows in parallel layers and there is no intermixing or disruption between the layers. As the Reynolds number increases, the inertial forces dominate and streamlines begin to loop back on themselves until, at higher Reynolds numbers, the flow becomes chaotic, or *turbulent*. Turbulence causes the formation of eddies of many different length scales. The actual values of the Reynolds number for onset of turbulence depend on how the gas flow is bounded. For instance, laminar flow occurs in a circular duct when the flow Reynolds number is less than about 2000, while turbulent flow occurs for Reynolds numbers above 4000. In the intermediate range, the flow is called the *transition flow*, and is sensitive to the previous history of the gas motion. For instance, if the gas velocity is increased into this transition range slowly, the flow may remain laminar. When a gas passes around a suspended object, such as a sphere, flow is laminar for particle Reynolds numbers below about 0.1. Laminar flow at very small Reynolds number $\ll 1$, which is the case with most aerosol particles, is called *creeping flow*.

Since it is often expensive and difficult to test collection and measurement systems at full scale and *in situ*, small-scale water (or other liquid) models operating at the same Reynolds number as the system being studied are a useful alternative. Dye injection into the flow stream allows visualization of the streamlines. Such models can operate on a smaller physical scale with a slower time response, so that it is easy to observe the time evolution of flow patterns. The same technique can be used to model the behavior of particles.

EXAMPLE 2-1

Silica particles of 10 μm diameter are removed by a 0.30 m diameter ventilation duct at 20 m/s. Assuming that the gravitational settling velocity of this particle is 1 cm/s [0.01 m/s], calculate the flow and particle Reynolds numbers at 293 K [20 °C].

Answer: The relevant parameters for the flow Reynolds number are the duct diameter and the air flow velocity in the duct (from Eq. 2-5).

$$Re_f = 65{,}000V \cdot d = 65{,}000 \left(20 \frac{\text{m}}{\text{s}}\right) 0.30\,\text{m} = 3.90 \times 10^5$$

The relevant parameters for the particle Reynolds number are the particle diameter and the gravitational settling velocity perpendicular to the gas flow.

$$Re_p = 65{,}000V \cdot d = 65{,}000 \left(0.01 \frac{\text{m}}{\text{s}}\right) 10 \times 10^{-6}\,\text{m}$$
$$= 6.5 \times 10^{-3}$$

The flow Reynolds number exceeds 4000, indicating turbulent flow in the ventilation duct. The particle Reynolds number is less than one, indicating the flow around the particle can be laminar. However, it is not in this case because the gas flow is turbulent.

2.2.5 Boundary Layer

A boundary layer in a flow is defined as a region near a boundary, usually a solid surface, where the influence of fluid viscosity is particularly important. The fluid velocity must fall to zero at the boundary itself. When flow starts along a surface, either in time or space, the boundary layer consists only of the gas at the surface, where the relative velocity is zero. At low Reynolds numbers, the boundary layer grows until steady state conditions are reached. For the circular duct example above, the boundary layer grows into a parabolic flow profile that fills the cylindrical duct. At higher Reynolds numbers (in the turbulent regime) or during abrupt changes in flow conditions, the boundary layer can become separated from the surface. The development of the boundary layer and its relationship to the overall flow depends on the object immersed in the fluid. Many excellent texts are available on this topic (see e.g. Schlicting 1979; White 1986).

2.2.6 Stagnation Flow

Stagnation occurs when all of the kinetic energy of the fluid is converted into static pressure such that the local fluid velocity, at the *stagnation point*, is zero. This is where the static pressure is highest. This usually occurs when there is a flow past a bluff body, for example, flow past an impactor stage. Stagnation occurs at the surface of the bluff body, at points where a streamline intersects with the body. It is a particularly

important concept in describing the flow near an aerosol inlet or a sampler.

2.2.7 Poiseuille Flow

Many instrument systems use cylindrical tubing to transport the aerosol from one place to the other. Understanding the flow patterns within the tubing is important for predicting the particle loss that occurs within the tubing as well as predicting the distribution of particles within the tubing. If a gas begins to flow in a cylindrical tube, the friction at the wall slows the gas velocity relative to the motion in the center of the tube. At low Reynolds numbers, the dominating friction force produces a characteristic laminar parabolic velocity profile. The gas velocity in the center of the tube for this *Poiseuille flow* is twice that of the average velocity in the tube. Poiseuille flow does not become established immediately. A common rule of thumb is to assume it takes 10 tube diameters for this equilibrium flow to be effectively established.

2.2.8 Flow Through Bends, Constrictions, and Expansions

There is a wide variety of flow situations for which empirical or experimentally verified theoretical solutions exist. For instance, when a gas passing through a cylindrical tube under laminar flow conditions negotiates a 90° bend, the cylindrical symmetry of the flow pattern in the tube is reduced to a plane of symmetry. Thus, the flow symmetry must also be reduced. Two circulation patterns, sometimes described as secondary flow to differentiate them from the primary flow along the tube axis, are set up on either side of the plane of the bend as shown in Figure 2-1. This secondary flow causes mixing of the gas as well as increased inertial forces on particles suspended in the gas (Tsai and Pui 1990). In tubing used to transport aerosols, bends are generally undesirable because of increased particle loss.

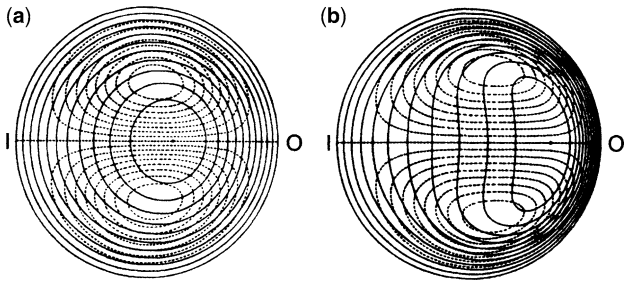

Figure 2-1 Secondary flow streamlines and primary flow velocity contours at a short distance downstream from the exit plane of a 90° bend in a tube. The flows are calculated at two Dean numbers ($De = Re/\sqrt{bend\ radius/tube\ radius}$). **(a)** $De = 17$ and **(b)** $De = 107$. From McConalogue and Srivastava (1968). Reproduced with permission of the Royal Society.

For various reasons, there are often constrictions or expansions in a tube carrying a gas. A constriction will force the gas to increase in velocity and be focused in the center of the tubing. After this contraction region, or *vena contracta*, the gas flow eventually expands again to fill the tubing and reestablishes an equilibrium pattern. These disturbances will also cause increased particle deposition.

When a gas flows from an initial tube diameter into a suddenly expanded section or into free space, the flow pattern may persist for many initial tube diameters downstream. If the expansion of the tube is very slight, the flow does not separate from the walls and the flow pattern can expand smoothly to fill the increased diameter of the tube. In general, the angle between the wall and the tube axis needs to be less than 7° to avoid flow separation from the tube wall.

2.2.9 Gas Density

The density of a gas, ρ_g, is related to its temperature, T, and pressure, P, through the *equation of state*

$$P = \rho_g \frac{R_u}{M} T = \rho_g RT \qquad \text{(Eq. 2-7)}$$

where ρ_g is the gas density ($1.192\ kg/m^3$ [$1.192 \times 10^{-3}\ g/cm^3$] for air at NTP), T is the absolute gas temperature in degrees Kelvin, M is the molecular weight in kg/mol, and R_u is the universal gas constant ($= 8.31\ Pa \cdot m^3/mol \cdot K$ [8.31×10^7 dyne $\cdot$ cm/mol $\cdot$ K]). In air, the effective molecular weight is 0.0289 kg/mol [28.9 g/mol]. Thus, the specific gas constant for air is $R = 288\ Pa \cdot m^3/kg \cdot K$ [2.88×10^6 dyne $\cdot$ cm/g $\cdot$ K]. One atmosphere equals 101 kPascal, where $1\ Pa = 1\ N/m^2 = 10\ dyne/cm^2$.

2.2.10 Viscosity

Gas viscosity is primarily due to the momentum transfer that occurs during molecular collisions. These frequent and rapid collisions tend to damp out differences in bulk gas motion as well as impede the net motion of particles relative to the gas. Thus, the mobility of a particle in a force field depends on the aerodynamic drag exerted on the particle through the gas viscosity. Fluid dynamic similitude, as expressed by Reynolds number, depends on gas viscosity η. Therefore, knowledge of the gas viscosity is important when dealing with aerosol particle mechanics. The viscosity can be related to a reference viscosity η_r and a reference temperature, T_r, as follows:

$$\eta = \eta_r \left(\frac{T_t + S_u}{T + S_u}\right) \left(\frac{T}{T_r}\right)^{3/2} \qquad \text{(Eq. 2-8)}$$

where S_u is the Sutherland interpolation constant (Schlichting 1979). Note that viscosity is independent of pressure.

TABLE 2-1 Properties for Several Gases at NTP (293.15 K and 101.3 kPa)

Gas	η (10^{-6} Pa · s)	S_u (K)	ρ_g (kg/m^3)	λ (μm)
Air	18.203	110.4	1.205	0.0665
Ar	22.292	141.4	1.662	0.0694
He	19.571	73.8	0.167	0.192
H_2	8.799	66.7	0.835	0.123
CH_4	10.977	173.7	0.668	0.0537
C_2H_6	9.249	223.2	1.264	0.0328
i-C_4H_{10}	7.433	255.0	2.431	0.0190
N_2O	14.646	241.0	1.837	0.0433
CO_2	14.673	220.5	1.842	0.0432

Source: Adapted from Rader (1990).

In SI units, viscosity is expressed in Pa · s. In cgs units, viscosity is expressed in dyne-s/cm^2, also referred to as poise or P. For air at 293 K, the viscosity is 1.833×10^{-5} Pa · s [183.3 μpoise] and S = 110.4 K. The interpolation formula is fitted to the data over the range 180–2000 K (Schlichting 1979). Reference values of viscosity and Sutherland constants for other gases are presented in Table 2-1.

2.3 SLIP FLOW REGIME

As noted earlier, the continuum flow description ignores the discrete molecular nature of the fluid when describing its own properties and its influence on the particle. Aerosol particles, large or small, are constantly bombarded from all directions by a great number of gas molecules. When a particle is much larger than the mean distance between the two molecules in the surrounding gas, the flow can be described as a continuum flow. However, as the particle size becomes smaller, below about 1 μm, the individual collisions have relatively greater influence on a particle's motion. In the extreme case where the particle size is smaller than the mean distance between the molecules, called *mean free path*, the particle can *slip* through the vacuum that exists between the molecules before colliding with another molecule in its path. This is called *slip flow regime* and can occur in any aerosol system for small particles at atmospheric pressure or, for larger particles where local static pressures are significantly lower than atmospheric. A dimensionless parameter called the *Knudsen number* is used to describe continuum and slip flow regimes and is defined below.

2.3.1 Gas Mean Free Path

The *average velocity of a molecule*, $\overline{V}$, is a function of its molecular weight, M, and the gas temperature, T. In air ($M_{air} = 0.0289$ kg/mol) at normal temperature and pressure (NTP: 20 °C, 1 atm), this molecular velocity is 463 m/s. Using these reference values for air, the average velocity can be estimated for other gases and temperatures as follows.

$$\overline{V} = \overline{V}_r \left(\frac{T}{T_r}\right)^{1/2} \left(\frac{M_r}{M}\right)^{1/2} \qquad \text{(Eq. 2-9)}$$

Mean free path, λ, is the mean distance a molecule travels before colliding with another molecule. In air at 293 K and atmospheric pressure, the mean free path, λ_r, is 0.0664 μm. The mean free path is an abstraction that is determined from a kinetic theory model that relates it to the coefficient of viscosity. Using these reference values, λ is determined for other pressures and temperatures (Willeke 1976).

$$\lambda = \lambda_r \left(\frac{101}{P}\right)\left(\frac{T}{293}\right)\left(\frac{1 + 110/293}{1 + 110/T}\right) \qquad \text{(Eq. 2-10)}$$

where P is in kPa and T in K. If the unit of atmosphere is used for pressure, the factor of 101 used in Equation 2-10 is substituted by one. The factor of 110 (K) is the Sutherland constant and the value changes for different gases. The mean free path and the average molecular velocity are parameters that are frequently used to predict bulk properties of a gas, such as thermal conductivity, diffusion, and viscosity. Mean free paths for other gases are presented in Table 2-1.

2.3.2 Knudsen Number

The *Knudsen number*, *Kn*, relates the gas molecular mean free path to the physical dimension of the particle, usually the *particle radius*, r_p.

$$Kn = \frac{\lambda}{r_p} = \frac{2\lambda}{d_p} \qquad \text{(Eq. 2-11)}$$

where d_p is the physical diameter of the particle. The Knudsen number is somewhat counterintuitive as an indicator of particle size since it has inverse size dependence. $Kn \ll 1$ indicates continuum flow and $Kn \gg 1$ indicates free molecular flow. The intermediate range, approximately $Kn = 0.4$ to 20, is usually referred to as the transition or slip flow regime.

2.4 DRAG FORCE AND MOBILITY

2.4.1 Continuum Regime

Drag force, sometimes called air resistance, refers to the force that opposes the relative motion of a particle in air or gas. Drag force is induced by the motion of the particle, and acts in the opposite direction of motion. It is a function of a particle's velocity with respect to the gas surrounding it.

Drag force can be obtained by solution of Navier–Stokes equations (Eqs. 2-1 and 2-2) for a particle moving in air by

using appropriate boundary conditions. Stokes, in 1851, solved the above set of equations by assuming that the inertial force term on the left side of Equation 2-1 is negligible (i.e., $Re \ll 1$ in Eq. 2-3) and obtained the following expression, now widely known as Stokes' law:

$$F_{\text{drag}} = 3\pi\eta V d_{\text{p}} \qquad \text{(Eq. 2-12)}$$

where V is the particle velocity with respect to gas, and d_{p} is particle diameter. Externally applied forces on an aerosol particle are opposed and rapidly balanced by the aerodynamic drag force. An example of this is a skydiver: the gravitational force pulling the skydiver toward the earth is eventually balanced by the air resistance, and the diver reaches a final falling speed of about 63 m/s (140 miles/hour).

Derivation of Equation 2-12 assumes that the particle is spherical. The particle drag for shapes other than spheres is usually difficult to predict theoretically. Therefore, for particles of other shapes, a *dynamic shape factor* χ is introduced that relates the motion of the particle under consideration to that of a spherical particle

$$F_{\text{drag}} = 3\pi\eta V \chi d_{\text{v}} \qquad \text{(Eq. 2-13)}$$

where d_{v} is the *volume equivalent diameter* defined as the diameter of a sphere composed of the particle bulk material with no voids that has the same mass as the particle in question. The shape factor is sometimes related to the *mass equivalent diameter*, d_{m}, defined as the diameter of a sphere of equivalent mass. When the equivalent volume is composed of particle bulk material with no void, $d_{\text{v}} = d_{\text{m}}$. However, if the material includes internal voids, $d_{\text{v}} > d_{\text{m}}$. If we determine the shape factors and equivalent diameters for particles that we wish to measure, the behavior of the particles can be predicted when they are influenced by various force fields, for example, gravity or electrostatic.

2.4.2 Slip Regime

The continuum regime ($Kn \ll 1$) drag force F_{drag} is given by Equation 2-12 above. However, in slip regime ($Kn \gg 1$), the particle can *slip* through the space between the molecules before colliding with another molecule or object in its path. This effectively leads to increased velocity of the particle, and reduced drag force compared to that predicted by the Stokes' law. To accommodate for this difference, a correction, C_{c}, known as *slip correction factor*, is introduced. An empirical fit to air data for particles gives the following equation (Allen and Raabe 1985).

$$C_{\text{c}} = 1 + Kn[\alpha + \beta \exp(-\gamma/Kn)] \qquad \text{(Eq. 2-14)}$$

Various values for α, β, and γ have been reported. However, it is important to use the mean free path with which these constants were determined. The value of λ used in Equation 2-11 should also be consistent with the derivation of the slip coefficient constants. The following constants are consistent with $\lambda_{\text{r}} = 0.0664$ μm at NTP. For solid particles, $\alpha = 1.142$; $\beta = 0.558$; $\gamma = 0.999$ (Allen and Raabe 1985). For oil droplets, $\alpha = 1.207$; $\beta = 0.440$; $\gamma = 0.596$ (Rader 1990). C_{c} for other gases such as CO_2 and He are similar within a few percent. The slip correction and viscosity values are better determined than most other aerosol-related parameters and are therefore reported with a higher degree of precision.

For pressures other than atmospheric, the slip correction changes because of the pressure dependence of mean free path on Kn and the following may be used for solid particles:

$$C_{\text{c}} = 1 + \frac{1}{P\, d_{\text{p}}}[15.60 + 7.00 \exp(-0.059\, P\, d_{\text{p}})] \qquad \text{(Eq. 2-15)}$$

where P is the absolute pressure in kPa and d_{p} is the particle diameter in μm (Hinds 1999).

C_{c} is greater than 1 in molecular and transition regime, and approaches the value of 1 in the continuum regime. For instance, $C_{\text{c}} = 1.02$ for 10-μm particles; 1.15 for 1-μm particles, and 2.9 for 0.1-μm particles. Note that the shape factor and the slip correction must be consistent with the type of equivalent diameter used in the same equation; see Chapter 23 for further details.

Using the slip correction factor, modified drag force on the particle in slip regime can be expressed as,

$$F_{\text{drag}} = \frac{3\pi\eta V \chi\, d_{\text{v}}}{C_{\text{c}}} \qquad \text{(Eq. 2-16)}$$

2.4.3 Drag Coefficient

Drag force given by Stokes' law in Equation 2-12 is applicable for $Re_{\text{p}} < 0.1$, known as *Stokes regime*. At higher Re_{p}, inertial forces dominate, and the actual drag is more than that predicted by the Stokes' law. A general expression for the drag force, which modifies Stokes drag, can be written as follows,

$$F_{\text{drag}} = \frac{\pi}{8} C_{\text{d}} \rho_{\text{g}} V^2 d_{\text{p}}^2 \qquad \text{(Eq. 2-17)}$$

where, C_{d} is known as *drag coefficient* and relates the drag force to the velocity pressure,

$$C_{\text{d}} = \frac{F_{\text{drag}}/\text{area}}{\frac{1}{2}\rho_{\text{g}} V^2}$$

Thus drag coefficient, C_{d}, for a spherical particle is the ratio of the resistance pressure due to aerodynamic drag (drag

force/cross-sectional area) to the velocity pressure of the flow toward the sphere (based on the relative velocity between the particle and the suspending gas). When the inertial force pushing the gas aside is much smaller than the viscous resistance force, that is, $Re_p < 0.1$, the drag coefficient, C_d, is expressed in terms of gas flow parameters

$$C_d = \frac{24}{Re_p} \quad Re_p < 0.1 \qquad \text{(Eq. 2-18)}$$

This relationship is accurate within 1% in the Re_p range indicated. If 10% accuracy is acceptable, Equation 2-18 can be used up to $Re_p < 1.0$.

For larger Re_p, empirical relationships for C_d have been developed to extend Stokes' law beyond Stokes regime. Figure 2-2 shows the relationship of the drag coefficient to particle Reynolds number over a wide range of Reynolds numbers.

For Re_p above 0.1, Sartor and Abbott (1975) developed the following empirical relationship:

$$C_d = \frac{24}{Re_p}(1 + 0.0196\,Re_p) \quad 0.1 \le Re_p < 5 \qquad \text{(Eq. 2-19)}$$

and Serafini (Friedlander 1977, p. 105) obtained the following relationship:

$$C_d = \frac{24}{Re_p}(1 + 0.158\,Re_p^{2/3}) \quad 5 \le Re_p < 1000 \qquad \text{(Eq. 2-20)}$$

Note that these relationships have been derived from data taken with smooth spheres. Similar relationships have been derived and reviewed for particles such as droplets, solid spheroids, disks and cylinders (Clift et al. 1978, p. 142). Typically, Re_p is based on the equatorial diameter for disks and spheroids and on the cylinder diameter for cylinders, though other definitions can be used. Particles with extreme shapes may have a significantly different drag coefficient.

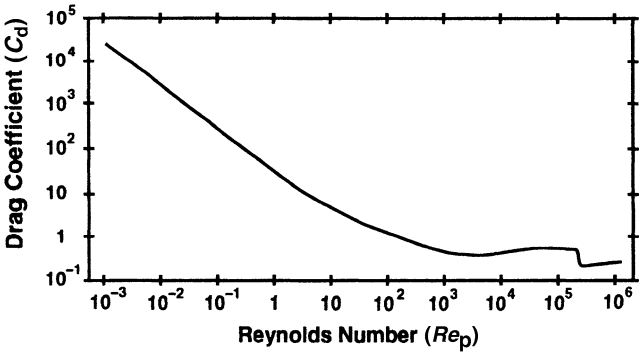

Figure 2-2 Drag coefficient as a function of particle Reynolds number for spherical particles.

For instance, C_d for fibers is up to four times lower than for spheres with $Re_p < 100$ when the fiber diameter is used as the characteristic dimension in the Reynolds number expression, Equation 2-4.

Thus, by using the appropriate form of the drag coefficient (Eqs. 2-18, 2-19, or 2-20) and including the shape factor and slip coefficient, the drag force can be calculated over a wide range of particles and conditions

$$F_{drag} = \frac{\pi C_d \rho_g V^2 \chi^2 d_v^2}{8 C_c} \qquad \text{(Eq. 2-21)}$$

2.4.4 Mechanical Mobility

Another important quantity often used in describing particle motion is its *mechanical mobility*, B, defined as the velocity produced by a unit force on the particle, and mathematically defined as,

$$B = \frac{C_c}{3\pi\eta d_p} \qquad \text{(Eq. 2-22)}$$

Units of B are $m/N \cdot s$ [$cm/dyne \cdot s$]. B is a convenient aerosol property that combines particle size with some of the properties of the suspending gas. Inverse of mobility B, called friction coefficient f, has also been used in the literature. The friction coefficient should not be confused with drag coefficient C_d described earlier.

2.5 BROWNIAN DIFFUSION

The random movement of gas molecules causes gas and particle diffusion if there is a concentration gradient. For instance, in a diffusion denuder, SO_2 gas molecules may diffuse to an absorbing surface due to their high diffusivity. Sulfate particles, which are larger and therefore have lower diffusivity, will mostly be transported through the device. Thus, the SO_2 gas molecules are separated from the sulfate particles.

2.5.1 Molecular Diffusion

Diffusion always causes net movement from a higher concentration to a lower one. The *net flux* of gas molecules, J, is in the direction of lower concentration. Thus, in simple one-dimensional diffusion,

$$J = -D\frac{\partial C_g}{\partial x} \qquad \text{(Eq. 2-23)}$$

where x is the direction of diffusion, C_g is the concentration, and D is a proportionality constant referred to as the *diffusion coefficient*. The diffusion coefficient for a gas with molecular

weight, M, is (Hinds 1999, p. 27)

$$D = \left(\frac{3\sqrt{2}\pi}{64 C_g d_{molec}^2}\right)\left(\frac{RT}{M}\right)^{1/2} \qquad \text{(Eq. 2-24)}$$

where C_g is the number of gas molecules/m^3 and d_{mole}^2 is the molecular collision diameter (3.7×10^{-10} m for air). The diffusion coefficient of "air" molecules at 293 K is 1.8×10^{-5} m^2/s. The above equation predicts a diffusion coefficient that is approximately 10% below the correct value (Hinds 1999, p. 27).

2.5.2 Particle Diffusion

Small particles can achieve significant diffusive motion in much the same manner as that described for gas molecules. The difference is only in the particle size and shape. Because of their large inertia and large surface area over which the bombardment by the gas molecules is averaged, large particles diffuse more slowly than small particles. For particles in a gas, the *diffusion coefficient* or *diffusivity*, D, can be computed by

$$D = \frac{kTC_c}{3\pi\eta d_p} = kTB \qquad \text{(Eq. 2-25)}$$

where k, the Boltzmann constant, is 1.38×10^{-23} N · m/K [1.38×10^{-16} dyne · cm/K] and B is the mechanical mobility defined earlier.

Particle diffusion, also referred to as *Brownian motion*, occurs because of the relatively high velocity of small particles and it is sometimes useful to estimate how far, on the average, these particles move in a given time. The *root mean square (rms) distance*, x_{rms}, that the particles can travel in time, t, is

$$x_{rms} = \sqrt{2Dt} \qquad \text{(Eq. 2-26)}$$

Table 2-2 shows x_{rms} for particles of various size after a period of 10 s.

EXAMPLE 2-2

Aerosol particles of 0.01-μm diameter are drawn into the deep lung regions of a person breathing them whose alveoli can be approximated by 0.2 mm diameter spheres. Estimate if these particles are likely to deposit in this area of the lung during a breath-hold period of 4 s. Assume body temperature is 330 K [37 °C].

Answer: We note that calculation of x_{rms} (Eq. 2-26) requires knowledge of the diffusion coefficient, which in turn requires the slip correction factor and viscosity. To simplify the calculation, let us assume for the moment that the diffusion is taking place at room temperature. Thus, the air viscosity is 183 μpoise and the mean free path is 0.0665 μm. (For a more accurate estimate of these parameters at body temperature use Equations 2-8 and 2-10, respectively.)

The slip correction factor can be determined from Equation 2-14 using constants for solid particles

$$C_c = 1 + Kn[1.142 + 0.558\ \exp(-0.999/Kn)]$$

$$C_c = 1 + \frac{2 \cdot 0.0665\ \mu m}{0.01\ \mu m} \times \left[1.142 + 0.558 \exp\left(-0.999 \frac{0.01\ \mu m}{2 \cdot 0.0665\ \mu m}\right)\right] = 23.1$$

We then estimate the diffusion coefficient, using Equation 2-25.

$$D = \frac{kTC_c}{3\pi\eta d_p}$$

$$D = \frac{\left(1.38 \times 10^{-23} \frac{N \cdot m}{K}\right)(293\ K)(23.1)}{3 \cdot 3.14 \cdot (1.84 \times 10^{-5}\ Pa \cdot s)\left(0.01\ \mu m \times 10^{-6} \frac{m}{\mu m}\right)}$$

$$= 5.45 \times 10^{-8} \frac{m^2}{s}$$

$$\left[D = \frac{\left(1.38 \times 10^{-16} \frac{dyne \times cm}{K}\right)(293\ K)(23.1)}{3 \cdot 3.14 \cdot (1.84 \times 10^{-4}\ poise)\left(0.01\ \mu m \times 10^{-4} \frac{cm}{\mu m}\right)}\right.$$

$$\left. = 5.45 \times 10^{-4} \frac{cm^2}{s}\right]$$

Finally, using Equation 2-26

$$x_{rms} = \sqrt{2Dt} = \sqrt{2\left(5.45 \times 10^{-8} \frac{m^2}{s}\right)(4\ s)}$$

$$= 6.60 \times 10^{-4}\ m\ [0.0660\ cm] = 0.660\ mm$$

we find that at room temperature, the *rms* displacement by diffusion is much larger than the alveolar size. At the elevated temperature in the lung (37° C) the particles are expected to move faster and diffuse further. If this air temperature is used in the calculation of the diffusion coefficient, x_{rms} is 0.675 mm. Thus, we know that most of these particles are likely to be collected in the alveolar space of the lung. A more exact analysis can be made by considering such factors as the spherical geometry of the alveoli, the location of the particles within the alveoli, and the air temperature.

When the air temperature dependence is also included in the calculation of viscosity and mean free path, the *rms* displacement calculation results in 0.661 mm.

2.5.3 Péclet Number

The amount of convective transport of particles toward an object may be related to the diffusive transport through the

TABLE 2-2 Particle Parameters for Unit Density Particles at NTP

Particle Diameter, d_p (μm)	Slip Correction Factor, C_c	Settling Velocity, V_{grav} (m/s)	Relaxation Time, τ (s)	Stopping Distance, S $V_0 = 10$ m/s (m)	Mobility, B (m/N · s)	Diffusion Coefficient, D (m^2/s)	rms Brownian Displacement in 10 s (m)
0.00037[a]			2.6×10^{-10}	2.5×10^{-9}	9.7×10^{15}	1.8×10^{-5}[b]	2.8×10^{-2}
0.01	23.04	6.95×10^{-8}	7.1×10^{-9}	7.1×10^{-8}	1.4×10^{13}	5.5×10^{-8}	1.0×10^{-3}
0.1	2.866	8.65×10^{-7}	8.8×10^{-8}	8.8×10^{-7}	1.7×10^{11}	6.8×10^{-10}	1.2×10^{-4}
1	1.152	3.48×10^{-5}	3.5×10^{-6}	3.5×10^{-5}	6.8×10^{9}	2.7×10^{-11}	2.3×10^{-5}
10	1.015	3.06×10^{-3}	2.3×10^{-4}	2.3×10^{-3}	6.0×10^{8}	2.4×10^{-12}	7.0×10^{-6}
100	1.002	2.61×10^{-1}	1.3×10^{-2}	0.13	5.9×10^{7}	2.4×10^{-13}	2.2×10^{-6}

[a]Average diameter of a molecule in air.
[b]Calculated using Equation 2-24.

dimensionless *Péclet number*, *Pe*,

$$Pe = \frac{Ud_c}{D} \qquad \text{(Eq. 2-27)}$$

where d_c is the significant dimension of the particle collecting surface and U is the upstream gas velocity toward the surface. The larger the value of *Pe*, the less important is the diffusional process (Licht 1988, p. 226). *Pe* is often used in the description of diffusional deposition on filters. For further discussion of diffusion in the context of aerosol instrumentation, see Chapters 6, 7, 15, 16, and 32.

2.5.4 Schmidt Number

The ratio of the Péclet number, Equation 2-27, to the Reynolds number, Equation 2-4, is referred to as the *Schmidt number*, *Sc*. It expresses the ratio of kinematic viscosity to diffusion coefficient.

$$Sc = \frac{\eta_g}{\rho_g D} = \frac{\nu}{D} \qquad \text{(Eq. 2-28)}$$

As the Schmidt number increases, convective mass transfer increases relative to Brownian diffusion of particles. It has been used for describing diffusive transport in flowing fluids (convective diffusion), especially in the development of filtration theory (Friedlander 1977). *Sc* is relatively independent of temperature and pressure near standard conditions.

2.6 PARTICLE MIGRATION IN EXTERNAL FORCE FIELDS

2.6.1 Migration in Gravitational Force Field

The *gravitational force*, F_{grav}, is proportional to particle mass, m_p, and gravitational acceleration, g,

$$F_{grav} = m_p g = (\rho_p - \rho_g) v_p g \approx \rho_p v_p g \qquad \text{(Eq. 2-29)}$$

where ρ_g is the gas density. The gravitational pull depends on the difference between the density of the particle and that of the surrounding medium. For a particle in water, this buoyancy effect is significant. For a particle in air, the buoyancy effect can be neglected for compact particles, since the particle density is generally much greater than the density of the gas. If the particle is spherical, particle volume v_p can be replaced with $\pi d_p^3/6$

$$F_{grav} = \frac{\pi}{6} d_p^3 \rho_g g \qquad \text{(Eq. 2-30)}$$

The gravitational field of the earth was mentioned in the previous chapter. This field exerts a force pulling a particle down. As the particle begins to move, the gas surrounding the particle exerts an opposing drag force, which, after a short period of acceleration, equals the gravitational force and the particle reaches its terminal settling velocity. By equating the drag force, Equation 2-17 (with slip correction factor C_c added), to the gravitational force, Equation 2-30, and using Equation 2-18 for C_d and Equation 2-4 for Re_p, the following relationship is obtained for the spherical particle settling velocity, V_{grav}, in the Stokes regime,

$$V_{grav} = V_{ts} = \frac{\rho_p d_p^2 g\, C_c}{18\eta} \quad Re_p < 0.1 \qquad \text{(Eq. 2-31)}$$

To reflect the equilibrium between the two opposing forces, this velocity is also referred to as *terminal settling velocity*, V_{ts}. For spherical particles with negligible slip ($C_c = 1$) and $1 < d_p < 100$, this equation reduces to the following at NTP

$$V_{grav} \cong 3 \times 10^{-8} \rho_p d_p^2 \qquad [V_{grav} \cong 0.003 \rho_p d_p^2] \qquad \text{(Eq. 2-32)}$$

where ρ_p is in kg/m^3 [g/cm^3] and d_p is in μm. Spherical particles, for example, droplets, are common in nature and their motion can be described mathematically. Therefore,

the behavior of nonspherical particles is often referenced to spherical particles through comparison of their behavior in a gravitational field.

EXAMPLE 2-3

An open-faced filter cassette samples at 2 L/min (3.33×10^{-5} m^3/s [33.3 cm^3/s]) over its inlet face of about 35 mm diameter. If the cassette is held facing downward, can a 25 μm diameter particle with a density of 3000 kg/m^3 [3 g/cm^3] be drawn upward onto the filter in calm air?

Answer: The cassette samples at a flow rate Q over a cross-sectional filter area A. The upward air velocity, U, is

$$U = \frac{Q}{A} = \frac{3.33 \times 10^{-5}\,\mathrm{m^3/s}}{\pi\left(\frac{0.035\,\mathrm{m}}{2}\right)^2} = 0.0346\,\mathrm{m/s}\,[3.46\,\mathrm{cm/s}]$$

The gravitational settling velocity of the 25 μm particle is, from Equation 2-32

$$V_{grav} = 3 \times 10^{-8}\rho_p d_p^2 = 3 \times 10^{-8}\left(3000\frac{\mathrm{kg}}{\mathrm{m^3}}\right)\left(25\,\mu\mathrm{m}\cdot 10^{-6}\frac{\mathrm{m}}{\mu\mathrm{m}}\right)^2$$

$$\left[V_{grav} = 0.003\,\rho_p d_p^2 = 0.003\left(3\frac{\mathrm{g}}{\mathrm{cm^3}}\right)(0.0025\,\mathrm{cm})^2\right]$$

$$= 0.0563\,\mathrm{m/s}\,[5.63\,\mathrm{cm/s}] > 0.0346\,\mathrm{m/s}\,[3.46\,\mathrm{cm/s}]$$

The particle cannot be drawn upward into the sampler.

This is also the principle of a vertical elutriator, which prevents particles above a certain size from passing through the device. However, in some implementations of this device, for example, the cotton dust elutriator, inlet effects complicate the penetration efficiency.

A number of instruments, including the horizontal and the vertical elutriators (Chapters 6 and 8), use settling velocity to separate particles according to size. For instance, aerosol particles of a certain size, d_p, initially spread throughout a quiescent rectangular chamber or room of height H_c, will settle at a constant velocity, V_{grav}. After some time, t, the particle concentration in the chamber, $N(t)$, will be

$$N(t) = N_0\left(1 - \frac{V_{grav}t}{H_c}\right) \qquad \text{(Eq. 2-33)}$$

where N_0 is the initial particle concentration in the chamber. After time t, a vertical distance of $V_{grav} \cdot t$ is cleared of particles. The same relationship determines the concentration of particles in a rectangular channel with air flowing through it (a horizontal elutriator). At some distance downstream of the entrance to the channel where the aerosol concentration is N_0, the concentration will be $N(t)$, where t is the time needed to reach that distance.

The above discussion of particle settling describes the behavior of particles in still air, a condition that is not often achieved in the environment or even in the laboratory. When the gas in a container undergoes continual and random motion, such as in a room with several randomly directed fans, the particles undergo *stirred settling*. The time-dependent concentration, $N(t)$, under these conditions is also expressed in terms of an initial particle concentration, N_0, the gravitational settling velocity in still air, V_{grav}, and the height of the container, H_c.

$$N(t) = N_0 \exp\left(\frac{-V_{grav}t}{H_c}\right) \qquad \text{(Eq. 2-34)}$$

This equation applies to any container shape with vertical walls and a horizontal bottom. This indicates that even under stirred or turbulent conditions larger particles (higher settling velocities) will settle out more rapidly than smaller particles, even though some of the large particles may persist in the air for a long time because of the exponential decay. Note that the forms of Equations 2-33 and 2-34 are similar except for the exponential decay when stirring takes place during settling. This similarity in form occurs for all such comparisons of uniform and stirred settling.

2.6.1.1 Aerodynamic and Stokes Diameter The *aerodynamic diameter*, d_a, of a particle is the diameter of a standard-density ($\rho_0 = 1000\,\mathrm{kg/m^3}$) sphere that has the same gravitational settling velocity as the particle in question, and is given by,

$$d_a = d_p\left(\frac{\rho_p}{\rho_0}\right)^{1/2} \qquad \text{(Eq. 2-35)}$$

Thus, aerodynamic diameter standardizes shape (spherical) and density (standard density) of aerosol particles, and allows comparison of settling behavior of particles of various shapes and densities using a single measure. It is the most commonly used diameter, particularly in applications involving particle deposition in respiratory systems.

EXAMPLE 2-4

What is the aerodynamic diameter of a spherical particle that is 3 μm in diameter and has a particle density of 4000 kg/m^3 [4 g/cm^3]? Ignore the slip correction factors.

Answer: From Equation 2-35

$$d_a = d_p\left(\frac{\rho_p}{\rho_0}\right)^{1/2} = 3\,\mu\mathrm{m}\left(\frac{4000}{1000}\right)^{1/2} = 6\,\mu\mathrm{m}$$

This indicates that a 6 μm standard-density particle gravitationally settles at the same velocity as the 3 μm particle with the higher density.

Another definition that is also commonly used is the *Stokes diameter*, d_s, which is the diameter of a spherical particle with the same density and gravitational settling velocity as the particle in question. The aerodynamic diameter can be related to the Stokes diameter through the settling velocity equation

$$\rho_p d_s^2 = \rho_0 d_a^2 \qquad \text{(Eq. 2-36)}$$

2.6.1.2 Relaxation Time and Stopping Distance Using the Stokes settling velocity relationship (Eq. 2-31), several useful particle parameters can be defined. The first is the *particle relaxation time*

$$\tau = \frac{\rho_p d_p^2 C_c}{18\eta} \qquad \text{(Eq. 2-37)}$$

This is the time a particle takes to reach $(1-1/e)$ or 0.63 of its final velocity when subjected to an external force field (i.e. gravity in the above equation). The relaxation time of a particle indicates how quickly a particle adjusts to transient force conditions. It has units of time. The relaxation time is typically quite short as indicated in Table 2-2. Use of this parameter simplifies the expression for *gravitational settling velocity* to

$$V_{grav} = \tau g \qquad \text{(Eq. 2-38)}$$

Quite often, a particle, rather than starting from rest in a gravitational field, is injected into the air with an initial velocity, V_0. For instance, such a particle might be released from a rotating grinding wheel. The product of the relaxation time and the initial particle velocity is referred to as the *stopping distance*, S

$$S = V_0 \tau \qquad \text{(Eq. 2-39)}$$

where S has units of distance. Values of S for an initial velocity of 10 m/s are given in Table 2-2. The concept of stopping distance is useful, for example, in impactors when evaluating how far a particle moves across the air streamlines when the flow makes a right-angle bend.

Since Equation 2-31 is accurate only in the Stokes regime, the following empirical relationship can be used at higher Re_p (Mercer 1973, p. 41)

$$S = \frac{\rho_p d_p}{\rho_g}\left(Re_0^{1/3} - \sqrt{6}\arctan\left(\frac{Re_0^{2/3}}{\sqrt{6}}\right)\right) \quad 1 < Re_p < 400 \qquad \text{(Eq. 2-40)}$$

where Re_0 is the Reynolds number of the particle at the initial velocity.

2.6.1.3 Stokes Number When flow conditions change suddenly, as in case of the particle traveling toward the collection surface of an impactor, the ratio of the stopping distance to a characteristic dimension, d, is defined as the Stokes *number*, *Stk*.

$$Stk = \frac{S}{d} \qquad \text{(Eq. 2-41)}$$

The characteristic dimension depends on the application, for example in fibrous filtration it is the diameter of the fiber; in axisymmetric impaction flow it is the radius or diameter of the impactor nozzle. For a given percent particle removal, the Stokes number value is therefore application specific. For example, the Stokes number of an impactor with one or several identical circular nozzles is

$$Stk = \frac{\rho_p d_p^2 V C_c}{9\eta d_j} \qquad \text{(Eq. 2-42)}$$

where d_j is the impactor jet diameter in meters and V is the particle velocity in the jet. V is assumed to be equal to the gas velocity in the jet. For further discussion of instruments and devices based on inertial forces, see Chapters 6, 7, 8, 12, and 14.

EXAMPLE 2-5

A grinding wheel, used in a machine shop, dislodges many particles and projects them from the contact point toward the receiving hood of the ventilation system. A particle of a certain size and density is projected 1 cm away. How far will a particle of twice this size be projected? Estimate the projected distance when the speed of the grinding wheel is doubled.

Answer: The projected distance is proportional to the stopping distance. From Equations 2-37 and 2-39

$$S = V_0\tau \propto V_0\rho_p d_p^2$$

The stopping distance depends on the square of the particle diameter, so a particle that is two times larger will project four times the distance to 4 cm. At twice the grinding wheel speed, the particle will come off at approximately twice the initial velocity, resulting in a doubling of the distance to 2 cm.

The above stopping distance equation assumes that the particle is in the Stokes regime. If the particle diameter and velocity are such that Re_p is larger than 0.1, the stopping distance will be somewhat less than quadrupled for the larger particle. This is because the drag increases faster with diameter outside the Stokes regime (see Fig. 2-2). Similarly, increasing the initial velocity also increases Re_p and results in somewhat less than doubling of the distance.

2.6.2 Migration in Electric Field

Application of electrostatic forces is particularly effective for submicrometer particles for which gravity forces are weak because of the d_p^3 dependence (Eq. 2-30). On a large scale, removal of aerosols by electrostatic forces is practiced in electrostatic precipitators. In aerosol sampling and measurement instruments, electrostatic forces are applied to precipitate or redirect either all aerosol particles or those in a specific size range.

For a particle with a total charge equal to n times the elementary unit of charge, e, the *electrostatic force*, F_{elec}, in an *electric field* of intensity, E, is

$$F_{elec} = neE \qquad \text{(Eq. 2-43)}$$

EXAMPLE 2-6

A 0.5-μm diameter standard-density particle has been charged with 18 elementary units of charge. Calculate the electrical force on the particle when it passes between two flat parallel plates (e.g., an electrostatic precipitator) located at a distance of 2 cm from each other, with a potential difference of 5 kV across them. Compare the electrical and the gravitational force on the particle.

Answer: The electric field between the plates is

$$E = \left(\frac{5000\,\text{V}}{0.02\,\text{m}}\right) = 2.5 \times 10^5\,\text{V/m}$$

$$\left[E = \left(\frac{5000\,\text{V}}{2\,\text{cm}}\right)\left(\frac{1\,\text{stat V}}{300\,\text{statV}}\right) = 8.33\,\text{statV/cm}\right]$$

Using Equation 2-43

$$F_{elec} = neE = 18(1.6 \times 10^{-19}\,\text{C})(2.5 \times 10^5\,\text{V/m}) = 7.2 \times 10^{-13}\,\text{N}$$

$$[F_{elec} = neE = 18(4.8 \times 10^{-10}\,\text{statC})(8.33\,\text{statV/cm}) = 7.2 \times 10^{-8}\,\text{dyne}]$$

One newton (N) in SI units equals 10^5 dyne in the cgs system of units. Using Equation 2-30:

$$F_{grav} = \frac{\pi}{6} d_p^3 \rho_p g = \frac{\pi}{6}(0.5 \times 10^{-6}\,\text{m})^3(1000\,\text{kg/m}^3)(9.80\,\text{m/s}^2)$$

$$\left[F_{grav} = \frac{\pi}{6}(0.5 \times 10^{-4}\,\text{cm})^3(1\,\text{g/cm}^3)(980\,\text{cm/s}^2)\right]$$

$$= 6.41 \times 10^{-16}\,\text{N}\ [6.41 \times 10^{-11}\,\text{dyne}]$$

Comparing the two forces

$$\frac{F_{elec}}{F_{grav}} = \frac{7.2 \times 10^{-13}\,\text{N}}{6.41 \times 10^{-16}\,\text{N}} = 1120$$

The electric force exceeds the gravity force by over a thousand times.

Electrostatic forces can affect particle motion, and to a certain extent, gas motion as well. These forces can be important during particle generation, transport, and measurement. Depending on the number of charges on a particle and the level of surrounding electric field, the force on that particle can range anywhere from zero to the largest of any force discussed here. If a particle is placed in an electric field described by Equation 2-43, it will reach a terminal velocity, V_{elec}, when the field and drag forces are equal.

$$V_{elec} = \frac{neEC_c}{3\pi\eta d_p} \qquad \text{(Eq. 2-44)}$$

The electronic charge e is 1.602×10^{-19} coulombs (C) [4.803×10^{-10} statcoulombs (statC)]. This terminal or *drift velocity* can also be written in terms of the particle mobility, B,

$$V_{elec} = neEB \qquad \text{(Eq. 2-45)}$$

or, including the electric charge, the *particle electrical mobility*, $Z = neB$,

$$V_{elec} = ZE \qquad \text{(Eq. 2-46)}$$

where the electrical mobility, Z, has units of velocity/electric field or $\text{m}^2/\text{V}\cdot\text{s}$ [$\text{cm}^2/\text{statV}\cdot\text{s}$], that is, unit electrical mobility is a drift velocity of 1 m/s in a 1 V/m field. One statvolt (cgs unit) is equal to 300 volts (V).

EXAMPLE 2-7

Aerosol emissions from a foundry are sampled into an electrostatic precipitator for collection onto an electron microscope grid. A power supply is used to apply a potential of 5000 V across the precipitator with a plate spacing, H, of 0.01 m. The aerosol flows through the precipitator at a uniform velocity of 0.02 m/s. The particles of concern have an electrical mobility of $3.33 \times 10^{-9}\,\text{m}^2/\text{V}\cdot\text{s}$. What is the minimum plate length, L, that will precipitate all of these particles?

Answer: For a potential of 5000 V, the precipitation time, t_e, in the electric field is

$$t_e = \frac{H}{V_{elec}} = \frac{H}{ZE} = \frac{0.01\,\text{m}}{\left(3.33 \times 10^{-9}\,\frac{\text{m}^2}{\text{V}\cdot\text{s}}\right)\left(\frac{5000\,\text{V}}{0.01\,\text{m}}\right)} = 6\,\text{s}$$

In cgs units, the mobility is converted to $0.01\,\text{cm}^2/\text{statV}\cdot\text{s}$ and the spacing is 1 cm.

$$\left[t_e = \frac{1\,\text{cm}}{\left(0.01\,\frac{\text{cm}^2}{\text{statV}\cdot\text{s}}\right)\left(\frac{16.7\,\text{statV}}{1\,\text{cm}}\right)} = 6\,\text{s}\right]$$

The transit time t_t for the air flow at velocity U must equal or exceed this time.

$$t_t = \frac{L}{U} \geq t_e$$

$$L \geq 6\,\text{s}\,(0.02\ \text{m/s}) = 0.12\ \text{m}\ [12\ \text{cm}]$$

The simplest electric field is uniform, for example, between two large parallel plates

$$E = \frac{\Delta V}{x} \qquad \text{(Eq. 2-47)}$$

where x (in SI units) is the distance between the plates and ΔV is the difference in potential (volts). The field between two concentric tubes or between a tube and a concentric wire is also used for electrostatic precipitation. In this case the field is dependent on the radial distance, r, from the axis

$$E = \frac{\Delta V}{r\ \ln(r_o/r_i)} \qquad \text{(Eq. 2-48)}$$

where ΔV is the difference in potential between the outer tube and inner tube (or wire) of radius r_o and r_i, respectively.

In the SI units, the force in newtons (N) on each of two particles with n_1 and n_2 unit charges on them is described by *Coulomb's law*

$$F_{elec} = \frac{n_1 n_2 e^2}{4\pi\varepsilon_0 r^2} = K_E \frac{n_1 n_2 e^2}{r^2} \qquad \text{(Eq. 2-49)}$$

where r in meters is the distance between the particles. The factor K_E, a proportionality constant that depends on the unit system, is 8.988×10^9 in SI units. This equation strictly applies only to point charges. However, it is a good approximation for the force between two particles or a particle at some distance from a charged object such as a sampler and indicates that the force drops off rapidly with distance. Aerosol particles, which typically carry a limited amount of charge because of their small surface area, are generally only affected electrically when they are quite close to another charged particle or close to a charged object.

In cgs units, Equation 2-49 is converted to give the force in dynes (dyne)

$$F_{elec} = \frac{n_1 n_2 e^2}{r^2} \qquad \text{(Eq. 2-50)}$$

where r is in centimeters, the electronic charge is 4.80×10^{-10} statC, and the proportionality constant K_E is unity. For further discussion of charged particle dynamics, see Chapters 15, 18, 19, 20, and 32.

2.6.3 Migration in Other External Force Fields

Particle transport is governed by a variety of other forces. Very small particles approach the behavior of the molecules of the surrounding gas, that is, they diffuse readily and have little inertia; they can be affected by light pressure, acoustic pressure, and thermal pressure. In a similar fashion to gravitational and electrical forces, other forces can be used to cause particle motion and, thus, size-selective measurement. These same forces can also cause particles to be lost rapidly in the sampling inlet or on measurement instrument surfaces. Other forces not mentioned may have some effects but are generally much weaker than the ones mentioned here. For instance, magnetic forces are typically several orders of magnitude smaller than electrostatic forces, but have been used for fiber alignment (Chapter 23).

2.6.3.1 Thermophoresis Particles in a thermal gradient are bombarded more strongly by gas molecules on the hotter side and are therefore forced away from a heat source. Thus, heated surfaces tend to remain clean, while relatively cool surfaces tend to collect particles. This process is called *thermophoresis*, from the Greek "carried by heat." For particles smaller than the mean free path (λ), the thermophoretic velocity, V_{th}, is independent of particle size and is (Waldmann and Schmitt 1966)

$$V_{th} = \frac{0.55\,\eta}{\rho_g}\,\nabla T \quad d_p < l \qquad \text{(Eq. 2-51)}$$

where ∇T is the thermal gradient in K/m. There is a slight increase (on the order of 3%) in the velocity of rough-surfaced particles versus spherical solids or droplets.

For particles larger than λ, the thermophoretic velocity depends on the ratio of the thermal conductivity of the gas to that of the particle and also on the particle size. For large conductive aerosol particles, the thermophoretic velocity may be about 5 times lower than for small, nonconductive ones. To calculate the thermophoretic velocity, the molecular accommodation coefficient (H) is needed.

$$H \cong \left(\frac{1}{1 + 6\,\lambda/d_p}\right)\left(\frac{k_g/k_p + 4.4\,\lambda/d_p}{1 + 2\,k_g/k_p + 8.8\,\lambda/d_p}\right) \qquad \text{(Eq. 2-52)}$$

where k_g and k_p are the thermal conductivities of the gas and particle, respectively. The thermal conductivity of air is 0.026 W/m · K [5.6×10^{-5} cal/cm · s · K], while that for particles ranges from 66.9 W/m · K for a metal (iron) to 0.079 W/m · K for an insulator (asbestos) (Mercer 1973, 166). The thermally induced particle velocity is then (Waldmann and Schmidt 1966)

$$V_{th} = \frac{-3\,\eta\,C_c H}{2\rho_g T}\,\nabla T \quad d_p > \lambda \qquad \text{(Eq. 2-53)}$$

Thermophoresis is relatively independent of particle size over a wide range and has been used for collecting small samples for electron microscopy in thermal precipitators. The sampling rate of these instruments is low because of the difficulty of maintaining a thermal gradient and, thus, thermal precipitators have not been scaled up for large volume use (Chapter 8).

2.6.3.2 Photophoresis Photophoresis is similar to thermophoresis in that particle motion is caused by thermal gradients at the particle surface, except that in this case the heating is caused by light absorption by the particle rather than by an external source. Light incident on a particle may be preferentially absorbed by the side near the light source or, under certain circumstances of weak absorption and focusing, by the far side of the particle. Thus, in the former case the particle will be repelled from the light source while in the latter, called reverse photophoresis, it will be attracted.

2.6.3.3 Electromagnetic Radiation Pressure Electromagnetic radiation can have a direct effect on particle motion by transferring momentum to the particle. Light impinging on a particle can be reflected, refracted, or absorbed. The fraction of momentum transfer from the light beam to the particle depends on the geometric cross section of the particle as well as the average direction of the scattered light. If a significant fraction of the light is absorbed by the particle, photophoresis, as described above, will be more important in deciding particle motion. Radiation pressure has been used to trap particles in focused laser beams and manipulate them for further study.

2.6.3.4 Acoustic Pressure Acoustic waves, either stationary, as in a resonant box, or traveling in open space can be reflected, diffused, or absorbed by particles. Particle motion in an acoustic field includes oscillation in response to the gas motion, circulation in the acoustic field, or net drift in some direction. Such waves have been used to increase particle coagulation or agglomeration, or in other cases, to enhance droplet evaporation or condensation (Hesketh 1977, p. 97). A resonant acoustic system has also been used to measure particle aerodynamic diameter by measuring a particle's ability to oscillate in response to the air motion (Mazumder et al. 1979; Chapter 14).

2.6.3.5 Diffusiophoresis and Stephan Flow When the suspending gas differs in composition from one location to another, diffusion of the gas takes place. This gas diffusion results in suspended particles acquiring a net velocity as a function of the gas diffusion. This phenomenon is known as *diffusiophoresis*. The particles are pushed in the direction of the larger molecule flow. The force is a function of the molecular weight and diffusion coefficients of the diffusing gases and is largely independent of the particle size.

A special case of diffusiophoresis occurs near evaporating or condensing surfaces. A net flow of the gas-vapor mixture away from an evaporating surface is set up that creates a drag on particles. The converse situation holds for a condensing surface, that is, gas and particles will flow toward the surface. This net motion of the gas-vapor mixture is called Stephan (also spelled Stefan) flow and can cause the motion of particles near these surfaces (Fuchs 1964, p. 67). Stephan flow can affect particle collection in industrial scrubbers and scavenging of the environment by growing cloud droplets. To increase particle collection by Stephan flow, the vapor must be supersaturated. Diffusiophoretic velocities are generally only significant for very small particles. For instance, diffusiophoresis of 0.005 to 0.05 μm diameter particles was found to have the following net *deposition velocity*, V_{diff}, toward surfaces condensing water vapor (Goldsmith and May 1966)

$$V_{\text{diff}} = 1.9 \times 10^{-3} \frac{dP}{dx} \qquad \text{(Eq. 2-54)}$$

where the deposition velocity is in m/s and dP/dx is the pressure gradient of the diffusing vapor in Pa/m. Note that in condensing and evaporating droplets, thermophoretic effects can also be important.

2.7 LIST OF SYMBOLS

C_c	Cunningham slip correction factor
B	mechanical mobility
C_d	drag coefficient
C_g	concentration of gas, number of molecules per unit volume
d	characteristic dimension of the object
D	diffusion coefficient or diffusivity
d_a	aerodynamic diameter
d_c	significant dimension of the particle collecting surface
d_j	impactor jet diameter
d_m	mass equivalent diameter
d_{molec}	molecular collision diameter (3.7×10^{-10} m for air)
d_p	physical diameter of the particle
d_s	Stokes diameter
d_v	volume equivalent diameter
E	electric field intensity
e	elementary unit of charge

F_{drag} drag force
F_{elec} electrostatic force
F_{grav} gravitational force
H_c height of the container or chamber (Eq. 2-34)
H molecular accommodation coefficient (Eq. 2-52)
J net flux of gas molecules
k Boltzmann constant
K_E proportionality constant in Coulomb's law
k_g thermal conductivity of the gas
Kn Knudsen number
k_p thermal conductivity of particle
l_c dimensional characteristic quantity for length
M molecular weight in kg/mol
Ma Mach number
N particle concentration
$N(t)$ particle concentration at time t
N_0 initial particle concentration
n number of elementary units of charge
P, p pressure of the gas
Pe Péclet number
r radial distance from the axis (Eq. 2-48)
r distance between the two particles in Coulomb's law (Eq. 2-49)
r_p particle radius (Eq. 2-11)
r_i radius of inner tube
r_o radius of outer tube
R_u universal gas constant
Re Reynolds number
Re_f flow Reynolds number
Re_0 Reynolds number of the particle at the initial velocity
Re_p particle Reynolds number
S_u Sutherland interpolation constant
S stopping distance
Sc Schmidt number
Stk Stokes number
Str Strouhal number
T absolute gas temperature in K
∇T thermal gradient
t_c dimensional characteristic quantity for time
T_r reference temperature
U dimensional characteristic quantity for velocity
$\mathbf{u}$ local velocity vector
U_{sonic} velocity of sound
$\overline{V}$ average velocity of a molecule
V particle velocity in the jet
V_0 initial velocity
V_{diff} diffusive deposition velocity
V_{elec} drift or migration velocity in electric field
V_{grav} particle settling velocity in gravitational field
V_{th} thermophoretic velocity
V_{ts} terminal settling velocity
ΔV difference in potential (volts)
x distance between the plates in SI units (Eq. 2-47)
x_{rms} root mean square (rms) distance
Z particle electrical mobility
η dynamic viscosity of gas
η_r reference viscosity of gas
λ Mean free path of gas
ν kinematic viscosity of gas
ρ_g gas density
τ particle relaxation time
χ dynamic shape factor

2.8 REFERENCES

Allen, M. D., and O. G. Raabe. 1985. Slip correction measurements of spherical solid aerosol particles in an improved Millikan apparatus. *Aerosol Sci. Tech.* 4: 269–286.

Clift, R., J. R. Grace, and M. E. Weber. 1978. *Bubbles, Drops, and Particles*. New York: Academic.

Fuchs, N. 1964. *The Mechanics of Aerosols*. Oxford: Pergamon. Reprinted 1989. Mineola, NY: Dover.

Goldsmith, P., and F. G. May. 1966. In *Aerosol Science*. C. N. Davies (ed.) London: Academic.

Friedlander, S. K. 1977. *Smoke, Dust and Haze*. New York: John Wiley and Sons.

Hesketh, H. E. 1977. *Fine Particles in Viscous Media*. Ann Arbor, MI: Ann Arbor Science Publishers.

Hinds, W. C. 1999. *Aerosol Technology*. New York: John Wiley and Sons.

Licht, W. 1988. *Air Pollution Control Engineering: Basic Calculations for Particulate Collection*. New York: Marcel Dekker.

Mazumder, M. K., R. E. Ware, J. D. Wilson, R. G. Renninger, F. C. Hiller, P. C. McLeod, R. W. Raible, and M. K. Testerman. 1979. SPART analyzer: Its application to aerodynamic size measurement. *J. Aerosol Sci.* 10: 561–569.

McConalogue, D. J., and R. S. Srivastava. 1968. Motion of a fluid in a curved tube. *Proc. Roy. Soc. A.* 307: 37–53.

Mercer, T. T. 1973. *Aerosol Technology in Hazard Evaluation*. New York: Academic.

Rader, D. J. 1990. Momentum slip correction factor for small particles in nine common gases. *J. Aerosol Sci.* 21: 161–168.

Sartor, J. D., and C. E. Abbott. 1975. Prediction and measurement of the accelerated motion of water drops in air. *J. Appl. Meteor.* 14(2): 232–239.

Schlichting, H. 1979. *Boundary-Layer Theory*. New York: McGraw Hill.

Tsai, C. J., and D. Y. H. Pui. 1990. Numerical study of particle deposition in bends of a circular cross-section–laminar flow regime. *Aerosol Sci. Technol.* 12: 813–831.

Waldmann, L., and K. H. Schmitt. 1966. Thermophoresis and diffusiophoresis of aerosols. In *Aerosol Science*. C. N. Davies (ed.). London: Academic.

White, F. M. 1986. *Fluid Mechanics*. New York: McGraw-Hill.

Willeke, K. 1976. Temperature dependence of particle slip in a gaseous medium. *J. Aerosol Sci.* 7: 381–387.

3

PHYSICAL AND CHEMICAL PROCESSES IN AEROSOL SYSTEMS

WILLIAM C. HINDS

Department of Environmental Health Sciences, University of California–Los Angeles, School of Public Health, Los Angeles, California

3.1 INTRODUCTION

Aerosols, by their nature, are somewhat unstable in the sense that concentration and particle properties change with time. These changes can be the result of external forces, such as the loss of larger particles by gravitational settling, or they may be the result of physical and chemical processes that serve to change the size or composition of the particles. This chapter addresses the latter category of processes. They all involve mass transfer to or from a particle. This transfer may be the result of molecular transfer between the particle and the surrounding gas, for example, condensation, evaporation, nucleation, adsorption, absorption, and chemical reaction, or it may result from interparticle mass transfer, such as by coagulation.

Processes that cause physical or chemical changes in the particulate phase influence the particle size distribution of nearly all aerosols. These processes contribute in an essential way to the earth's hydrological cycle. They are involved in the formation of photochemical smog and are key to shaping the atmospheric aerosol size distribution. These processes play a significant role in many occupational aerosol exposures and in the operation of the condensation nuclei counters described in Chapters 17 and 32. They are central to industrial aerosol processing and the generation of test aerosols.

Condensation, thermal coagulation, and adsorption are related processes that rely on the diffusion of molecules or particles to a particle surface. Evaporation is the opposite of condensation and is governed by the same laws. Reactions may be non-growth processes that change the composition or density of an aerosol particle with little or no change in particle size. Because the processes discussed in this chapter are related and may be occurring simultaneously, it is necessary to look at each process separately in order to obtain an accurate picture of the changes that occur. Furthermore, these processes depend on particle size in a complex way, so a single

Aerosol Measurement: Principles, Techniques, and Applications, Third Edition. Edited by P. Kulkarni, P. A. Baron, and K. Willeke

particle approach for much of the analysis that follows will be adopted. We rely on the concepts of mean free path and diffusion coefficient, defined in Chapter 2.

3.1.1 Definitions

The *partial pressure* of a vapor is a way of expressing the concentration of that vapor in a volume of a gas mixture. It is the pressure the vapor would exert if it were the only component present. This pressure, expressed as a fraction of the ambient pressure, is the fractional concentration of the vapor. Air at 293 K [20 °C or 68 °F] and 50% relative humidity has a partial pressure of water vapor of 1.17 Pa [8.8 mm Hg], which means that the air–water vapor mixture is $1.17/101$ $[= 8.8/760] = 1.2\%$ water vapor on a volume basis.

The *vapor pressure* or *saturation vapor pressure* is a unique property of any liquid at a given temperature. It represents the minimum partial pressure of that liquid's vapor that must be maintained at the gas–liquid interface to prevent evaporation. This is a condition required for mass equilibrium, no net transfer of molecules at the liquid surface, that is, no net condensation or evaporation. Vapor pressure as defined here is for a flat liquid surface, but, as will be explained below, a slightly greater partial pressure is required to maintain mass equilibrium around an aerosol particle. The partial pressure of vapor in a sealed chamber containing a liquid will eventually reach the vapor pressure of the liquid at the temperature of the container.

The vapor pressure of water in kPa and mm Hg at a temperature T in K is given by

$$p_s = \exp\left(16.7 - \frac{4060}{T-37}\right)\text{kPa}$$
$$= \exp\left(18.72 - \frac{4060}{T-37}\right)\text{mm Hg} \qquad \text{(Eq. 3-1)}$$

for T from 273 to 373 K.

For aerosol condensation and evaporation processes, it is the ratio of the partial pressure of vapor to the saturation vapor pressure that is important. This ratio is called the *saturation ratio*, S_R. When the saturation ratio is equal to one, the mixture is described as *saturated*; when it is greater than one, the mixture is *supersaturated*; and when less than one, it is *unsaturated*.

Nucleation or *nucleated condensation* refers to the process of initial formation of a particle from vapor. This process is usually facilitated by the presence of small particles, called condensation nuclei, that serve as sites for condensation.

Adsorption is the process whereby vapor molecules attach to solid surfaces. It is most important for porous solids, such as activated charcoal, that have large surface areas. *Absorption* refers to the process of vapor molecules transferring from the gas phase to the liquid phase.

For aerosol particles, *condensation* occurs when the rate of vapor molecules arriving at a particle's surface is greater than that for molecules leaving. It results in a net growth of the particle. *Evaporation* is the reverse of condensation and results in a net loss of molecules and a shrinkage of the particle.

EXAMPLE 3-1

Saturated air coming from the ocean at 293 K [20 °C] is carried by air currents up the side of a mountain to an altitude of 1 km. Assuming this represents adiabatic expansion to a pressure of 89 kPa [670 mm Hg], what would be the saturation ratio of this air mass if no condensation occurred?

Answer: The absolute temperature of the air mass after an adiabatic expansion of saturated air from p_1 to p_2 is given by

$$T_2 = T_1\left(\frac{p_2}{p_1}\right)^{0.28} = 293\left(\frac{89.0}{101}\right)^{0.28} = \left[293\left(\frac{670}{760}\right)^{0.28}\right] = 283 \text{ K}$$

At 283 K the saturation vapor pressure for water is given by Equation 3-1

$$p_s = \exp\left(16.7 - \frac{4060}{283-37}\right) = 1.22 \text{ kPa} = [9.1 \text{ mm Hg}]$$

The saturation ratio is the ratio of the actual partial pressure of vapor, 2.34 kPa [17.6 mm Hg] (by Eq. 3-1 at 293 K), to the saturation vapor pressure for the ambient temperature, 1.22 kPa [9.1 mm Hg].

$$S_R = \frac{2.34}{1.22} = \left[\frac{17.6}{9.3}\right] = 1.92$$

3.1.2 The Kelvin Effect

Saturation vapor pressure has been defined as the partial pressure required for mass equilibrium (no net evaporation or condensation) for a flat liquid surface. Because liquid aerosol particles have a sharply curved surface, a greater partial pressure is required to maintain mass equilibrium for a droplet than for a flat liquid surface at a given temperature. This increase in the partial pressure of vapor required for mass equilibrium increases with decreasing particle size. This effect is called the *Kelvin effect*. The saturation ratio required for mass equilibrium (no net condensation or evaporation) for a droplet of diameter d_p is given by the Kelvin equation:

$$S_R = \exp\left(\frac{4\gamma M}{\rho_p R T d_p}\right) \qquad \text{(Eq. 3-2)}$$

where γ, M, and ρ_p are the surface tension, molecular weight, density of the liquid, respectively, and R is the gas constant. Thus, 0.1- and 0.01-μm diameter water droplets require an environment with a saturation ratio of least 1.022 and 1.24, respectively, to prevent evaporation. Evaporation will occur if the saturation ratio is less than that given by Equation 3-2, even if the saturation ratio is greater than one. Likewise,

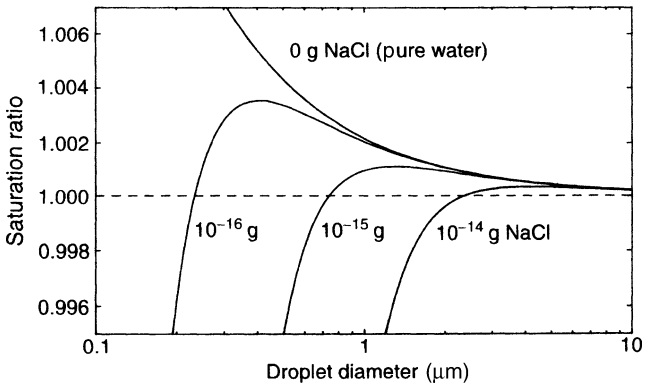

Figure 3-1 Saturation ratio versus droplet size for pure water and droplets containing the indicated mass of sodium chloride at 293 K [20 °C]. Adapted from Hinds (1999).

if the saturation ratio is greater than that required by the Kelvin equation, then condensation and growth will occur. For a given supersaturation, the minimum droplet size required to prevent evaporation is given by Equation 3-2 and is referred to as the *Kelvin diameter* for that condition. The Kelvin effect is illustrated by the line labeled pure water in Figure 3-1.

EXAMPLE 3-2

What saturation ratio is required to prevent growth or evaporation of 0.05-μm pure water droplets?

Answer: Use the Kelvin equation, Equation 3-2:

$$S_R = \exp\left(\frac{4\gamma M}{\rho_p R T d_p}\right)$$

where $\gamma = 0.0727\ \text{N/m}$; $M = 0.018\ \text{kg/mol}$; $\rho_p = 1000\ \text{kg/m}^3$; $R = 8.31\ \text{J/K} \cdot \text{mole}$; $T = 293\ \text{K}$; and $d_p = 5 \times 10^{-8}\ \text{m}$.

Substituting in gives

$$S_R = \exp\left(\frac{4 \times 0.0727 \times 0.018}{1000 \times 8.31 \times 293 \times 5 \times 10^{-8}}\right) = \exp(0.043)$$
$$= 1.044$$

3.2 CONDENSATION

3.2.1 Growth Rate

When a droplet of pure liquid is in a supersaturated environment that exceeds the saturation ratio requirement given by the Kelvin equation, the droplet grows by condensation of vapor on its surface. The rate of growth depends on the saturation ratio and the particle size. It is controlled by the rate of arrival of vapor molecules at the droplet surface. Initially the droplet will usually be less than the mean free path of the surrounding gas λ (0.066 μm at standard conditions, see Chapter 2) and the rate of arrival of vapor molecules is governed by the kinetic theory of gases. The growth rate, the rate of increase in droplet diameter, is given by Hinds (1999) as

$$\frac{d(d_p)}{dt} = \frac{2\alpha_c(p_\infty - p_d)}{\rho_p\sqrt{2\pi RT/M}} \quad \text{for } d_p < \lambda \qquad \text{(Eq. 3-3)}$$

where α_c is the condensation coefficient, the fraction of arriving molecules that stick, approximately 0.04 (see Barrett and Clement 1988); p_∞ is the partial pressure of vapor in the neighborhood of the droplet, but away from the droplet surface, and p_d is the partial pressure of vapor at the droplet surface as given by the Kelvin equation. The application of Equation 3-3 to obtain the growth rate in m/s [cm/s] requires that pressure be expressed in Pa [dyne/cm^2] (note that, mm Hg × 1330 = dyne/cm^2), density of the liquid in kg/m^3 [g/cm^3], temperature in K, and molecular weight in kg/mol [g/mol]. The gas constant R is 8.31 J/K · mol [8.31×10^7 dyne · cm/K · mol].

Once a droplet's size is greater than the mean free path, the rate of arrival of vapor molecules is governed by the rate of molecular diffusion to the droplet surface. Under these conditions the rate of growth is given by

$$\frac{d(d_p)}{dt} = \frac{4D_v M}{\rho_p d_p R}\left(\frac{p_\infty}{T_\infty} - \frac{p_d}{T_d}\right)\varphi \quad \text{for } d_p > \lambda \qquad \text{(Eq. 3-4)}$$

where D_v is the diffusion coefficient of the vapor molecules, $2.4 \times 10^{-5}\ \text{m}^2/\text{s}$ [$0.24\ \text{cm}^2/\text{s}$] for water vapor at 293 K [20 °C], the subscript ∞ refers to conditions removed from the particle, the subscript d refers to conditions right at the droplet surface. During rapid condensation ($S_R > 1.05$) the temperature of the droplet T_d will be greater than the surrounding air due to the release of heat of vaporization. The droplet temperature due to heating during condensation or cooling during evaporation can be estimated by (Hinds 1999),

$$T_d = T_\infty + \frac{(6.65 + 0.345T_\infty + 0.0031T_\infty^2)(S_R - 1)}{1 + (0.082 + 0.00782T_\infty)S_R} \qquad \text{(Eq. 3-5)}$$

where T_d and T_∞ are in °C. The quantity p_d in Equations 3-3 and 3-4 is evaluated at T_d by Equation 3-1.

The last factor in Equation 3-4, φ, corrects for complications in the calculation of mass transfer by diffusion within one mean free path of the particle surface. This correction is known as the Fuchs correction. The Fuchs correction factor φ is given by Davies (1978) as

$$\varphi = \frac{2\lambda + d_p}{d_p + 5.35(\lambda^2/d_p) + 3.42\lambda} \qquad \text{(Eq. 3-6)}$$

This factor can be omitted with little error for growing or evaporating droplets larger than about 2 μm.

Equations 3-3 to 3-5 apply only to pure materials, that is, single component liquids without any dissolved salts or impurities.

EXAMPLE 3-3

What is the rate of growth by condensation for a 5-μm water droplet at a saturation ratio of 1.04 and a temperature of 293 K [20 °C]?

Answer: Since 5 μm is greater than the mean free path (0.066 μm) we can use Equation 3-4. We can neglect φ because $d_p > 2$ μm.

$$\frac{d(d_p)}{dt} = \frac{4D_v M}{\rho_p R d_p}\left(\frac{P_\infty}{T_\infty} - \frac{P_d}{T_d}\right)$$

where $D_v = 2.4 \times 10^{-5}$ m^2/s [0.24 cm^2/s]. Because $S_R < 1.05$, $T_d \approx T_\infty = 293$ K and $p_d \approx p_s$ at 293 K [20 °C]. Saturation vapor pressure p_∞ is given by Equation 3-1 for $T = 273 + 20 = 293$ K

$$p_s = \exp\left(16.7 - \frac{4060}{293 - 37}\right) = 2.318 \text{ kPa} = 2318 \text{ Pa}$$

$$p_\infty = 1.04 \times p_s = 1.04 \times 2.318 = 2.411 \text{ kPa} = 2411 \text{ Pa}$$

Substituting in gives

$$\frac{d(d_p)}{dt} = \frac{4(2.4 \times 10^{-5})0.018}{1000(8.31)5 \times 10^{-6}}\left(\frac{2410}{293} - \frac{2318}{293}\right)$$
$$= 4.159 \times 10^{-5}(0.317) = 1.32 \times 10^{-5} \text{ m/s}$$
$$= 13.2 \text{ μm/s}$$

3.2.2 Time Required for Growth

The time required for a droplet to grow from d_1 to d_2 can be obtained by integrating Equation 3-4 over the size limits.

$$t = \frac{\rho_p R(d_2^2 - d_1^2)}{8D_v M\left(\frac{p_\infty}{T_\infty} - \frac{p_d}{T_d}\right)} \quad \text{for } d_1 \gg \lambda \qquad \text{(Eq. 3-7)}$$

3.3 NUCLEATION

3.3.1 Homogeneous

The preceding section described the growth process for pure materials once the droplets have been formed. The initial formation of the droplet from a vapor is a more complicated process. Droplets can be formed in the absence of condensation nuclei, but this process, called *homogenous nucleation* or *self-nucleation*, requires large saturation ratios, usually in the range of 2 to 10, which normally occur only in special laboratory or chemical process situations. Pure water vapor at 293 K [20 °C] and at a saturation ratio of 3.5 or greater spontaneously forms droplets by homogeneous nucleation. This corresponds to a Kelvin diameter of 0.0017 μm and suggests that molecular clusters of about 90 molecules are necessary for this process. A detailed description of homogeneous nucleation is given by Sienfeld and Pandis (1998).

3.3.2 Heterogeneous

The more common formation mechanism is *nucleated condensation* or *heterogenous nucleation*. This process relies on existing submicrometer particles, called *condensation nuclei*, to serve as sites for condensation. Our natural atmosphere contains thousands of these nuclei in each cubic centimeter of air. To a first approximation, insoluble nuclei serve as passive sites on which condensation occurs for supersaturated conditions. Under supersaturated conditions, a solid nucleus with a wettable surface will have on its surface an adsorbed layer of vapor molecules. If the nucleus has a diameter greater than the Kelvin diameter for a particular condition of supersaturation, the nucleus "looks like" a droplet to surrounding vapor molecules and vapor will condense on its surface. Once condensation starts, droplet growth continues as described by Equations 3-3 and 3-4.

The situation with soluble nuclei is more complex and more important. Our normal atmosphere contains large numbers of soluble nuclei formed as the solid residue left behind after the water has evaporated from a droplet containing dissolved material. Many are sodium chloride nuclei formed from droplets of sea water created by the action of waves and bubbles in the oceans. Because these soluble nuclei have a strong affinity for water, they facilitate the initial formation of droplets and enable their growth to occur at lower saturation ratios than would be the case for insoluble nuclei.

Because of the complex effect the presence of dissolved salt has on the rate of growth of a droplet, Equations 3-3 and 3-4 cannot be used to determine growth rates for such droplets. The stabilization time for droplets containing salt is described by Ferron and Soderholm (1990). In general, dissolved salts increase the rate of growth and decrease the rate of evaporation compared to pure liquids. As a droplet grows by the addition of water vapor, the concentration of salt becomes more and more dilute. Consequently, it is convenient to characterize the amount of salt in a droplet not by its concentration but by the mass of salt in the droplet, a quantity that remains constant during condensation or evaporation processes. The mass of salt is also equal to the mass of the original salt nucleus upon which the droplet formed.

When a dissolved salt is present in a droplet there are two competing effects at work as the droplet evaporates or grows. As a droplet evaporates the concentration of salt increases, because only the water leaves. This strengthens the ability of the dissolved salt to hold water in the droplet. The other effect is the Kelvin effect, which results in an increase in the equilibrium vapor pressure required for a droplet as its

size decreases. The relationship between saturation ratio and particles size for droplets containing dissolved salts is illustrated in Figure 3-1 by the three lines, called *Kohler curves*, labeled with their mass of dissolved salt.

3.3.3 Equilibrium Conditions

As with pure materials, the region above a given Kohler curve in Figure 3-1 represents a growth region and below the curve represents an evaporation region. Thus, if the saturation ratio is greater than 1.002, any droplet (or nucleus) containing more than 10^{-15} g of sodium chloride will grow to a large droplet, although its growth rate will slow as it gets larger, as predicted by Equation 3-4. When environmental conditions and particle size give a location on Figure 3-1 that is below the curve, the particle will shrink until it reaches the curve. If above the curve, and below and to the left of the peak, it will grow until it reaches the curve. Thus, the portion of the curve to the left of the peak represents a true equilibrium region and droplets will remain at their size as long as environmental conditions stay constant. This is true even if the saturation ratio is less than 1.0. Thus, there are a large number of particles in the atmosphere that will experience an increase in their size with an increase in relative humidity and a decrease with a decrease in relative humidity. The line for pure water does not have this type of equilibrium region. It represents only a demarcation between the growth (above) and evaporation (below) regions. As droplets continue to grow, the concentration of dissolved salts decreases, eventually reaching the point where the droplets behave the same as pure water, and their curves in Figure 3-1 merge with that for pure water.

3.4 EVAPORATION

3.4.1 Rate of Evaporation

The process of evaporation of a pure liquid droplet (no dissolved salts) is similar to the process of growth, except that it proceeds in the opposite direction. Evaporation will occur when the ambient partial pressure of vapor is less than the saturated vapor pressure ($p_\infty < p_s$). The rate of particle shrinkage due to evaporation can be predicted by Equation 3-4. During evaporation, the term in parentheses will be negative, giving a negative growth rate, which represents shrinkage due to evaporation.

For volatile particles such as water or alcohol, the quantity p_d must be evaluated at the cooler conditions prevailing at the droplet surface, T_d, which is given by Equation 3-5.

For particles larger than about 50 μm, an additional correction must be included to account for the disruption in the diffusion of vapor away from the droplet surface caused by the settling of the droplet. This effect increases the rate of evaporation of 50- and 100-μm droplets by 10 and 31%, respectively. More detailed information on this effect is given by Davies (1978) and Fuchs (1959).

3.4.2 Drying Time

Figure 3-2 gives droplet lifetimes or drying times, that is, the time for evaporation from an initial diameter to zero for pure water droplets at three conditions of relative humidity. The graph was obtained by numerical integration of Equation 3-4 from the initial size to zero. For particles initially larger than about 2 μm at standard conditions, φ in Equation 3-4 can be neglected and the equation integrated to give droplet lifetimes.

$$t = \frac{R\rho_p d_p^2}{8D_v M\left(\frac{p_d}{T_d} - \frac{p_\infty}{T_\infty}\right)} \quad \text{for initial } d_p > 2\,\mu\text{m} \quad \text{(Eq. 3-8)}$$

Table 3-1 gives droplet lifetimes for four materials at standard conditions. It illustrates the wide range of droplet lifetimes for different materials. The effect of material properties on droplet lifetime is, to a first approximation, proportional to $\rho_p/D_v M$.

EXAMPLE 3-4

Water droplets 60 μm in diameter are sprayed into air with 50% relative humidity at 293 K [20 °C]. How long before they evaporate completely?

Answer: Use Equation 3-8:

$$t = \frac{R\rho_p d^2}{8D_v M\left(\frac{p_d}{T_d} - \frac{p_\infty}{T_\infty}\right)}$$

where:

$R = 8.31\ \text{J/K} \cdot \text{mol}$
$\rho = 1000\ \text{kg/m}^3$
$d_p = 6 \times 10^{-5}\ \text{m}$
$D_v = 2.4 \times 10^{-5}\ \text{m}^2/\text{s}$
$T_\infty = 293\ \text{K}\ [20\ ^\circ\text{C}]$
$p_\infty = 0.5 \times 2.34\ \text{kPa} = 1.17\ \text{kPa} = 1170\ \text{Pa}$
$T_d = 286.4\ \text{K}$ (by Equation 3-5 with $T_\infty = 20\ ^\circ\text{C}$)
p_d is given by Equation 3-1 at 286.4 K

Substituting into Equation 3-8 gives

$$t = \frac{8.31 \times 1000 \times (6 \times 10^{-5})^2}{8 \times (2.4 \times 10^{-5}) \times 0.018\left(\frac{1523}{286.4} - \frac{1170}{293}\right)} = 6.5\ \text{s}$$

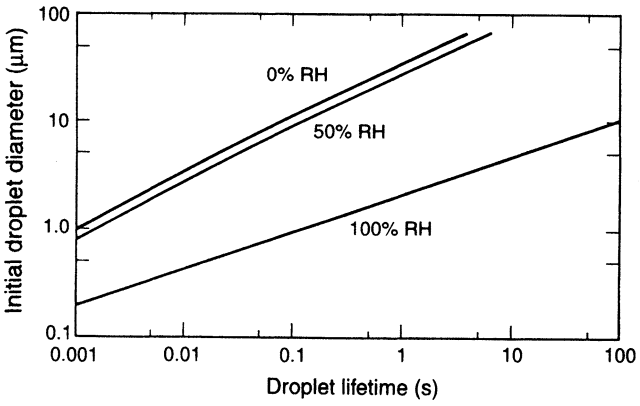

Figure 3-2 Drying times for pure water droplets at 293 K [20 °C]. RH is relative humidity. Reprinted from Hinds (1999), with permission.

3.5 COAGULATION

Coagulation is an aerosol growth process that results from the collision of aerosol particles with each other. If the collisions are the result of Brownian motion, the process is called *thermal coagulation*; if they are the result of motion caused by external forces, the process is termed *kinematic coagulation*. Thermal coagulation is in some ways analogous to growth by condensation, except that it is other particles diffusing to a particle's surface rather than molecules that causes the growth. It differs from condensation in that a supersaturation is not required, and it is a one-way process of growth with no equivalent process corresponding to evaporation. The result of many collisions between particles is an increase in average particle size and a decrease in aerosol number concentration. In the absence of any loss or removal mechanisms, there is no change in volume or mass concentration as a result of coagulation.

To understand the process, we look first at a simplified description of coagulation called *simple monodisperse coagulation* or *Smoluchowski coagulation*. The latter is named after the person who developed the original theory in 1917. This approach illustrates the process well, is useful for analyzing many situations, and is the basis for further refinements.

3.5.1 Simple Monodisperse Coagulation

For simple monodisperse coagulation we make the simplifying assumptions that the particles are monodisperse, they will stick if they contact one another, and they grow slowly. The latter two are valid assumptions for most aerosol particles and situations. Aerosol particles exhibit Brownian motion and diffuse like gas molecules, but their diffusion occurs at a much slower pace; consequently, the diffusion coefficients for aerosol particles are about a million times smaller than those for gas molecules.

The derivation developed by Smoluchowski is based on the diffusion of other particles to the surface of each particle [see Hinds (1999)]. It gives the rate of change (decrease) in aerosol number concentration as

$$\frac{dN}{dt} = -KN^2 \qquad \text{(Eq. 3-9)}$$

where N is particle number concentration and K is the coagulation coefficient. For particles larger than the gas mean free path, K is given by

$$K = 4\pi d_p D = \frac{4kTC_c}{3\eta} \quad \text{for } d_p > \lambda \qquad \text{(Eq. 3-10)}$$

where D is the particle diffusion coefficient m^2/s [cm^2/s], η is the gas viscosity in $Pa \cdot s$ [$g/cm \cdot s$], and k is Boltzmann's constant, 1.38×10^{-23} J/K [1.38×10^{-16} dyne $\cdot$ cm/K]. The coagulation coefficient has units of m^3/s [cm^3/s] when number concentration is expressed in particles/m^3 [particles/cm^3]. The coagulation coefficient is only slightly dependent on particle size being proportional to slip correction factor C_c. For particles less than 0.5 μm, an additional correction, due to distortion of the concentration gradient within one mean free path of the particle's surface, must be applied [see Hinds (1999)]. Table 3-2 gives coagulation coefficients for different size particles at standard conditions.

TABLE 3-1 Droplet Lifetime for Selected Materials[a]

Initial Droplet Diameter (μm)	Droplet Lifetime (s)			
	Ethyl alcohol	Water	Mercury	Dioctyl phthalate
0.01	4×10^{-7}	2×10^{-6}	0.005	1.8
0.1	9×10^{-6}	3×10^{-5}	0.3	740
1	3×10^{-4}	0.001	1.4	3×10^{4}
10	0.03	0.08	1200	2×10^{6}
40	0.4	1.3	2×10^{4}	4×10^{7}

Source: Adapted from Hinds (1999).

[a]Calculated by Equation 3-4 for vapor-free air at 293 K [20 °C].

TABLE 3-2 Coagulation Coefficients for Selected Particle Sizes at 293 K [20 °C][a]

Particle Diameter (μm)	Coagulation Coefficient (m^3/s)
0.05	9.9×10^{-16}[b]
0.1	7.2×10^{-16}[b]
0.5	5.8×10^{-16}[b]
1	3.4×10^{-16}
5	3.0×10^{-16}

Source: Adapted from Hinds (1999).

[a]For coagulation coefficients in cm^3/s multiply table values by 10^6.

[b]Includes additional correction factors. See Hinds (1999).

TABLE 3-3 Time Required for Selected Coagulation Processes[a]

Initial Number Concentration (m^{-3})	Time for Number Concentration to Halve (s)	Time for Particle Size to Double (s)
10^{18}	0.002	0.014
10^{16}	0.2	1.4
10^{14}	20	140
10^{12}	2000 (33 min)	14,000 (4 h)
10^{10}	200,000 (55 h)	1,400,000 (16 d)

Source: Adapted from Hinds (1999).

[a]Assumes simple monodisperse coagulation with $K = 5 \times 10^{-16}\,m^3/s$ [$5 \times 10^{-10}\,cm^3/s$].

In the usual situation, the extent of particle size increase is sufficiently limited that the coagulation coefficient can be considered a constant, and the rate of coagulation is proportional only to number concentration squared. Thus, coagulation is a rapid process at high number concentration and a slow one at low concentrations.

As a practical matter, the net effect of coagulation over some period of time is a more useful quantity than the rate of coagulation. The change in number concentration over a period of time t is obtained by integrating Equation 3-9 to get

$$N(t) = \frac{N_0}{1 + N_0 K t} \qquad \text{(Eq. 3-11)}$$

where $N(t)$ is the number concentration at time t and N_0 is the initial number concentration. Number concentration must be expressed in particles/m^3 for K in m^3/s [particles/cm^3 for K in cm^3/s].

As number concentration decreases, particle size increases, but, for a contained system with no losses, total particle mass will remain constant. If number concentration decreases to one half of its original value, then the same mass (and volume) will be contained in half as many particles, so each particle will have twice its original mass (and volume). For liquid particles, particle size is proportional to the cube root of particle volume and, consequently, it is also proportional to the inverse cube root of number concentration.

$$d(t) = d_0 \left(\frac{N_0}{N(t)} \right)^{1/3} \qquad \text{(Eq. 3-12)}$$

Thus an eight-fold reduction in particle number concentration results in a doubling of particle size. Equations 3-11 and 3-12 can be combined to give a more direct expression for the change in particle size due to coagulation over a period of time t

$$d(t) = d_0 (1 + N_0 K t)^{1/3} \qquad \text{(Eq. 3-13)}$$

Equations 3-12 and 3-13 are correct for liquid droplets and approximately correct for solid particles that form compact clusters. Table 3-3 gives the time required for various initial concentrations to reach one half their number concentration and the time for particle size to double. It is apparent from Table 3-3 that whether or not coagulation can be neglected depends on the concentration and time scale under consideration. Thus, over a period of a few minutes, coagulation is only important if particle number concentration exceeds $10^{12}/m^3$.

3.5.2 Polydisperse Coagulation

The previous description of coagulation is accurate enough for a wide variety of situations, but it requires the assumption of a monodisperse aerosol. In the real world, we usually have a polydisperse aerosol, and the situation is more complicated. Because the coagulation process is governed by the rate of diffusion of particles to the surface of each particle, the process is enhanced when small particles with their high diffusion coefficients diffuse to a large particle with its large surface. A ten-fold difference in particle size produces a three-fold increase in coagulation rate, and a hundred-fold difference results in more than a twenty-five-fold increase in coagulation rate. To use Equations 3-11 or 3-13 for polydisperse aerosols requires the use of numerical methods, because the coagulation for every combination of particle sizes has a different value of K and has to be calculated separately (Zebel 1966). For the case of coagulation of an aerosol with a lognormal size distribution having a count median diameter (CMD) and a geometric standard deviation σ_g, an equation derived by Lee and Chen (1984) can be used to calculate the average coagulation coefficient $\overline{K}$:

$$\overline{K} = \frac{2kT}{3\eta} \left[1 + \exp(\ln^2 \sigma_g) + \left(\frac{2.49\lambda}{\text{CMD}} \right) \times [\exp(0.5 \ln^2 \sigma_g) + \exp(2.5 \ln^2 \sigma_g)] \right] \qquad \text{(Eq. 3-14)}$$

This value of $\overline{K}$ can be used in place of K in Equation 3-11 to predict the change in number concentration over a period of time t for which there is only a modest change in CMD.

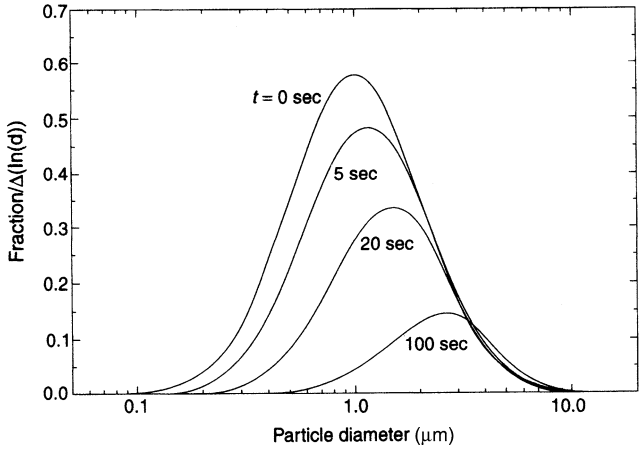

Figure 3-3 Effect of coagulation on particle size distribution. $N_0 = 10^{14}/\text{m}^3$ $[10^8/\text{cm}^3]$; initial count median diameter = 1.0 μm; initial geometric standard deviation = 2.0. Reprinted from Hinds (1999), with permission.

Equation 3-13 can be used with $\overline{K}$ to predict the increase in CMD over a time period for which $\overline{K}$ is approximately constant. For this type of calculation it is reasonable to assume that σ_g remains constant for modest changes in particle size. For large changes in particle size, calculation can be done as a series of steps, each with a constant but different value of $\overline{K}$. Figure 3-3 shows the effect of polydisperse coagulation on number concentration and particle size distribution for the indicated initial condition.

EXAMPLE 3-5

A. An iron oxide fume has an initial number concentration of $10^{13}/\text{m}^3$. Assuming the aerosol is monodisperse with a diameter of 0.2 μm, what will be the number concentration and particle size after two minutes? Assume standard conditions.

B. Repeat the above example for a polydisperse aerosol having a CMD of 0.2 μm and σ_g of 2.0. Assume σ_g remains constant.

Answer:

A. Use Equation 3-11:

$$N(t) = \frac{N_0}{1 + N_0 K t}$$

where $N_0 = 10^{13}/\text{m}^3$

$$K = \frac{4kTC_c}{3\eta}$$

$$= \frac{4(1.38 \times 10^{-23})293 \times 1.88}{3(1.81 \times 10^{-5})} = 5.6 \times 10^{-16}\ \text{m}^3/\text{s}$$

$t = 120\,\text{s}$

Substituting in

$$N(t) = \frac{10^{13}}{1 + 10^{13}(5.6 \times 10^{-16})120} = 5.98 \times 10^{12}/\text{m}^3$$

Use Equations 3-12 or 3-13 to determine the change in diameter:

$$d(t) = d_0\left(\frac{N_0}{N(t)}\right)^{1/3} = 0.2\left(\frac{10^{13}}{5.98 \times 10^{12}}\right)^{1/3} = 0.24\ \mu\text{m}$$

B. Use Equation 3-14 to get $\overline{K}$

$$\overline{K} = \frac{2kT}{3\eta}\left[1 + \exp(\ln^2\sigma_g) + \left(\frac{2.49\lambda}{\text{CMD}}\right) \times [\exp(0.5\ln^2\sigma_g) + \exp(2.5\ln^2\sigma_g)]\right]$$

$$\overline{K} = \frac{2(1.38 \times 10^{-23}) \times 293}{3(1.81 \times 10^{-5})}\left[1 + \exp[\ln^2(2.0)] + \left(\frac{2.49 \times 0.066}{0.2}\right)\left(\exp[0.5\ln^2(2.0)] + \exp[2.5\ln^2(2.0)]\right)\right]$$

$$= 1.489 \times 10^{-16}[6.986]$$

$$= 1.04 \times 10^{-15}\,\text{m}^3/\text{s}$$

Substituting into Equation 3-11 using $\overline{K}$ instead of K gives

$$N(t) = \frac{N_0}{1 + N_0\overline{K}t} = \frac{10^{13}}{1 + 10^{13}(1.04 \times 10^{-15})120}$$

$$= 4.45 \times 10^{12}/\text{m}^3$$

$$\text{CMD}_2 = 0.2\left(\frac{10^{13}}{4.45 \times 10^{12}}\right)^{1/3} = 0.26\,\mu\text{m}$$

3.5.3 Kinematic Coagulation

Kinematic coagulation is a coagulation process whereby the relative motion between particles is created by external forces rather than by Brownian motion. Brief descriptions of several such mechanisms are given below. In all cases, the greater the particle number concentration the greater the rate of coagulation. In general, there are no simple equations that describe these processes in a complete way. More detailed information is given by Fuchs (1964) and Hinds (1999).

Because particles of different sizes settle at different rates, there is a relative motion between settling particles of different sizes. The aerodynamics of the collision process is complicated and the collision efficiency is low except in the case of very large particles, such as raindrops, settling through micrometer-sized or larger-sized aerosol particles.

A similar process occurs when particles are projected through an aerosol at high velocity. This is an important mechanism for the capture of particles by spray droplets in certain kinds of wet scrubbers used for gas cleaning.

Gradient or *shear coagulation* occurs for particles moving in a flow velocity gradient. Particles on slightly different streamlines in a velocity gradient travel at different velocities and faster particles eventually overtake the slower ones. If the

particles are big enough, particle contact occurs by interception.

In turbulent flow, particles follow a complex path having strong velocity gradients. Relative motion between particles arises from these gradients and from inertial projection of the particles. The resulting coagulation is called *turbulent coagulation*. This mechanism is most effective when the turbulent eddy size is the same order of magnitude as the particle stopping distance. This mechanism is only important for particles larger than about 1 μm. Generally, the more intense the turbulence the more coagulation that results from this mechanism.

Finally, there is *acoustic coagulation*, where intense sound waves are used to create relative motion between particles. Depending on their size, particles respond to high intensity sound waves differently; large particles may be unaffected, whereas small particles oscillate with the sound waves. The relative motion that results leads to collisions and the process is called acoustic coagulation. Generally, sound pressure levels exceeding 120 dB are required to produce significant coagulation.

3.6 REACTIONS

Compared to bulk materials, aerosol particles have very high ratios of surface area to mass. For example, 1 g of standard density material ($1000\,kg/m^3$) when divided into 0.1-μm particles has a surface area of $60\,m^2$. Because of their large specific surface (surface area per gram), aerosols participate actively in many kinds of interaction between gas molecules and liquid or solid particles. This property accounts for many of the special characteristics of nanoparticles. Particles can undergo three kinds of reactions: reactions between compounds within a particle, reactions between particles of different chemical composition, and reactions between a particle and one or more chemical species in the surrounding gas phase. In the first case, reactions are governed by the usual chemical kinetics. The second case is most likely controlled by the rate of arrival of other particles, which is described by the coagulation process given above. Once dissimilar particles contact each other, reactions proceed by chemical kinetics. The third case may be controlled by the rate of arrival of the appropriate gas molecules at the particle surface. The rate of arrival of gas molecules is described by the condensation growth equations given in this chapter. Absorption and adsorption are related processes that also have as one of their necessary steps the arrival of gas molecules at a particle's surface.

These processes can be thought of as having three mass transfer steps in series, any one of which may be the rate-controlling step. First, there is diffusion of specific gas molecules to the surface of the particle. Next is the transfer across the interface or reaction at the interface. Finally, there is diffusion into the solid or liquid particle.

3.6.1 Reaction

In the case of a chemical reaction between the suspending gas and a particle, any of the three steps given above may control the rate of reaction. For solid particles, diffusion into the interior will be relatively slow even though the distances involved are small. Diffusion into the interior of liquid particles will be more rapid and may be augmented by internal circulation. If the reaction is controlled by the rate of arrival of gas molecules at the particle surface, then the maximum rate of reaction is given by

$$R_R = \frac{2\pi d_p D_v p}{kT} \quad \text{for } d_p > \lambda \qquad \text{(Eq. 3-15)}$$

where R_R is the rate of reaction in molecules per seconds. This is equivalent to a condensation process (Hinds 1999) under uniform temperature conditions. This situation is called a *diffusion controlled* reaction. The process can continue until all molecules of the particle have reacted.

3.6.2 Absorption

The process whereby gas molecules dissolve in a liquid droplet is called *absorption*. In this process the transfer at the interface is usually not controlling, but diffusion in either the gas phase or liquid phase may be. The process can continue until the limit of solubility of the gas in the liquid is reached. This limit may change with temperature or the presence of other dissolved components.

3.6.3 Adsorption

Adsorption is the transfer of gas molecules from the surrounding gas to a solid surface. There are two types of adsorption that can occur on the surface of a solid particle: physical adsorption, or *physisorption*, and chemical adsorption, or *chemisorption*. Physisorption is a physical process where gas molecules are held to a particle's surface by van der Waals' forces. It occurs for all gases when the ambient temperature is below their critical temperature. It is a rapid and readily reversible process. Because the adsorption process is rapid, the diffusion of gas molecules to the particle surface is usually the rate-limiting step. The relationship between the amount of adsorbed gas and the partial pressure of the gas or vapor at a given temperature is called the *adsorption isotherm*. Physisorption is usually not significant if the saturation ratio is below 0.05, but can lead to an adsorbed layer several molecules thick when the saturation ratio is 0.8 or greater. For a particle in adsorption equilibrium, a reduction in the partial pressure of the vapor will lead to a transfer

of adsorbed vapor molecules from the particle's surface to the gas.

The process of adsorption is similar to the process of condensation. Highly porous materials, like activated carbon, have enormous surface areas and contain numerous small pores and capillaries that facilitate molecular attachment on their surface and inhibit evaporation. The isotherms for highly porous materials will differ significantly from those for smooth solids.

Chemisorption is similar, except that chemical bonds are formed to hold the gas molecules on the particle's surface. It can occur above or below the critical temperature of the gas. In chemisorption, only a monolayer can form and, unlike physisorption, the process is not easily reversible because the chemical bonds are much stronger than van der Waals' forces. Either the rate of gas-phase diffusion or the rate of reaction can control the rate of this process. The rate of transfer slows as a complete monolayer is approached. In some cases molecules are first held to the surface by physisorption and then slowly react to attach by chemisorption. In other cases a physisorption layer may form on top of a chemisorption layer.

3.7 REFERENCES

Barrett, J.C., and Clement, C.F. 1988. Growth rates for liquid drops. *J. Aerosol Sci.* 9: 223–242.

Davies, C.N. 1978. Evaporation of airborne droplets. In *Fundamentals of Aerosol Science*, D.T. Shaw (ed.). New York: John Wiley and Sons. pp. 135–164.

Ferron, G.A., and Soderholm, S.C. 1990. Estimation of the times for evaporation of pure water droplets and for stabilization of salt solution particles. *J. Aerosol Sci.* 21: 415–429.

Fuchs, N.A. 1959. *Evaporation and Droplet Growth in Gaseous Media*. Oxford: Pergamon.

Fuchs, N.A. 1964. *The Mechanics of Aerosols*. Oxford: Pergamon.

Hinds, W.C. 1999. *Aerosol Technology*, 2nd ed. New York: John Wiley and Sons.

Lee, K.W., and Chen, H. 1984. Coagulation rate of polydisperse particles. *Aerosol Sci. Tech.* 3: 327–334.

Sienfeld, J.H., and Pandis, S.N. 1998. *Atmospheric Chemistry and Physics*. New York: John Wiley and Sons.

Zebel, G. (1966). Coagulation of aerosols. In *Aerosol Science*, C.N. Davies (ed.). London: Academic. pp. 31–58.

4

SIZE DISTRIBUTION CHARACTERISTICS OF AEROSOLS

WALTER JOHN
195 Grover Lane, Walnut Creek, California

4.1 BASIC CONCEPTS OF PARTICLE SIZE AND SIZE DISTRIBUTIONS

4.1.1 Definitions of Particle Size

Size is probably the most fundamental parameter describing aerosol particles. To satisfy the definition of an aerosol, the particles must be suspended in a gas. This implies that the particles are small enough to be suspended for an appreciable time, an arbitrary criterion. Conventionally, the upper size limit is considered to be about 100 μm; such particles have a settling velocity of 0.25 m/s and experience a drag force deviating appreciably from that calculated from Stokes' law. The lower size limit is likewise arbitrary, usually taken to be a few nm, the size of molecular clusters. Over this enormous range of five decades, the properties and behavior of aerosols change greatly.

For a spherical particle of unit density, the size can be simply characterized by the geometric diameter. For particles of arbitrary shape and density, an equivalent diameter is used. The *aerodynamic diameter* is defined as the diameter of a spherical particle of unit density having the same terminal settling velocity as that of the particle in question. The aerodynamic diameter is useful for particles having appreciable inertia, that is, those larger than about 0.5 μm. Particles smaller than about 0.5 μm undergo Brownian motion and are characterized by the *diffusive diameter*, the diameter of a particle that has the same diffusion coefficient as the particle in question. The *electrical mobility diameter* is the diameter of a spherical particle with the same electrical mobility as that of particle in question. The *Stokes diameter* is the diameter of a spherical particle having the same density and settling velocity as the particle in question. An *optical diameter* is defined as the diameter of a particle having the same response in an instrument that detects particles by their interaction with light. There are a number of diameter definitions used to describe particles measured by microscopy.

The appropriate particle size definition depends primarily on the type of measurement made. For example, the aerodynamic diameter would be used to analyze the data from a

Aerosol Measurement: Principles, Techniques, and Applications, Third Edition. Edited by P. Kulkarni, P. A. Baron, and K. Willeke

cyclone, a cascade impactor, or an aerodynamic particle sizer (APS). The diffusive diameter would be used for a diffusion battery measurement, the mobility diameter for a differential mobility analyzer and, obviously, the optical diameter with an optical particle counter.

4.1.2 Size Distributions

The particles in an aerosol are seldom uniform in size. A particle population in which all the particles have the same size would be said to be *monodisperse*. The most nearly monodisperse aerosols are those generated in the laboratory, typically with a spread in particle diameter of a few percent. (The spread is more precisely characterized by the geometric standard deviation, defined below.) Conventionally, a spread of less than about 10–20% (i.e., with a geometric standard deviation of 1.1 to 1.2) is considered monodisperse. Aerosols that have a larger range in size are said to be *polydisperse*. Both monodisperse and polydisperse aerosols consist of particles with sizes distributed over a certain range. In order to describe particle populations quantitatively, it is necessary to have a mathematical description of their size distributions.

The simplest size distribution would be a histogram of the number of particles in successive size intervals. Data for such a histogram could be obtained by sampling an aerosol with a cascade impactor and counting the number of particles on each stage with the aid of a microscope. The size intervals would be determined from the known cutpoints of each stage. Finer size intervals would be afforded by the use of an instrument such as the APS. With sufficiently fine intervals, the distribution would become a *differential size distribution.* Since the dependent variable or the ordinate of the plot is the number of particles, such a distribution is called a *number distribution.* If $\mathrm{d}N$ is the number of particles in the size interval from d_p to $d_\mathrm{p} + \mathrm{d}d_\mathrm{p}$, where d_p is the particle diameter, the number distribution function $n(d_\mathrm{p})$ is defined as

$$\mathrm{d}N = n(d_\mathrm{p})\mathrm{d}d_\mathrm{p} \qquad \text{(Eq. 4-1)}$$

Because the particle diameter typically ranges over several orders of magnitude, it is convenient to use $\mathrm{d}\ln d_\mathrm{p}$ (or $\mathrm{d}\log d_\mathrm{p}$) for the size interval, and the number distribution becomes

$$\mathrm{d}N = n(\ln d_p)\mathrm{d}\ln d_\mathrm{p} \qquad \text{(Eq. 4-2)}$$

Similarly, if $\mathrm{d}S$ is the total surface area of the particles in the same differential size interval, then the *surface area size distribution* is

$$\mathrm{d}S = s(\ln d_p)\mathrm{d}\ln d_\mathrm{p} \qquad \text{(Eq. 4-3)}$$

Two additional size distributions are frequently used, the *volume distribution* and the *mass distribution*:

$$\begin{aligned} \mathrm{d}V &= v(\ln d_p)\mathrm{d}\ln d_\mathrm{p} \\ \mathrm{d}M &= m(\ln d_p)\mathrm{d}\ln d_\mathrm{p} \end{aligned} \qquad \text{(Eq. 4-4)}$$

The data for one of the above distributions might be obtained directly by an appropriate particle sampler; for example, the mass distribution might be obtained by weighing the particle deposit on each of the stages of a cascade impactor. Alternatively, the number distribution might be obtained directly by an instrument such as an optical particle counter or an APS. In the absence of an instrument capable of measuring the surface distribution directly, it could be obtained by transforming the number distribution, that is, by taking

$$s(d_\mathrm{p}) = n(d_\mathrm{p}) \cdot \pi d_\mathrm{p}^2 \qquad \text{(Eq. 4-5)}$$

Likewise, the volume and mass distributions can be obtained from

$$\begin{aligned} v(d_\mathrm{p}) &= n(d_\mathrm{p}) \cdot \frac{\pi d_\mathrm{p}^3}{6} \\ m(d_\mathrm{p}) &= v(d_\mathrm{p}) \cdot \rho \end{aligned} \qquad \text{(Eq. 4-6)}$$

where ρ is the particle density.

While particle size distributions can be simply tabulated or plotted, it is convenient to fit the data to a function allowing the distribution to be characterized by only a few parameters. A variety of functions have been used for this purpose. Number distributions are frequently fitted to a power law. Mass distributions are commonly fitted to a lognormal function. The lognormal function is simply obtained from the normal function by using logarithmic variables. The lognormal distribution has a peak, a peak width, and, its most notable feature, a tail for large values of the independent variable, in this case the particle diameter. Aerosol size distributions from many different sources have been found to fit the *lognormal distribution*. The lognormal number distribution is:

$$n(\ln d_p) = \frac{N_T}{\sqrt{2\pi}\ln \sigma_\mathrm{g}} \exp\left[\frac{-(\ln d_\mathrm{p} - \ln \mathrm{CMD})^2}{2(\ln \sigma_\mathrm{g})^2}\right] \qquad \text{(Eq. 4-7)}$$

where N_T is the total number of particles, CMD is the count (number) median diameter (defined below), and σ_g is the geometric standard deviation, given by:

$$\ln \sigma_\mathrm{g} = \left[\frac{\int_0^\infty (\ln d_\mathrm{p} - \ln d_\mathrm{g})^2 \mathrm{d}n}{N_T - 1}\right]^{\frac{1}{2}} \qquad \text{(Eq. 4-8)}$$

σ_g is a measure of the width of the peak; if $d_{84\%}$ and $d_{16\%}$ are the diameters that include 84% and 16% of all the particles with diameters from zero to the diameter in question, then:

$$\sigma_g = \left(\frac{d_{84\%}}{d_{16\%}}\right)^{\frac{1}{2}} \qquad \text{(Eq. 4-9)}$$

In Equation (4-8), d_g is the geometric mean diameter, defined by:

$$\ln d_g = \frac{1}{N_T}\int_0^\infty (\ln d_p)\mathrm{d}n \qquad \text{(Eq. 4-10)}$$

For a lognormal distribution, the count median diameter, CMD, is equal to d_g. The lognormal function has a number of remarkable features. If the particle number distribution is lognormal, then the surface and volume distributions are also lognormal, and will be given by Equation 4-7 by replacing N by S or V, the total surface and volume, respectively, and by replacing CMD by the surface median diameter (SMD) and volume median diameter (VMD), respectively. The median diameters are related:

$$\begin{aligned} \mathrm{SMD} &= \mathrm{CMD}\exp(2\ln^2\sigma_g) \\ \mathrm{VMD} &= \mathrm{CMD}\exp(3\ln^2\sigma_g) \end{aligned} \qquad \text{(Eq. 4-11)}$$

The diameter corresponding to the peak of the lognormal distribution is called the *mode* diameter, and for a number distribution it is given by:

$$d_{\mathrm{mode}} = \mathrm{CMD}\exp(-\ln^2\sigma_g) \qquad \text{(Eq. 4-12)}$$

If, for example, experimental data for an aerosol mass distribution is found to fit the lognormal distribution, the distribution can be completely characterized by the mode diameter (or by the mass median diameter), the geometric standard deviation, and the total mass (integral of the differential mass distribution or the area under the curve). It is not unusual for the size distribution to have more than one mode, especially when there is more than one source of the aerosol. Then the distribution may be fit by a sum of lognormals.

Data on the aerosol concentration as a function of particle size can also be analyzed as discussed above. Elemental or chemical compound concentrations versus particle size can be treated as size distributions.

For more comprehensive treatments of the analysis of size distributions, the reader is referred to Chapter 22 of this book, and also Hinds (1999) and Friedlander (1977).

4.1.3 Use of Size Distribution Functions

The lognormal function is the most widely used for particle size distributions. There is no theoretical justification for such use. However, reasonably good fits are obtained to a variety of empirical data. Ambient particle size distributions are semi-quantitatively described by lognormals and the mathematical characteristics discussed above facilitate analysis.

The modified gamma distribution has also been used for atmospheric aerosols (Pruppacher and Klett 1980). The Weibull distribution fits aerosols from the fragmentation of rocks somewhat better than the lognormal according to Brown and Wohletz (1995). The Rosin–Rammler (1933) distribution is related to the Weibull distribution. In the modeling of the evolution of atmospheric aerosol, complexities are encountered in condensation and coagulation processes that require numerical rather than analytical treatment of the size distributions.

4.2 ATMOSPHERIC AEROSOLS

4.2.1 Introduction

Particles in the ambient atmosphere have diameters spanning the entire range within the definition of an aerosol. The particle sizes are determined by formation processes and subsequent physical and chemical processes in the atmosphere. Particle size is a key parameter in the transport and deposition of the ambient aerosol. The principal undesirable effects of ambient aerosol, including the respiratory health hazard, visibility reduction, and deposition to surfaces, depend on particle size. The effects on regional and global climate also depend on particle size. Therefore, the measurement and interpretation of particle size distributions in the atmosphere are essential to the overall understanding of the origin and the effects of ambient aerosol.

An early and widely used representation of the ambient particle size distribution was that of Junge (1963), who fitted the plot of the logarithm of particle number concentration versus the logarithm of particle radius with a simple power law. Later, Whitby (1978) showed that transforming atmospheric aerosol number distributions to volume distributions revealed three distinct size modes (peaks), which he labeled the nuclei, accumulation, and coarse modes (see Fig. 4-1). Most importantly, he interpreted each mode in terms of a different formation process leading to different particle characteristics. This model provided a fundamental basis for the understanding of the properties of ambient aerosol. The characteristics of the atmospheric aerosol depend on location, meteorological conditions, time of day, the status of sources, and other factors. Given this complexity, the Whitby trimodal model is a remarkable simplification that has proven to be very useful.

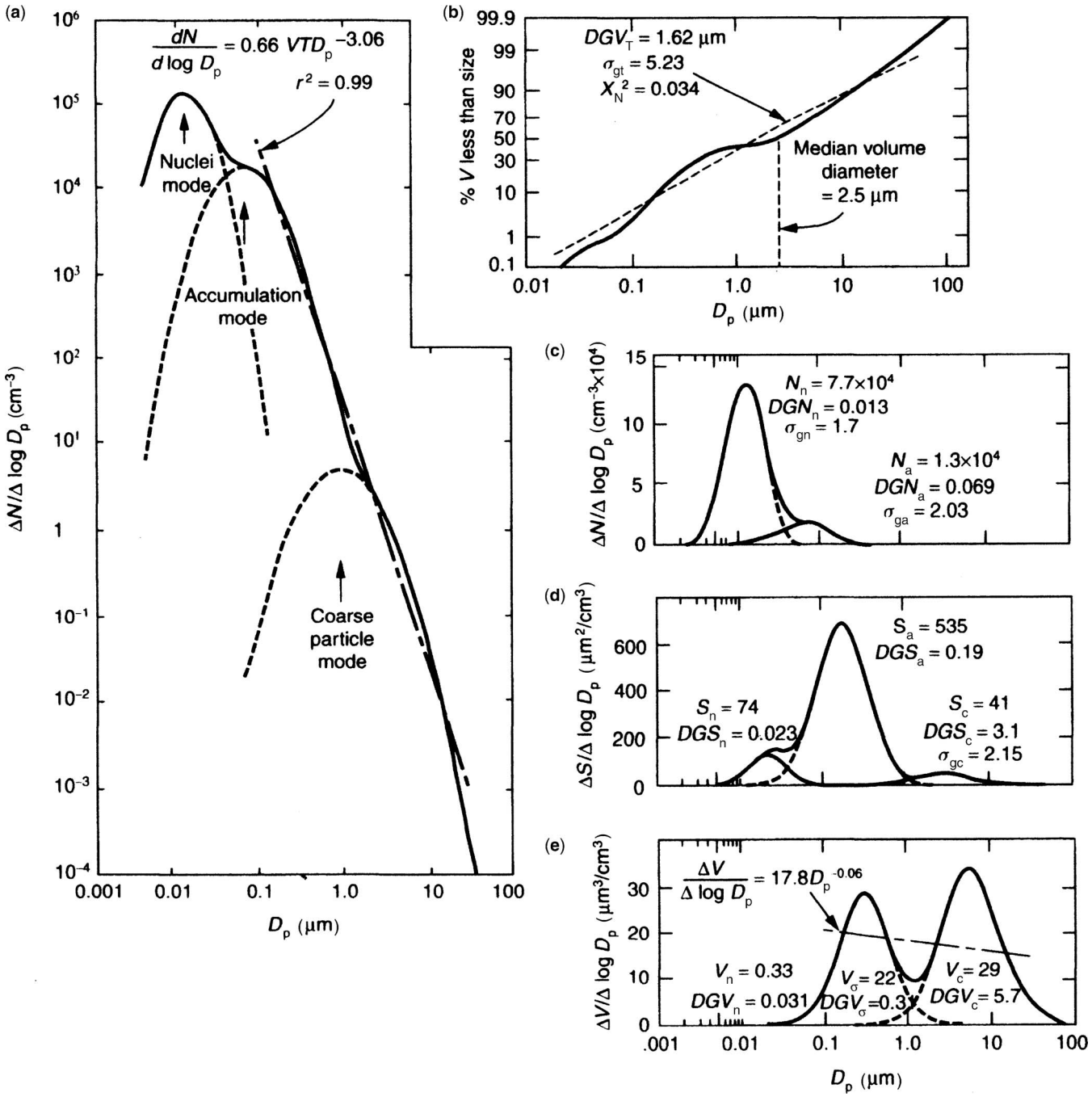

Figure 4-1 **(a)** Number distribution of an average urban model aerosol showing a fit to a power law distribution and as the sum of three lognormal distributions; **(b)** a cumulative plot of the fit to a single lognormal function; **(c)** number, **(d)** surface, and **(e)** volume distributions that have been fit to separate lognormals. (From Whitby and Svedrup, 1980, with permission of G. M. Hidy.)

In the following sections, the Whitby model will be discussed. Then each of the size ranges covered by the nuclei, accumulation, and coarse modes will be discussed, including more recent findings. The intent is not to review the vast literature on atmospheric size distributions, but rather to convey a broad understanding of the main features. Our knowledge of atmospheric size distributions is still incomplete despite decades of effort. The complexity of atmospheric processes presents difficult challenges to the measurement and modeling of ambient aerosol, which must be characterized by particle size and chemical composition and with temporal and spatial resolution.

4.2.2 The Whitby Model

Whitby (1978) described a trimodal distribution (Fig. 4-2) consisting of a nuclei mode in the size range 0.005 to 0.1 μm, an accumulation mode from 0.1 to 2 μm, and a coarse mode greater than 2 μm. Each mode was fitted by a lognormal function. In Table 4-1, the modal parameters for eight different types of atmospheres are listed (from Whitby and Sverdrup 1980).

Ambient particle size distributions typically have a minimum concentration between the accumulation and coarse modes, that is, near 2 μm. Whitby divided the particles into two main fractions: fine particles, with diameters <2 μm, and coarse particles, with diameters >2 μm. These two fractions have major differences both in origin and in physical and chemical characteristics (see Fig. 4-3). The fine fraction derives mainly from combustion, whereas the coarse fraction is generated by mechanical processes. The fine fraction includes the nuclei mode, which are transient particles formed by condensation and coagulation. The nuclei rapidly grow into the accumulation mode. According to Whitby, the accumulation mode also contains droplets formed by the chemical conversion of gases to vapors which condense. The coarse particle fraction contains windblown dust, sea spray, and plant particles.

4.2.3 Nuclei Mode, Size Range 0.005–0.1 μm

The smallest mode in the atmospheric aerosol, both in terms of particle size and mass concentration, is the nuclei mode, which, however, contains the highest number of particles. One of the largest databases on the nuclei mode remains that of Whitby and his collaborators. Analyzing the data as lognormal volume distributions, they obtained modal parameters including geometric mean particle diameters from 0.015–0.038 μm, and a mode geometric standard deviation of 1.7, in a variety of locations (Table 4-1). The mode diameter increases with time by less than a factor of three because the nuclei mode particles coagulate more rapidly with particles in the condensation mode (defined below) than with other particles in the nuclei mode. Extensive measurements by Reischl, Winklmayr, and John (1993) with an electrical mobility analyzer during the Southern California Air Quality Study (SCAQS) showed the nuclei mode to occur at a size consistent with the Whitby urban average value of 0.038 μm. Some recent data have shown two modes present in the size range of the nuclei mode.

Whitby (1978) has discussed the dominant role played by sulfur in the nucleation and growth of the nuclei mode. The nuclei mode is formed by photochemical reactions on gases in the atmosphere and by combustion. A striking demonstration of the photochemistry is afforded by the rapid appearance and growth of the nuclei mode at dawn. Because of its transient nature, the nuclei mode is significant only in the immediate vicinity of sources, for example, on a freeway.

There is considerable current interest in "ultrafine particles," loosely defined to be in the same size range as the nuclei mode, but with the emphasis near the lower end of the range. The interest stems from the possibility that particles this small might penetrate the tissue in the deep lung, leading to health effects (see Chapter 38).

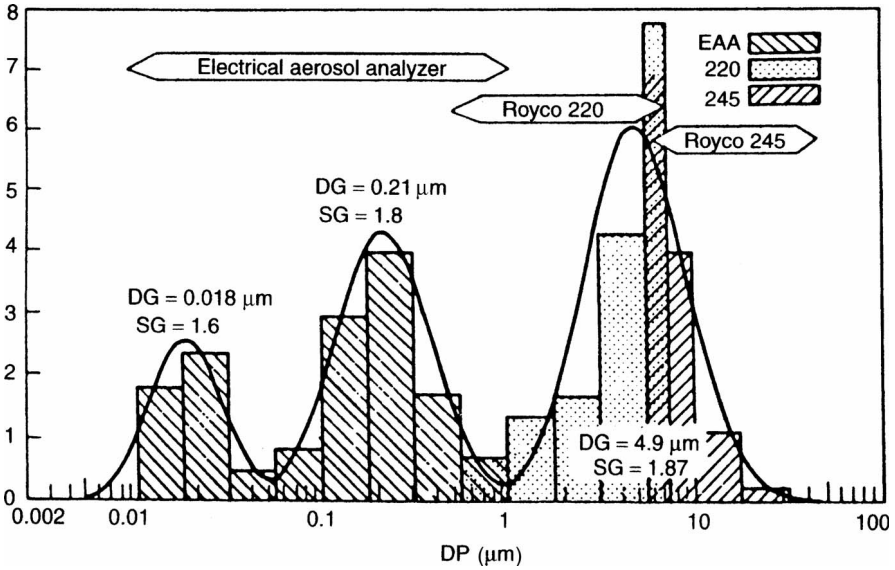

Figure 4-2 Trimodal particle volume distribution measured at the General Motors Milford Proving Grounds (29 October 1975). The size range measured with each instrument is indicated; the Royco®'s are optical particle counters, DG is the geometric mean particle diameter, and SG is the geometric standard deviation. Reprinted from Whitby (1978) with permission.

TABLE 4-1 Modal Parameters for Eight Typical Atmospheric Size Distributions

	Nuclei			Accumulation			Coarse		
Atmospheric Distribution	d_g (μm)	σ_g	V^a ($\mu m^3/cm^3$)	d_g (μm)	σ_g	V ($\mu m^3/cm^3$)	d_g (μm)	σ_g	V ($\mu m^3/cm^3$)
Marine, surface	0.019	1.6[b]	0.0005	0.3	2[b]	0.10	12	2.7	12
Clean continental background	0.03	1.6	0.006	0.35	2.1	1.5	6	2.2	5
Average background	0.034	1.7	0.037	0.32	2.0	4.45	6.04	2.16	25.9
Background and aged urban plume	0.028	1.6	0.029	0.36	1.84	44	4.51	2.12	27.4
Background and local sources	0.021	1.7	0.62	0.25	2.11	3.02	5.6	2.09	39.1
Urban average	0.038	1.8	0.63	0.32	2.16	38.4	5.7	2.21	30.8
Urban and freeway	0.032	1.74	9.2	0.25	1.98	37.5	6.0	2.13	42.7
Labadie coal power plant	0.015	1.5	0.1	0.18	1.96	12	5.5	2.5	24
Mean	0.029	1.66	0.26[c]	0.29	2.02	21.5[d]	6.3	2.26	25.9
Standard deviation	±0.007	±0.1	±0.33	±0.06	±0.1	±20	±2.3	±0.22	±13

[a]Volume of particles per volume of air.
[b]Assumed.
[c]Average omitting marine, urban and freeway, and Labadie.
[d]Average omitting marine.

Source: Reprinted from Whitby and Sverdrup (1980) with permission.

4.2.4 Accumulation Mode, Size Range 0.1–2 μm

This size range contains most of the fine particle mass. The U.S. Environmental Protection Agency (USEPA 1997) has established a particle standard for PM-2.5, that is, for particles with aerodynamic diameters smaller than 2.5 μm, based on the minimum in the ambient particle size distribution near 2.5 μm, and the fact that the accumulation mode consists mainly of combustion products, that is, anthropogenic emissions. Also, the USEPA considered PM-2.5 to present a respiratory health hazard. The 2.5-μm cutpoint is set lower than the 4-μm cutpoint of the respirable criteria of the American Conference of Governmental Industrial Hygienists (ACGIH; 1999) in order to exclude coarse mode particles.

The combustion of fossil fuels produces gases containing sulfur, nitrogen, and organic compounds. Complex reactions in the atmosphere result in the oxidation of the sulfur and nitrogen to produce particles in the accumulation mode containing inorganic compounds such as ammonium sulfate and ammonium nitrate. Organic and elemental carbon particles are also produced in the accumulation mode size range. Some of these chemicals are externally mixed, that is, they

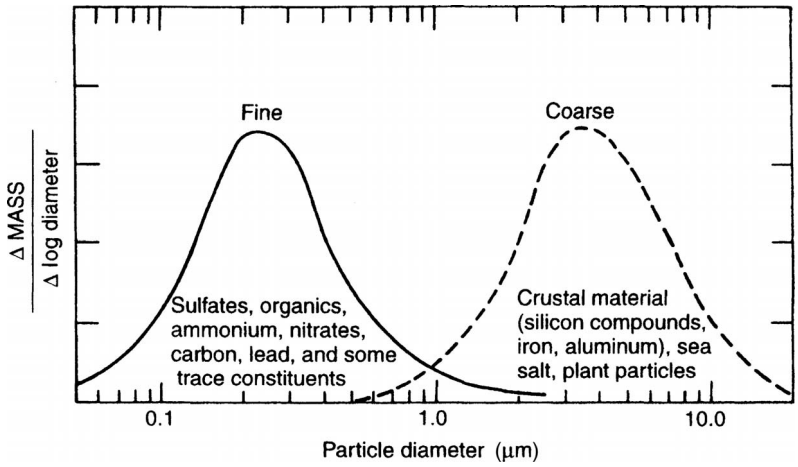

Figure 4-3 Schematic of typical urban aerosol composition by particle size fraction. The chemical species are listed in approximate order of relative mass contribution. From U.S. Environmental Protection Agency (1982).

are in separate particles, and some are internally mixed, being in the same particles. Since an internally mixed compound may have a concentration varying with particle size, the mode diameter of that compound may be different from that of the mode of the particles in question. Whether a compound is internally or externally mixed can sometimes be inferred indirectly from the size distributions, but is best determined directly by single particle analysis techniques such as microscopy and microprobe analysis (Chapter 10) or real-time mass spectrometers (Chapter 11; Prather et al. 1994).

Whitby described a single accumulation mode with a MMD of about 0.3 μm. In a study of sulfur aerosols in the Los Angeles area, Hering and Friedlander (1982) found the size distributions in the accumulation mode size range on different days to fall into two different types, depending on atmospheric conditions, namely, whether the air was relatively clean and dry or polluted and humid. During SCAQS, John et al. (1990) (Fig. 4-4) found two modes in the particle size distributions of inorganic ions in this size range. One mode, designated the *condensation mode* by John et al., had an average aerodynamic diameter of 0.2 μm. The other mode, named the *droplet mode*, had an average aerodynamic diameter of 0.7 μm. Both modes contained sulfate, nitrate, and ammonium ions (Table 4-2). Size distributions measured with differential mobility analyzers and optical counters by Eldering and Cass (1994) showed similar modal structure.

The condensation mode was named to reflect its formation and growth by condensation of gases either directly or indirectly through coagulation with nuclei mode particles. The rate of growth of particles in the condensation mode decreases with increasing particle size. Therefore, in the typical particle residence time in the atmosphere, the condensation mode does not grow much beyond 0.2 μm.

The other fine particle mode observed by John et al. (1990) was named the droplet mode because particle deposits in that

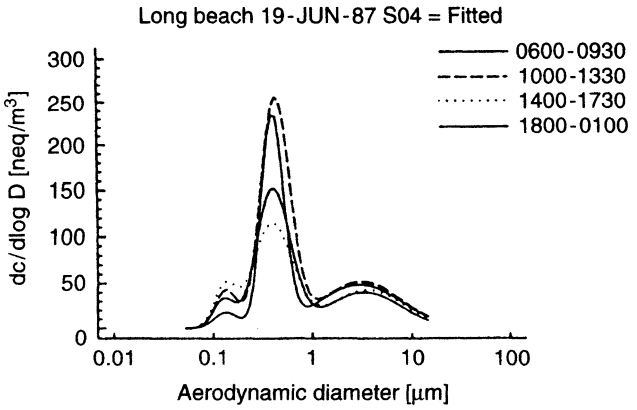

Figure 4-4 Sulfate particle size distribution measured in ambient air with a Berner cascade impactor. The sulfate ion concentrations are given in units of nanoequivalents per cubic meter of air. Reprinted from John et al. (1990) with permission.

size range showed evidence of being wet. The droplet mode averaged 0.7 μm in diameter, but the diameter ranged from near the condensation mode diameter of 0.2 μm up to a maximum of 1 μm. The total ion mass in the droplet mode averaged 6.5 times that in the condensation mode. It was pointed out by McMurry and Wilson (1983) and by Hering and Friedlander (1982) that the formation of particles as large as those in the droplet mode requires aqueous phase reactions involving sulfur. Meng and Seinfeld (1994) found a plausible mechanism for the formation of the droplet mode to involve the activation of condensation mode particles to form fog or clouds followed by aqueous phase reactions with ambient sulfur dioxide. Finally, evaporation of fog water leaves the droplets.

In addition to the condensation and droplet modes, John et al. observed a coarse ion mode (discussed in the next section). Because the geometric standard deviations do not

TABLE 4-2 Average Mode Parameters for Atmospheric Inorganic Aerosol Measured During the Southern California Air Quality Study of 1987

	Mode		
	Condensation[a]	Droplet[a]	Coarse[a]
	Summer		
Aerodynamic diameter (μm)	0.2 ± 0.1	0.7 ± 0.2	4.4 ± 1.2
σ_g	1.5 ± 0.2	1.7 ± 0.2	1.9 ± 0.3
Average concentration ($\mu g/m^3$)	5 ± 5	26 ± 21	13 ± 7
	Fall		
Aerodynamic diameter (μm)	0.2 ± 0.1	0.7 ± 0.3	5.5 ± 0.7
σ_g	1.5 ± 0.2	1.9 ± 0.5	1.8 ± 0.4
Average concentration ($\mu g/m^3$)	9 ± 8	40 ± 29	5 ± 4

[a]Means and standard deviations.

Source: Reprinted from John et al. (1990) with permission.

vary much (see Table 4-2), it is possible to characterize the modes by their mode diameters and concentrations. In Figure 4-5, a large data set has been summarized by plotting the relative mode concentrations versus the mode diameters. In Figure 4-5a, the sulfate data are seen to cluster in three modes that were relatively constant over the entire Los Angeles air basin during the summer of 1987. By contrast, Figure 4-5c shows that the nitrate data varied considerably. Prevailing westerly winds carry pollutants from the coastal sources toward the east, where ammonium converts the gaseous nitric acid to particulate ammonium nitrate. As a result, nitrate concentrations are higher in the eastern end of the air basin.

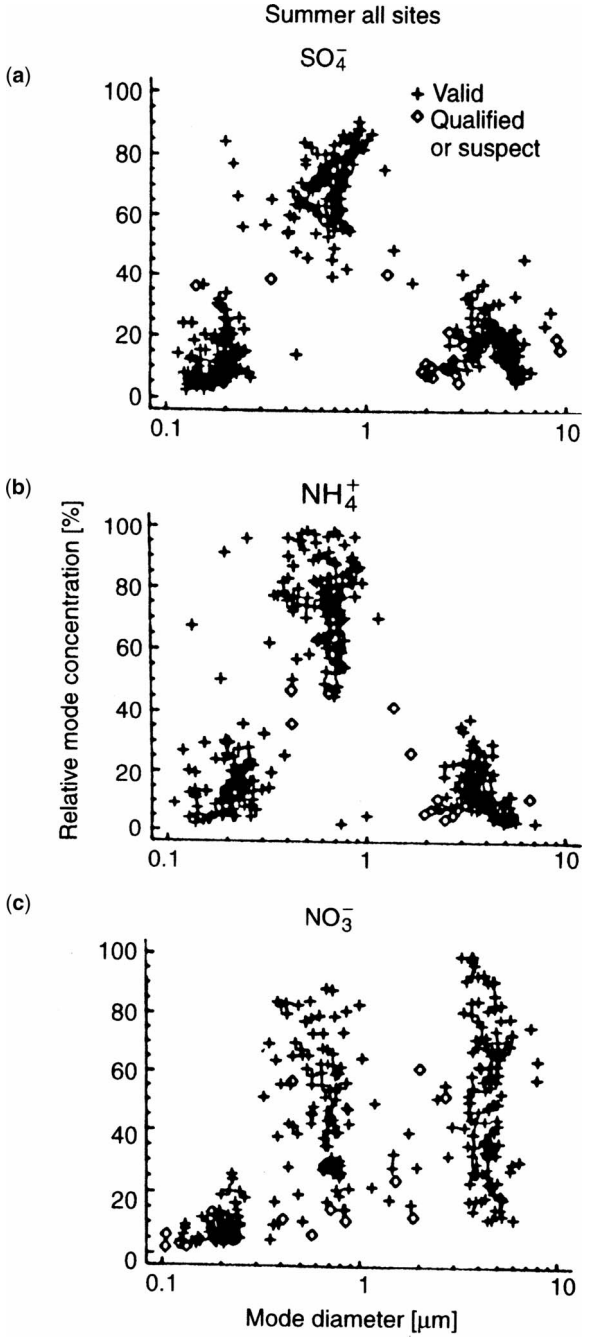

Figure 4-5 Relative mode concentration versus mode diameter for all sampling sites and all sampling periods during the summer SCAQS: **(a)** sulfate, **(b)** ammonium, and **(c)** nitrate. Reprinted from John et al. (1990) with permission.

There is appreciable overlap between the condensation and droplet modes. It is therefore misleading to quote a mass mean diameter over the fine particle range, since that mixes the two modes. Even when the modes overlap, the particles are a mixture of two different populations with different origins and compositions. The sulfate concentration in the droplet mode increases with increasing mode diameter, which is consistent with sulfur causing the formation of the mode. Others have observed sulfate size distributions peaking at 0.7 μm or larger. McMurry and Wilson (1983) reported sulfate particles as large as 3 μm in a power plant plume in Ohio. Georgi et al. (1986) observed sulfate in Hanover, Germany, peaking just above 1 μm and extending somewhat above 10 μm when the wind was from the east. Kasahara et al. (1994) reported sulfur distributions in Austria with mass mean diameters of 0.66 μm in Vienna and 0.65 μm in Marchegg. Koutrakis and Kelly (1993) found sulfate size distributions in Pennsylvania to peak at a geometric mean diameter of 0.75 μm. In Hungary, Meszaros et al. (1997) observed ammonium, nitrate, and sulfate modes in the range 0.5–1.0 μm, consistent with the droplet mode, but did not observe a condensation mode for these ions.

It appears that 0.7 μm is a typical mode diameter in many different locations, but the mode diameter varies considerably, depending on conditions. The mode diameter increases with residence time and can even exceed the large size limit of the accumulation mode. The size of the droplet mode has great significance for atmospheric visibility (John 1993). A mode aerodynamic diameter of 0.7 μm corresponds to a geometric diameter of 0.57 μm, assuming a density of 1.5. This size is almost exactly on the peak of the light-scattering curve for sunlight. Thus, the droplet mode dominates visibility reduction; there is a smaller reduction due to extinction by particles of elemental carbon. Sloan et al. (1991), in a study of visibility in Denver, observed two modes in the sulfate and nitrate size distributions with sizes consistent with condensation and droplet modes.

Koutrakis and Kelly (1993) found the size of sulfate particles in Pennsylvania to depend on relative humidity (RH) and acid content. Their data show the effect of RH to be most pronounced on ammonium bisulfate particles. Aerosols in Pennsylvania were found to contain little nitrate, most of the nitrate being in gaseous nitric acid. In the SCAQS, nitrate and sulfate ions were closely balanced by ammonium ion; this is typical for California aerosols, which are nearly neutral. This is to be contrasted with typical aerosols in the eastern United States, which are acidic.

The accumulation mode size range also includes elemental and organic carbon particles. In general, carbon data are more uncertain than that of the inorganics because of the complexity of the organics and associated experimental difficulties. Measurements by McMurry (1989) during SCAQS indicate a bimodal distribution with one mode in the condensation mode, but the other mode at a somewhat smaller diameter than the inorganic droplet mode. Venkataraman and Friedlander (1994) measured size distributions of polycyclic aromatic hydrocarbons (PAHs) and elemental carbon. Peaks were found at about 0.1 and 0.7 μm. Similar size distributions were found for aliphatic carbon, carbonyl carbon (Pickle et al. 1990), and organonitrates (Mylonas et al. 1991). Meszaros et al. (1997) found peaks for PAHs in the accumulation size range.

Milford and Davidson (1985) have summarized the size distributions of 38 particulate trace elements, which were mostly taken with cascade impactors. Most have a dominant peak in the accumulation mode size range with a smaller peak at about 3–5 μm.

4.2.5 Coarse Mode, Size Range >2 μm

Ambient coarse mode particles have been much less studied than fine mode particles because of concerns regarding the respiratory health effects of the fine particles. Whereas the sampling of fine particles poses problems because of their volatility and complex chemistry, the coarse particles pose difficult sampling problems because of their inertia.

Whitby and Sverdrup (1980) reported an average coarse mode diameter of 6.3 ± 2.3 μm for extensive measurements with optical counters in a variety of locations. However, other modes have been observed, some considerably larger than 6 μm. The largest particles suspended in the atmosphere are in a size mode that will be referred to here as the *giant coarse mode* to distinguish it from a smaller coarse mode to be discussed later. The giant particles can only be observed by *in situ* techniques or collected by special samplers such as the Noll rotary impactor (NRI) or the wide range aerosol classifier (WRAC), which have very large inlets. Noll et al. (1985) measured coarse modes with mass median diameters ranging from 16 to 30 μm, with an average mode diameter of 20 μm and a standard deviation of 2.0 (see Fig. 34-6 in Chapter 34 of this book). Measurements by Lundgren et al. (1984) are in general agreement. The particles consist of mineral particles derived from soil, biological particles, and sea salt.

The classical studies of Bagnold (1941) and Gillette and co-workers (Gillette 1974; Gillette et al. 1972, 1974) have explained how windblown dust is generated. Direct aerodynamic entrainment of soil particles is relatively insignificant. A process called saltation involves turbulent bursts that eject particles from the ground that are approximately 100 μm in diameter. Subsequently, these particles impact the surface at a shallow angle, dislodging smaller particles that can then be entrained in the air. Noll and Fang (1989) have proposed an explanation for the selective suspension of particles in the giant coarse mode size range by atmospheric turbulence. Particles that are too large fall out rapidly under gravity. Particles with too little inertia follow the eddies and do not acquire any net upward velocity from the wind. There is an intermediate size small enough to allow the particles to acquire upward velocity but with sufficient inertia to sustain an upward momentum. Corroborating evidence was obtained by Noll and Fang from sampling with a collection plate.

Biological particles frequently consist of pollens, which are fairly monodisperse, and generally 20 μm or more in diameter. Large plant fragments are also present in the coarse mode. The sampling of biological particles is discussed in Chapter 24. In urban areas, road dust generated by vehicles is found in the giant coarse mode. Particles of rubber containing mineral inclusions are seen. Coarse sea salt particles are found in coastal areas.

Measurements with cascade impactors find coarse modes with diameters typically ranging from 5 to 10 μm. These instruments are incapable of sampling the giant coarse mode, but the smaller modes that have been reported appear to be well within the capability of the samplers. The data suggest the existence of a coarse particle mode at a smaller size than the giant coarse mode. The smaller coarse mode will be referred to as the *coarse mode* here. This mode is further discussed in detail in Chapter 34.

Gillette et al. (1974) found soil aerosol size distributions to be similar to the size distribution of bulk soil particles that were separated in a water suspension. When the bulk soil particles were separated in water containing detergent, there was an excess of particles smaller than 5 μm compared to the aerosol, implying that the forces producing the aerosol were not strong enough to completely deagglomerate the soil. They also observed that the shapes of the aerosol size distributions were insensitive to wind conditions, implying that aerodynamic suspension was not operating. By sampling at various heights above the ground, Gillette et al. (1972) measured aerosol size distributions during periods of vertical flux. By converting his number distributions to volume distributions, it can be estimated that the MMD of the soil aerosol was about 9 μm. This is evidence of another source of a coarse mode smaller than the giant coarse mode. The distinction between the coarse mode and the giant coarse mode has an implication for aerosol composition because the ratio of clay to silt in soil varies with particle size.

It is well-known that in coastal areas, nitrate is found in the coarse aerosol fraction as a result of the reaction of gaseous nitric acid with sea salt (Savoie and Prospero 1982, Harrison and Pio 1983, Bruynseels and Van Grieken 1985, Wall et al. 1988). During the summer SCAQS study, the wind was primarily from the Pacific Ocean. John et al. (1993) observed a coarse ion mode containing nitrate, sulfate, chloride, sodium, ammonium, magnesium, and calcium. The mean mode diameter was 4.4 μm and the geometric standard

deviation was 1.9. This mode could be called the *coarse ion mode*. Wall et al. (1988) pointed out that small NaCl particles will be completely converted to $NaNO_3$, whereas large NaCl particles will be only partially converted. This leads to a nitrate mass distribution that has the same shape as that of the NaCl mass distribution for particles smaller than the NaCl mode diameter, but for larger particles, the distribution is truncated relative to that of the NaCl.

Coarse nitrate is also seen in continental air, formed by the reaction of gaseous nitric acid with alkaline soil particles and, at night, possibly by the reaction of N_2O_2 with soil particles (Wolff 1984). The nitrate on soil particles is not associated with ammonium.

Venkataraman et al. (1999) measured size distributions of polycyclic hydrocarbons (PAHs) in India, finding nonvolatile PAHs to peak in the accumulation mode, but an average of 32% was in the coarse mode. Semi-volatile PAHs were predominantly in the coarse mode, averaging 60% in the coarse mode. Venkataraman and co-workers discuss the volatilization of the original particles in the nuclei or accumulation modes followed by adsorption of the organic compounds onto coarse mode particles. The presence of PAHs and nitrates in the coarse mode exemplifies the complexity of ambient aerosol composition since many of the substances in atmospheric aerosol are semi-volatile.

4.3 INDOOR AEROSOLS

Indoor aerosol usually refers to that in residences and offices as distinguished from that in industrial workplaces. Increasing emphasis is being placed on indoor aerosols, since people average 80–90% of their time indoors (Spengler and Sexton 1983). Three major studies have been made in recent years: the Harvard Six Cities Study (Spengler et al. 1981), the New York State Energy Research and Development Authority (ERDA) study (Sheldon et al. 1989), and the EPA PTEAM Study (Pellizzari et al. 1992). Some of the indoor aerosol derives from infiltration of atmospheric aerosol. In the above three studies, the fine particle fraction, defined as PM-2.5 or PM-3.5, had a concentration indoors averaging about twice that outdoors, but the indoor/outdoor ratio varies, depending on whether the outdoor concentration is high or low. In the PTEAM study, the ratio of PM-2.5 to PM-10 indoors was about 0.5.

In homes with smokers, tobacco smoke is the largest component of the indoor aerosol. Tobacco smoke particles coagulate rapidly in the first few minutes after emission, causing the size distribution to shift toward larger diameters. The number distribution of tobacco smoke typically peaks in the accumulation mode size range. In Figure 4-6, the number distribution measured by Keith and Derrick (1960) is compared to a theoretical calculation based on self-preserving size spectrum theory (Friedlander and Hidy 1969). Light-scattering measurements by Chung and Dunn-Rankin (1996) showed mainstream cigarette smoke to have a CMD of 0.14 μm for unfiltered cigarettes and 0.17 μm for filtered cigarettes, with GSDs of 2.1 and 2.0, respectively. The corresponding MMDs were 0.71 and 0.66 μm. Fresh sidestream smoke had a CMD of 0.27 μm. "Typical environmental tobacco smoke" measured with a scanning mobility particle sizer (Morawska and Jamriska 1997) gave a number

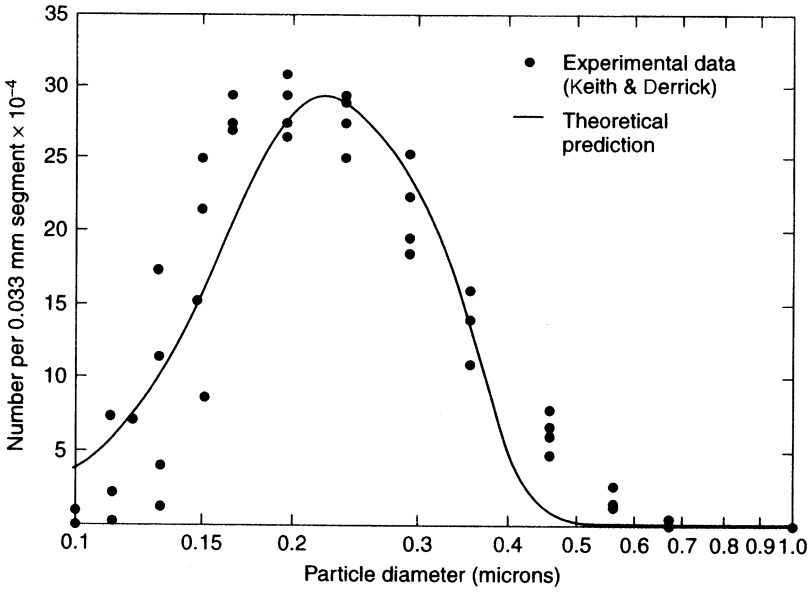

Figure 4-6 Comparison of experimental size distribution data for tobacco smoke with prediction based on self-preserving size spectrum theory. Reprinted from Friedlander (1977) with permission.

distribution with a lognormal shape, peaking at about 0.12 μm. Cigarette smoke particles will undergo hygroscopic growth in the human respiratory tract (Robinson and Yu 1998).

The next most significant source of indoor aerosol is from cooking. The size distribution parameters for smoke from cooking oils, sausages, and wood burning are listed in Table 4-3. The particles are in the accumulation size range. Table 4-3 also lists the soluble fraction of the smoke particles, which is low for the oils and sausages and high for wood smoke. Correspondingly, the oil and sausage smoke particles do not show hygroscopic growth whereas the wood smoke particles do (Dua and Hopke 1996).

Kerosene heaters, when present, contribute to indoor aerosol. The fine fraction (PM-2.5) of the indoor aerosol contains particles of soil, wood smoke, iron, and steel and particles from auto-related and sulfur-related sources (Spengler et al. 1981). Biological particles in indoor air include dander, fungi, bacteria, pollens, spores, and viruses. Walls, floors, and ceilings may release glass fibers, asbestos fibers, mineral wool, and metal particles. Aerosols are generated by consumer product spray cans. Paper products are a source of cellulose fibers, and clothing articles are sources of natural and synthetic organic fibers.

In homes where radon gas is present, radioactive aerosols may be formed by the attachment of radon daughters to suspended particles. Activity median diameters (AMD), from the size distribution of the radioactivity, are as small as a few nm but can also be considerably larger (Tu et al. 1991). Morawska and Jamriska (1997) have discussed the difficulties in measuring radon progeny and reference the extensive literature. See Chapter 28 for discussion of radioactive aerosols.

TABLE 4-3 Size Distribution Parameters of Indoor Smoke Aerosols and the Soluble Fraction

Product	CMD (nm)[a]	GSD[a]	Soluble Fraction[b]
Hollywood® Peanut Oil	199.1	1.62	0.076 ± 0.026
Mazola® Corn Oil	173.6	1.58	0.164 ± 0.008
Wesson® Canola Oil	238.9	1.61	0.203 ± 0.045
Wesson Vegetable Oil	168.3	1.68	0.128 ± 0.033
Sweet Italian sausages	73.8	1.55	0.456 ± 0.087
Wood burning with flame	80.3	1.90	0.714 ± 0.022
Wood burning without flame	55.1	1.31	0.924 ± 0.098
Particles in living room (wood burning in woodstove)	96.7	1.81	

[a]CMD = Count median diameter; GSD = geometric standard deviation.
[b]Means and standard deviations.

Source: Reprinted from Dua and Hopke (1996) with permission.

Particle size distributions have been measured in an office to determine the effect of the amount of outdoor air supplied and the occupation level (Owen et al. 1990).

Indoor aerosol and exposure assessment are discussed in Chapter 27.

4.4 INDUSTRIAL AEROSOLS

The characteristics of aerosols produced in industry are determined by the type of industry, the nature of the product, and the industrial operations. Detailed discussions of emissions from basic industries have been given (Stern 1968). Basic industries include petroleum refineries, nonmetallic mineral product industries, ferrous metallurgical operations, nonferrous metallurgical operations, inorganic chemical industry, pulp and paper industry, and food and feed industries. Power plants and incinerators are examples of stationary combustion sources. The properties of the aerosols emitted to the atmosphere depend on the material burned, combustion conditions, and the type of controls on the stacks.

Within an industry, aerosols are generated by processing activities. Welding produces fumes, chain aggregates of very fine particles. Mechanical operations such as grinding make coarse particles. Size distributions measured by Sioutas (1999) in an automotive machining facility show that, as expected, welding and heat-treating operations produce fine particles from the condensation of hot vapors while machining and grinding produce relatively large particles by breakup of solid material. Spray painting produces liquid droplets in the aerosol size range. The transport and handling of powdered materials produces dust aerosols. Ore, coal, and tailings give rise to fugitive emissions.

Workplace operations can produce aerosols of very large particles that are difficult to monitor or sample, yet may pose a respiratory hazard. The ACGIH (1999) recommends sampling such coarse aerosols according to the inhalable particulate mass criteria (IPM), which specifies the desired sampling efficiency up to 100 μm. An example is wood dust aerosol, which can cause nasal cancer (Hinds 1988). Workplace aerosol measurements are discussed in Chapter 25.

Aerosols in mines have long been investigated because of their ability to cause respiratory diseases, including pulmonary fibrosis, pneumoconiosis, and lung cancer. Indeed, work on mine aerosols has provided much of the existing aerosol sampling technology and the approach to sampling criteria for hazardous aerosols (Mercer 1973). The mechanical operations in coal mines produce coarse aerosols as expected, with a peak in the mass distribution at about 7 μm. However, if the mine contains diesel machinery, the mass distribution is bimodal, with a second peak at about 0.2 μm (Cantrell and Rubow 1990). Cavallo (1998) has published activity-weighted particle size distributions for two

uranium mines with diesel engines; the AMDs are in the 0.1- to 0.2-μm range.

4.5 GENERALIZED MODEL OF MODES IN PARTICLE SIZE DISTRIBUTIONS

In the preceding sections, the characteristics of particle size distributions for ambient aerosol, indoor aerosol, and industrial aerosol have been discussed. The size distributions generally have a wide range in particle size with modes (peaks) followed by long tails on the large particle end of the distributions. Whitby's model for ambient aerosol identifies three size modes, each with a different formation process. Data more recent than that included in Whitby's model provides evidence for a droplet mode and additional coarse particle modes in ambient air. The indoor and industrial aerosols also have particle size distributions with modes having sizes depending on the substances and processes involved in the aerosol production.

In general, aerosol production involves complex processes. The instant a particle is produced other processes begin, which may include coagulation, interactions with gases and other particles, evaporation, photochemistry, and transport. The resultant size distribution will vary temporally and spatially. A particle size distribution will evolve exhibiting a mode and a wide spread in particle size. The mode can be interpreted as the most probable particle size produced by the complex process. Conversely, the observation of a mode in a size distribution signifies a distinct particle production mechanism.

EXAMPLE 4-1

The number distribution of an aerosol is fitted by the function

$$n(\ln d_p) = \frac{N_T}{\sqrt{2\pi}\ln\sigma_g}\exp\left[\frac{-(\ln d_p - \ln \mathrm{CMD})^2}{2(\ln\sigma_g)^2}\right]$$

where $\sigma_g = 1.7$ and $\mathrm{CMD} = 0.30\ \mu\mathrm{m}$. Here N_T is the total number of particles/cm^3, CMD is the count median diameter, and σ_g is the geometric standard deviation.

(a) What is the volume median diameter?

(b) If σ_g were 20% larger, how much larger would the VMD be?

Answer:

(a) The distribution is lognormal, so that the volume median diameter, VMD, can be calculated from CMD and σ_g, using the relation

$$\mathrm{VMD} = \mathrm{CMD}\exp(3\ln^2\sigma_g) = 0.70\ \mu\mathrm{m}$$

(b) $\sigma_g = 2.04$ and $\mathrm{VMD} = 1.38\ \mu\mathrm{m}$, which is nearly double the original value. This illustrates the sensitivity to errors in the data when conversions are made from number-weighted to volume-weighted parameters.

4.6 LIST OF SYMBOLS

CMD	count (number) median diameter
d_{mode}	mode diameter
d_g	geometric mean diameter
d_p	particle diameter
$m(d_p)$	mass distribution
$n(d_p)$	number distribution
$s(d_p)$	surface area size distribution
$v(d_p)$	volume distribution
N_T	total number of particles
PM-2.5	particles with aerodynamic diameters smaller than 2.5 μm
SMD	surface median diameter
VMD	volume median diameter
ρ	particle density
σ_g	geometric standard deviation

4.7 REFERENCES

American Conference of Governmental Industrial Hygienists (ACGIH). 1999. *TLVs and BEIs*, app. D: Particle size-selective sampling criteria for airborne particulate matter. Cincinnati, OH: ACGIH.

Bagnold, R. A. 1941. *The Physics of Blown Sand and Desert Dunes*. London: Methuen.

Brown, W. K., and K. H. Wohletz. 1995. Derivation of the Weibull distribution based on physical principles and its connection to the Rosin-Rammler and lognormal distributions. *J. Appl. Phys.* 78:2758–2763.

Bruynseels, F., and R. Van Grieken. 1985. Direct detection of sulfate and nitrate layers on sampled marine aerosol by laser microprobe mass analysis. *Atmos. Environ.* 19:1969–1970.

Cantrell, B. K., and K. L. Rubow. 1990. Mineral dust and diesel exhaust aerosol measurements in underground metal and nonmetal mines. In *Proceedings of the VIIth International Pneumoconiosis Conference*, NIOSH Publication No. 90-108. Washington, DC: NIOSH, pp. 651–655.

Cavallo, A. J. 1998. Reanalysis of 1973 activity-weighted particle size distribution measurements in active U.S. uranium mines. *Aerosol Sci. Technol.* 29:31–38.

Chung, I.-P., and D. Dunn-Rankin. 1996. *In situ* light scattering measurements of mainstream and sidestream cigarette smoke. *Aerosol Sci. Technol.* 24:85–101.

Dua, S. K., and P. K. Hopke. 1996. Hygroscopic growth of assorted indoor aerosols. *Aerosol Sci. Technol.* 24:151–160.

Eldering, A., and G. R. Cass. 1994. An air monitoring network using continuous particle size distribution monitors: Connecting pollutant properties to visibility via Mie scattering calculations. *Atmos. Environ.* 28:2733–2749.

Friedlander, S. K. 1977. *Smoke, Dust, and Haze*. New York: John Wiley & Sons.

Friedlander, S. K., and G. M. Hidy. 1969. New concepts in aerosol size spectrum theory. In *Proceedings of the 7th International Conference on Condensation and Ice Nuclei*, J. Pkodzimek (ed.). Prague: Academia.

Georgi, B., K. P. Giesen, and W. J. Muller. 1986. Measurements of airborne particles in Hannover. In *Aerosols, Formation and Reactivity*, Proceedings of the Second International Aerosol Conference, 22–26 September 1986, Berlin (West). Oxford: Pergamon Press.

Gillette, D. A., I. H. Blifford, Jr., and C. R. Fenster. 1972. Measurements of aerosol size distributions and vertical fluxes of aerosols on land subject to wind erosion. *J. Appl. Meteor.* 11:977–987.

Gillette, D. A. 1974. On the production of wind erosion aerosols having the potential for long range transport. *J. de Recherches Atmospheriques*. 8:735–744.

Gillette, D. A., I. H. Blifford, Jr., and D. W. Fryrear. 1974. The influence of wind velocity on the size distributions of aerosols generated by the wind erosion of soils. *J. Geophys. Res.* 79:4068–4075.

Harrison, R. M., and C. A. Pio. 1983. Size differentiated composition of inorganic atmospheric aerosols of both marine and polluted continental origin. *Atmos. Environ.* 17:1733–1738.

Hering, S. V., and S. K. Friedlander. 1982. Origins of aerosol sulfur size distributions in the Los Angeles basin. *Atmos. Environ.* 16: 2647–2656.

Hinds, W. C. 1999. *Aerosol Technology*, 2 ed. New York: John Wiley & Sons.

Hinds, W. C. 1988. Basis for particle size-selective sampling for wood dust. *Appl. Ind. Hyg.* 3:67–72.

John, W. 1993. Multimodal size distributions of inorganic aerosol during SCAQS. In *Southern California Air Quality Study, Data Analysis*, Proceedings of an International Specialty Conference, July 1992, Los Angeles, CA. Pittsburgh, PA: Air & Waste Management Association, p. 167.

John, W., S. M. Wall, J. L. Ondo, and W. Winklmayr. 1990. Modes in the size distributions of atmospheric inorganic aerosol. *Atmos. Environ.* 24A:2349–2359.

Junge, C. E. 1963. *Air Chemistry and Radioactivity*. New York: Academic Press.

Kasahara, M., Takahashi, K., Berner, A. and O. Preining. 1994. Characteristics of Vienna aerosols sampled using rotating cascade impactor. *J. Aerosol Sci.* 25S1:S53–S54.

Keith, C. H., and Derrick, J. E. 1960. Measurement of the particle size distribution and concentration of cigarette smoke by the "conifuge". *J. Colloid Sci.* 15:340–356.

Koutrakis, P., and B. P. Kelly. 1993. Equilibrium size of atmospheric aerosol sulfates as a function of particle acidity and ambient relative humidity. *J. Geophys. Res.* 98:7141–7147.

Lundgren, D. A., B. J. Hausknecht, and R. M. Burton. 1984. Large particle size distribution in five U.S. cities and the effect on the new ambient particulate matter standard (PM_{10}). *Aerosol Sci. Technol.* 7:467–473.

Mercer, T. T. 1973. *Aerosol Technology in Hazard Evaluation*. New York: Academic.

Meszaros, E., T. Barcza, A. Gelencser, J. Hlavay, G. Kiss, Z. Krivacsy, A. Molnar, and K. Polyak. 1997. Size distributions of inorganic and organic species in the atmospheric aerosol in Hungary. *J. Aerosol Sci.* 28:1163–1175.

McMurry, P. H. 1989. Organic and elemental carbon size distributions of Los Angeles aerosols measured during SCAQS. Final report to Coordinating Research Council, project SCAQS-6-1. Particle Technology Laboratory Report No. 713.

McMurry, P. H., and J. C. Wilson. 1983. Droplet phase (heterogeneous) and gas phase (homogeneous) contributions to secondary ambient aerosol formation as functions of relative humidity. *J. Geophys. Res.* 88:5101–5108.

Meng, Z., and J. H. Seinfeld. 1994. On the source of the submicrometer droplet mode of urban and regional aerosols. *Aerosol Sci. Technol.* 20:253–265.

Milford, J. B., and C. I. Davidson. 1985. The sizes of particulate trace elements in the atmosphere—A review. *APCA J.* 33:1249–1260.

Morawska, L., and M. Jamriska. 1997. Determination of the activity size distribution of radon progeny. *Aerosol Sci. Technol.* 26:459–468.

Mylonas, D. T., D. T. Allen, S. H. Ehrman, and S. E. Pratsinis. 1991. The sources and size distributions of organonitrates in Los Angeles aerosol. *Atmos. Environ.* 25A:2855–2861.

Noll, K. E., A. Pontius, R. Frey, and M. Gould. 1985. Comparison of atmospheric coarse particles at an urban and non-urban site. *Atmos. Environ.* 19:1931–1943.

Noll, K. E., and K. Y. P. Fang. 1989. Development of a dry deposition model for atmospheric coarse particles. *Atmos. Environ.* 23:585–594.

Owen, M. K., D. S. Ensor, L. S. Hovis, W. G. Tucker, and L. E. Sparks. 1990. Particle size distribution for an office aerosol. *Aerosol Sci. Technol.* 13:486–492.

Pellizzari, E. D., K. W. Thomas, C. A. Clayton, R. C. Whitmore, H., Shores, S. Zelon, and R. Peritt. 1992. Particle total exposure assessment methodology (PTEAM): Riverside, California pilot study, vol. I (final report). EPA Report No. EPA/600/SR-93/050. Research Triangle Park, NC: U.S. Environmental Protection Agency, Atmospheric Research and Exposure Assessment Laboratory. Available from NTIS, Springfield, VA, PB93-166957/XAB.

Pickle, T., D. T. Allen, and S. E. Pratsinis. 1990. The sources and size distributions of aliphatic and carbonyl carbon in Los Angeles aerosol. *Atmos. Environ.* 24A:2221–2228.

Prather, K. A., T. Nordmeyer, and K. Salt. 1994. *Anal. Chem.* 66:1403–1407.

Pruppacher, H. R., and J. D. Klett. 1980. *Microphysics of Clouds and Precipitation*. Boston: Reidel.

Robinson, R. J., and C. P. Yu. 1998. Theoretical analysis of hygroscopic growth rate of mainstream and sidestream cigarette smoke particles in the human respiratory tract. *Aerosol Sci. Technol.* 28:21–32.

Rosin, P., and E. Rammler. 1933. The laws governing the fineness of powdered coal. *J. Inst. Fuel* 7: 29–36.

Savoie, D. L., and J. M. Prospero. 1982. Particle size distribution of nitrate and sulfate in the marine atmosphere. *Geophys. Res. Lett.* 9:1207–1210.

Sheldon, L. S., T. D. Hartwell, B. G. Cox, J. E. Sickles II, E. D. Pellizari, M. L. Smith, R. L. Perritt, and S. M. Jones. 1989. An investigation of infiltration and indoor air quality (final report). Contract No. 736-CON-BCS-85. Albany, NY: New York State Energy Research and Development Authority.

Sioutas, C. 1999. A pilot study to characterize fine particles in the environment of an automotive machining facility. *Appl. Occup. Environ. Hyg.* 14:246–254.

Sloan, C. S., J. Watson, J. Chow, L. Pritchett, and L. W. Richards. 1991. Size-segregated fine particle measurements by chemical species and their impact on visibility impairment in Denver. *Atmos. Environ.* 25A:1013–1024.

Spengler, J. D., D. W. Dockery, W. A. Turner, J. M. Wolfson, and B. G. Ferris, Jr. 1981. Long-term measurements of sulfates and particles inside and outside homes. *Atmos. Environ.* 15:23–30.

Spengler, J. D., and K. Sexton. 1983. Indoor air pollution: A public health perspective. *Science* 221:9–17.

Stern, A. C. (ed.). 1968.*Air Pollution*, vol. 111, *Sources of Air Pollution and Their Control*, 2 ed. New York: Academic.

Tu, K. W., E. O. Knutson, and A. C. George. 1991. Indoor radon progeny aerosol size measurements in urban, suburban, and rural regions. *Aerosol Sci. Technol.* 15:170–178.

U.S. Environmental Protection Agency. 1982. Air quality criteria for particulate matter and sulfur. EPA-600/882-029b, December 1982.

U.S. Environmental Protection Agency. 1997. National Ambient Air Quality Standards for Particulate Matter. Fed. Regist. 62 (138), July 18, 1997.

Venkataraman, C., and S. K. Friedlander. 1994. Size distributions of polycyclic aromatic hydrocarbons and elemental carbon. 2. Ambient measurements and effects of atmospheric processes. *Environ. Sci. Technol.* 28:563–572.

Venkataraman, C., S. Thomas, and P. Kulkarni. 1999. Size distributions of polycyclic aromatic hydrocarbons–gas/particle partitioning to urban aerosols. *J. Aerosol Sci.* 30:759–770.

Wall, S. M., W. John, and J. L. Ondo. 1988. Measurement of aerosol size distributions for nitrate and major ionic species. *Atmos. Environ.* 22:1649–1656.

Whitby, K. T. 1978. The physical characteristics of sulfur aerosols. *Atmos. Environ.* 12:135–159.

Whitby, K. T., and G. M. Sverdrup. 1980. California aerosols: Their physical and chemical characteristics. In *The Character and Origins of Smog Aerosols*, G. M. Hidy, P. K. Mueller, D. Grosjean, B. R. Appel, and J. J. Wesolowski (eds.). New York: John Wiley & Sons, p. 477.

Wolff, G. T. 1984. On the nature of nitrate in coarse continental aerosols. *Atmos. Environ.* 18:977–981.

5

AN APPROACH TO PERFORMING AEROSOL MEASUREMENTS

PRAMOD KULKARNI AND PAUL A. BARON

Centers for Disease Control and Prevention,[1] *National Institute for Occupational Safety and Health, Cincinnati, Ohio*

5.1 INTRODUCTION

Variety of methods and instruments are available to today's scientists and engineers making aerosol measurement, that range from filter-based sample collection for off-line laboratory analysis to sophisticated near-real-time instruments that detect the airborne particles and display size distribution and chemical data in real time. Instruments used for aerosol measurement frequently provide only an indirect measure of the desired particle property. For instance, commonly used optical particle counters measure an "optical size" that must then be converted to a physical or aerodynamic size—if needed—using assumptions about particle properties. Most instruments also only operate over a limited particle size range, and often two or more instruments, each using a different measurement principle, must be used to cover a wide size range. Therefore, the user must be able to assess the meaning and usefulness of data likely to be obtained with various instruments when selecting one for a specific application. Lack of recognition of measurement errors may affect the interpretation of aerosol measurements. Approaching the aerosol measurement process with an appropriate plan will reduce the likelihood of measurement errors.

[1]The findings and conclusions in this chapter are those of the authors and do not necessarily represent the views of the Centers for Disease Control and Prevention.

5.2 QUALITY ASSURANCE: PLANNING A MEASUREMENT

In most aerosol measurement applications, the challenges of selecting the instruments (with desired accuracy, precision, size and dynamic range) and the measurement strategy that

Aerosol Measurement: Principles, Techniques, and Applications, Third Edition. Edited by P. Kulkarni, P. A. Baron, and K. Willeke

will provide desired information often dominate the measurement approach. As a result, quality assurance principles, routinely used in analytical laboratories, often assume lesser importance. Many investigators prefer to address problems in a more ad hoc, investigative manner. However, an understanding of the principles of quality assurance can often be integrated into investigative approach with relatively little effort and with large gains in measurement accuracy and efficiency. Quality assurance principles have been developed over many years and most analytical laboratories around the world apply these principles on a routine basis to obtain reliable measurements. It has been recognized that reliable data are much more likely to be produced by laboratories under such conditions. To help improve the quality and reliability of measurements of environmental systems, the U.S. Environmental Protection Agency (USEPA 2008) has developed a quality assurance approach consisting of following steps: 1) State the problem, 2) identify the goals of the study, 3) identity information inputs, 4) define the boundaries of the study, 5) develop the analytical approach, 6) specify acceptance criteria, and 7) develop the plan for obtaining data. It should be noted that the approach is usually cyclic; these steps are repeated until an optimal measurement approach has been achieved.

Although a formal quality assurance process may be more appropriate for measurements targeted for regulatory compliance and may seem unnecessary for each aerosol measurement process (particularly in research applications) understanding the principles of a good quality assurance program can highlight or alert the practitioner of pitfalls in designing an experimental approach. The EPA's website on quality management has a wealth of information on the application of quality assurance programs to environmental measurements (USEPA, 2008).

5.3 MEASUREMENT ACCURACY

If "measurement processes are to serve both the practical needs of humankind and excellence in the pursuit of new scientific knowledge, they must be endowed with an adequate level of accuracy. . . . Control, and acceptable bounds for imprecision and bias are clearly prerequisites; but scientific conventions (communication) and scientific and technological means for approaching 'the truth' must also be considered" (Currie 1992). While nomenclature provides the basis for communication of accuracy and precision of measurements, the basis for developing the accuracy limits on measurements comes from experiments, assumptions, and scientific knowledge.

The discussion below presents various issues related to aerosol measurements that can affect the accuracy and precision of measurements. There are a variety of measurement techniques presented in the "Techniques" section of this book. The diversity of available techniques may leave one confused about what measurement techniques to choose from for a given application. However, based on the desired aerosol property, size and dynamic range, time resolution, instrument size and portability, resource constraints, and the accuracy and precision required, the choices are often reduced to one or two approaches. The first few chapters in the "Techniques" section deal with off-line techniques involving collection of particles on substrates for subsequent analysis in the laboratory (Chapters 7 to 10, and 12), while the remaining chapters describe real-time instruments that offer *in situ*, near-real-time measurement of particle properties (Chapters 11 to 18). The last two chapters in the "Techniques" section deal with the critical issues related to all instruments, that is, calibration of instruments (Chapter 21), and data inversion, statistical analysis, and presentation (Chapter 22).

5.4 SIZE RANGE

One of the first factors to consider in the selection of instrumentation for aerosol measurement is the size range of the aerosol. Chapter 4 presents typical size distribution characteristics of various aerosols encountered in atmospheric and industrial environments, and should help assess the approximate size range involved in similar environments. Additional examples are given in the following subsections and in the "Applications" section of this book. Very small aerosol particles can form and grow from chemical or photochemical reactions, condensational nucleation and growth, and coagulation or agglomeration. On the other hand, very large particles are likely to be formed from mechanical action, such as abrasion and crushing, while droplets can be formed by spraying and bubbling. The typical boundary between the small and large aerosol particles is about 1 μm, with the former aerosols rarely growing significantly above several micrometers and the latter aerosols rarely approaching below about 0.5 μm. The characteristics of the source of the aerosol can often give a clue to the particle size range likely to be produced. For example, hot processes such as smelting are likely to produce submicrometer fume particles; mechanical processes such as drilling tend to produce large particle dusts, while some processes such as welding and grinding may produce multimodal distributions covering a wide size range. A number of aerosol measurement instruments will be mentioned here with only a very cursory description of their detection mechanism and capabilities. Further details are provided in the chapters dedicated to specific instruments or techniques.

In the past forty years, aerosol measurement research has been quite active with explorations of different detection, classification, and analysis techniques. Some of these

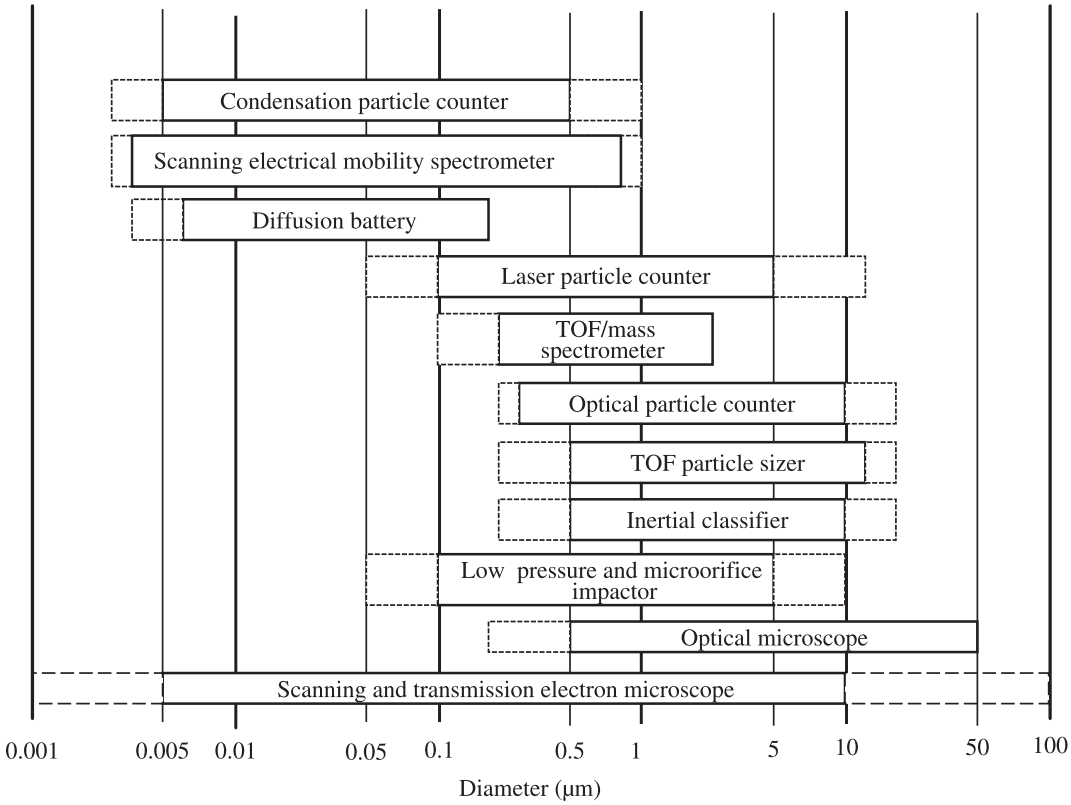

Figure 5-1 Measurement size range of some principal aerosol instruments.

techniques have become successful commercial instruments, while others have languished for a variety of reasons. The reasons include poor accuracy, precision, or sensitivity; lack of appropriate application, difficulty of use, overall size or weight, or high cost. There is a continual effort to build aerosol instruments that measure one or more useful aerosol properties over a wider size range. In most cases, the aerosol measurement process is a compromise, with the selection of the available instrumentation that measures an aerosol property closely related to that desired. In general, fewer the number of assumptions, calibration or empirical factors, greater is the likelihood of reliable or representative measurement. This makes the selection of instrumentation for a given application somewhat of an art. There are two general approaches to aerosol measurement: substrate-based collection, followed by laboratory analysis and *in situ* real-time measurement. The former is generally less expensive in terms of capital investment, but is more time consuming and gives time-integrated aerosol measurement. The latter approach requires much more expensive instrumentation, and usually gives size distribution information and nearly instantaneous results; however, it may not provide selective measurements. An overview of the size range of several types of commonly used classes of instruments is presented in Figure 5-1.

5.5 MEASUREMENT USING COLLECTION AND LABORATORY ANALYSIS

The most common collection technique involves the use of filters for collecting particles from the air. Most modern sampling filters are nearly 100% efficient for collecting all particle sizes (see Chapter 7). The filter is placed in a holder, the size of which depends largely on the application. If the sampling device is intended to be a stand-alone device that collects particles from an environment, the enclosure and inlet of the device must be appropriately designed to give accurate, or at least known, sampling efficiency. The aspiration (or entry) efficiency and internal losses in various devices is discussed in Chapter 6. Sampling devices are frequently designed for specific applications (such as atmospheric or workplace aerosol monitoring, aircraft-based measurements) and some of these are discussed in the chapters in the "Applications" section.

In addition to simply collecting all particles entering the sampling device, some instruments are designed to classify particles into two or more size fractions. Inertial separation devices, such as cyclones and impactors, are most commonly used for this purpose. A cyclone causes air to move in a swirling motion from which larger particles are deposited onto a

surface by centrifugal action, while impactors cause a more abrupt change in airflow direction, also causing larger particles, which are slow to respond to abrupt change, to be deposited onto a surface or substrate (Chapter 8). A cyclone or impactor is often placed before the filter as a "preclassifier" to simulate the removal of particles by the upper respiratory system, so that the material collected on the filter represents particles reaching the alveolar or other regions of interest in the lungs (Chapters 25 to 27).

Particles collected on the filter can be analyzed in many different ways. The sample on the entire filter can be subjected to gravimetric, chemical, radioactive, or biological analysis (Chapters 9, 12, 24, and 28) or individual particles on the filter can be subjected to various forms of microscopy, spectroscopy, or shape analysis (Chapters 10 and 23).

Classification or size distribution measurement of aerosols can be achieved by placing several classifiers in series in a 'cascade' arrangement. Typically, each stage collects larger particles than those in the subsequent stages. These devices have various names: cascade impactors, cascade centripeters, cascade cyclones, or diffusion batteries depending on the separation mechanism. The first three are inertial separators, while the latter separates particles by exploiting their Brownian diffusion. Inertial separators remove larger particles from the airstream first, depositing them onto a clean or greased surface, or a filter. The amounts collected on each stage of the cascade device can then be analyzed to allow calculation of the size distribution (Chapters 4 and 22). Generally, the size classification is performed in a series of steps in which the size cuts decrease by a factor of about 1.5–2 from one stage to the next.

For classification of particles in the submicrometer range, diffusion batteries can be used. These devices consist of several screens or collimated-hole structures that allow particles to diffuse to the surface (Chapter 16). The material collected on the screens can be analyzed, for example, for radioactivity or chemical composition. The size resolution of these devices is generally much poorer than that of impactors (Chapters 16 and 22) or electrical mobility techniques (Chapter 15), but they are relatively inexpensive.

5.6 MEASUREMENTS USING REAL-TIME INSTRUMENTS

5.6.1 Measurement of Substrate-Collected Particles

A wide range of physical and chemical principles have been applied to the detection and analysis of collected particles. Some of these approaches have resulted in semi-continuous or near-real-time instruments. For various reasons, few of these devices have survived as commercial instruments. Several of these techniques for measurement of aerosol mass concentration are described in Chapter 12. The most common aerosol particle property measured, particularly for regulatory compliance, is the mass of the aerosol constituent of interest.

The most direct approach to measurement of total particulate mass is the deposition of particles onto a vibrating surface and measurement of the change in resonant frequency. Two distinct types of instrument use this approach. The first uses a piezoelectric crystal as the collection surface. This provides high sensitivity and accurate mass measurement, but only for relatively small and 'sticky' particles and only in very limited regions on the surface of the crystal. Large particles (several micrometers) may not couple well to the vibrating surface and may be poorly detected. The crystal has vibrational nodes on its surface and the particles must be precisely deposited on the appropriate nodes to achieve consistent response. For more information on this technique, see Chapter 12 and Williams et al. (1993).

Another vibrational sensor is the Tapered Element Oscillating Microbalance (***R&P***).[2] The collection substrate, either a filter or an impaction surface, is placed at the end of a tapered vibrating tube. The amount of mass collected on the substrate is related to the decrease in the resonant vibrational frequency of the tube. This approach appears to have fewer artifacts, though variations in temperature, humidity, and pressure, and external vibrations can sometimes affect the accuracy of the measurement (Chapter 12).

Another approach to mass measurement is the use of β-radiation scattering from collected material (Chapter 12). The sample is placed between a β-radiation source and a detector. The radiation is scattered by the electron cloud around the atoms of the sample, attenuating the radiation reaching the detector. The amount of attenuation is approximately proportional to the mass of material, though materials with low atomic number, for example hydrogen, have reduced scattering efficiency and are thus underdetected. Hydrocarbon compounds thus require a different calibration than most other materials.

The Dekati Mass Monitor (DMM, ***DEK***; Chapter 12), has been developed to measure mass concentrations of automobile engine exhausts and provides near-real-time measures of particle mass concentration. DMM uses a combination of electric mobility measurement and impaction to measure mass concentration, and is based on the Dekati Electrical Low Pressure Impactor (ELPI, ***DEK***; Chapter 18).

5.6.2 Real-Time Measurement of Individual Airborne Particles

5.6.2.1 Particle Detectors Most real-time spectrometers require a particle detector or a sensor that responds quickly and efficiently to presence of each particle in the detection

[2]Refer to Appendix I for full manufacturer address indexed to three-letter codes.

zone. One of the widely used sensors is the optical particle counter (OPC; Chapter 13). In an OPC, particles pass through a sensing zone that is illuminated by either a broadband (white light) or a monochromatic (laser or light-emitting diode) source. If the instrument uses a laser, it may be called a laser particle counter (LPC). The light scattered by each particle is detected over a range of angles and converted to an electronic pulse that is a complex, but generally increasing, function of particle size. Light scattering provides a relatively inexpensive, nondestructive, high-speed technique for particle detection. An OPC can be used for obtaining information about individual particles or for determining total particle concentration, for example, in cleanrooms (Chapters 13 and 36). With the appropriate optics, OPCs can be designed so that the sensing volume is external to the instrument, thus allowing the measurement of particles in extreme environments, such as outside of aircraft in the atmosphere (Chapter 29) or in high temperature stacks or reactors (Chapter 35).

Optical particle counters are used as stand-alone instruments to detect and size particles. However, the light scattered by each particle has a complex dependence on the light source, the range of detection angles, the particle size, particle shape, and the particle refractive index. It is usually difficult to predict or compensate for the latter two factors in real-world situations and, thus, the sizing capability of OPCs is usually only approximate.

In the small particle size range, particle detection by light scattering loses sensitivity, with a lower limit of about 50 nm under optimum conditions. To detect particles smaller than this size range, condensation particle counters (CPC), also called a condensation nucleus counter (CNC), are used (Chapters 17 and 32). The CPC exposes particles to a supersaturated vapor that condenses onto particles. All the particles grow to approximately the same size (on the order of few micrometers) and can then be detected by light scattering. The CPC can detect particles down to about 1 nm (Chapter 32).

Aerosol electrometers, detectors that measure charge on aerosol particles, have also been used as particle detectors to sense and count particles (Chapter 18). These detectors require the particles be electrically charged. A sufficiently high flow rate of charged particles through a particulate filter housed in a Faraday cage induces electrical current which is then amplified and measured by the electrometers. Unlike particle-by-particle detection in CPCs, electrometers involve ensemble detection; the accuracy of measurement depends on charge distribution on particles, flow rate, and electrometer characteristics such as noise. Instruments based on these detectors are described in Chapter 18.

5.6.2.2 Spectrometers for Submicrometer Size Range

There are several forms of the electrical mobility classifier that allow size separation of submicrometer particles. These instruments operate by observing velocity of particles placed in a known electric field, carrying a known electrical charge. Particles that achieve a selected velocity in the electric field (i.e., a selected electrical mobility) pass through the classifier and can be detected downstream, usually with a CPC. Several of these devices have been developed and commercialized, each optimized for a specific size range or application (Chapters 15 and 32). Depending on the sample flow rate and other operating conditions, these instruments can provide size distribution measurements over the submicrometer range within a few minutes. Larger particles are not sized accurately because they are likely to retain multiple charges; whereas, smaller particles (below few nanometers) cannot be sized with high resolution due to their large Brownian diffusivity. When the electrical classification is used along with electrical detection, high time resolution measurements are possible. These electrical-sensing mobility spectrometers can provide size distribution measurement in times as small as 100 ms, albeit with much lower size resolution (Chapter 18). Electrical mobility classifiers have also been developed to measure particles below 3 nm with very high size resolution, but with limited size range (Chapter 32).

Diffusion batteries can also be used as direct-reading instruments, detecting the particles passing through the diffusive collecting elements with a CPC. However, because of the inherently lower resolution of the size separation elements, diffusion batteries have significantly lower size resolution than the electrical mobility classifiers. The size distribution must be deconvoluted from the diffusion battery's raw penetration data, and the deconvoluted spectra are subject to significant errors (Chapters 16 and 22). Although these devices are less expensive than the electrical mobility instruments, they have largely lost favor as real-time instruments and are used primarily as integral sampling devices.

5.6.2.3 Spectrometers for Large Particle Size Range

OPCs and LPCs are widely used to measure size distribution, which can operate over a relatively wide range of concentration and size. The LPC generally produces a higher intensity beam at the sensing volume, resulting in higher sensitivity to small particles. Solid-state lasers are available with a shorter wavelength that can also be used to detect smaller particles. These instruments provide rapid readout and moderate size resolution. They are subject to complex sizing errors which are a function of particle properties; however, for many applications they provide a low-cost solution. Some of the errors in sizing can be reduced by appropriate calibration with the aerosol being measured (Chapter 13).

The time-of-flight particle sizers, such as the aerodynamic particle sizer described in Chapter 14, sample the aerosol through a nozzle, accelerating the particles so that their velocity in the sensing zone is a function of particle aerodynamic diameter. The velocity of the particles is measured by the "time of flight" of the particles through the sensing zone.

The high acceleration through the nozzle can distort the shape of liquid particles, leading to non-Stokesian effects in the sizing procedure, and corrections usually have to be applied to obtain true aerodynamic diameter. However, the corrections, especially for known density and gas viscosity, are predicted from theory and can be accurately applied. These spectrometers can provide high resolution spectra in less than a minute and give reasonably accurate results. Because of the relative complexity of these instruments, the sizing and concentration errors, though usually not significant, sometimes can be subtle and difficult to correct (Chapter 14).

Over the recent years, significant advances have taken place in the development of aerosol mass spectrometers that provide near-complete analysis of particles (Chapter 11). These instruments are capable of providing number-weighted aerodynamic size distribution, as well as size-resolved chemical composition data in near real time. However, these instruments are rather bulky, expensive, and cumbersome to operate. There are significant limits to the size range and concentration that these instruments can measure; however, they can provide information virtually unattainable by other means.

5.7 AEROSOL MEASUREMENT ERRORS

Figure 5-2 summarizes some major sources of biases that may occur in aerosol measurement. The aerosol to be sampled may have particles anywhere in the size range 0.001–100 μm. Various portions of this range may be nondetectable with a given measurement technique. Particles smaller than about 20% of the wavelength of visible light (0.4–0.7 μm) are generally not detectable by optical means. Depending on the objective of measurement and the type of aerosol present, different portions of this 0.001- to 100-μm size range may be of interest. For instance, from the human health perspective, particles <10 μm are often important because the aerosol particles in this size range are likely to deposit in the biologically sensitive regions of the human respiratory system. Measurement of such aerosols will be used as an example in some of the following discussion.

5.7.1 Sampling and Transport

As the aerosol enters the sampling inlet of the aerosol measuring device, the ratio of ambient air velocity to sampling velocity, the air turbulence, as well as the size, shape, and orientation of the inlet may affect the sampling efficiency of the inlet (Chapter 6; Vincent 2007; Okazaki et al. 1987a,b). Generally, the larger particles enter less efficiently, as illustrated in Figure 5-2, because of properties producing inertial losses and particle settling. Various particle size preclassifiers, such as cyclones or elutriators, take advantage of these properties to impose size discrimination on sampled particles. Some of these devices or instruments are

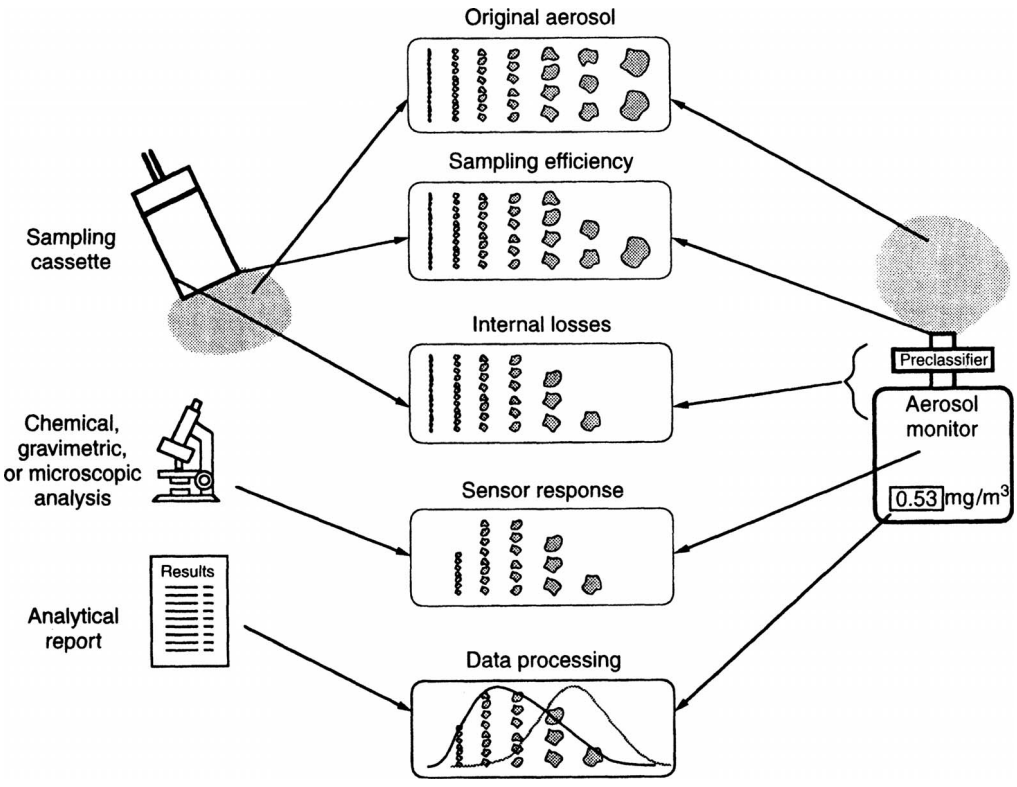

Figure 5-2 Schematic representation of some important biases in aerosol measurement. (Figure adapted from Willeke and Baron 1991.)

intentionally designed to allow only a certain fraction of particles to pass through for detection and analysis. Aerosol particles reaching the alveolar or gas exchange region of the lung, are defined as respirable aerosol. A cyclone is generally used to measure respirable aerosol (as defined by the American Conference of Governmental Industrial Hygienists [ACGIH]), while a horizontal elutriator is used for the British Medical Research Council (BMRC) definition of respirable aerosol (Vincent, 1999).

The tubing or transport line connecting the inlet to the collection device (e.g., filter) or sensor (e.g., detection region of a particle counter) is usually considered separately from the inlet or the point at which the aerosol enters the measurement device. For instance, in asbestos sampling, a length of tubing equal in diameter to the filter collection area, called a "cowl" (Baron 1994), connects the sampling inlet to the collecting filter. In a real-time instrument, the aerosol is generally transported from the inlet to the sensor via a tube or channel. Particle losses may occur in these channels due to electrostatic attraction, impaction, or gravitational settling and further reduce the aerosol concentration, generally in the upper size range, as illustrated in Figure 5-2. It is important to make the plumbing and transport lines out of conductive material to reduce electrostatic losses and, further, to minimize the length of these lines to reduce losses due to other forces. For small-inlet devices used for sampling submicrometer particles, diffusion may also contribute significantly to the losses. Chapter 6 discusses how to estimate losses resulting from various mechanisms in sampling lines and inlets.

The measured size-dependent sampling efficiencies for the open- and closed-face 37-mm cassettes (Buchan et al. 1986), both widely used in industrial hygiene sampling with filters, have been multiplied by the corresponding values of an example lognormal size distribution with a median diameter, $d_{50} = 5.0$ μm, and a geometric standard deviation, $\sigma_g = 2.0$ (Fig. 5-3). These samplers are used for a variety of aerosol measurements and a smaller diameter version of the cassette is used for asbestos exposure measurement Taylor et al. (1984). Two sampling efficiency curves are calculated for an open- and a closed-face sampler hanging down with the inlet perpendicular to a horizontally moving wind stream of 100 cm/s; the third curve was calculated from measurements with the sampler on a mannequin facing the wind under the same wind conditions. The mannequin-mounted sampler curves were nearly identical for closed- and open-faced cassettes, so a single average curve has been drawn for this case. It is apparent that the airflow conditions near the sampler inlet can significantly affect the collection efficiency of the sampler. The bluff mannequin body reduced the effect of wind speed on the sampler inlets. As pointed out in Chapter 6, the inlet efficiency is greatest when the air flow velocity and direction in the sampler and surrounding air are exactly or nearly matched. In Figure 5-3, there is a size-dependent reduction in particle

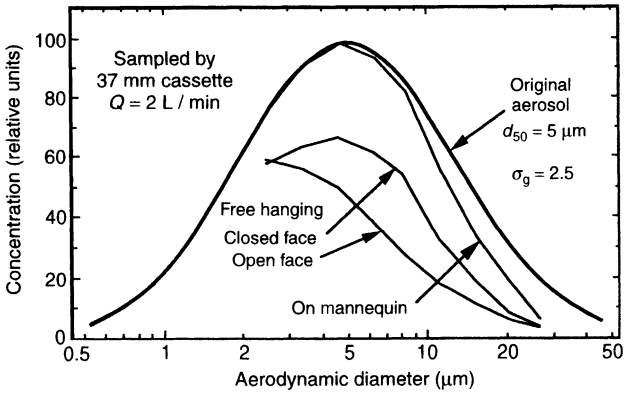

Figure 5-3 Sampling and transport biases in several cassette configurations. Sampling efficiency data were taken from Buchan et al. (1986) and smoothed. Cassettes hung on a bluff body (a mannequin) appear to have smaller biases than free-hanging ones. (Figure adapted from Willeke and Baron 1991.)

concentration relative to the true concentration that varies with sampler placement.

Electrostatic attraction to the cassette inlet and its walls reduces the amount collected on the filter, especially if the cassette is constructed of nonconducting material (Baron and Deye 1990). The loss increases with the number of electrical charges on the aerosol particles and on the sampler and decreases with increasing sampling rate. The number of charges on airborne particles depends on the process producing the particles, the air humidity, or the amount of water on the particle surface during release, and the length of time the particles have been airborne (Chapter 18). Real-time instruments may have similar sampling and transport losses depending on the design of the inlet and the section leading to the sensor (Liu et al. 1985).

5.7.2 Detector Response and Sensitivity

When the particles collected on a filter are analyzed by optical microscopy, many of the smaller particles may not be detected by the microscopist, with none being counted below a certain size, say 0.3 μm. Thus the measurements obtained by the microscopist will be biased as they will not account for any particles below 0.3 μm. Such a bias is also exhibited by all sensors or detectors in real-time instruments within a certain window of particle size or operating parameters.

Figure 5-4 illustrates the bias introduced by detector using an example aerodynamic particle sizer (APS, ***TSI***), a time-of-flight aerosol spectrometer that uses a detector relying on scattered light from particles (described in Chapter 14). A lognormal size distribution with mass median aerodynamic diameter $d_{50} = 1$ μm and $\sigma_g = 2.5$ is calculated to simulate the measured aerosol (Fig. 5-4). Based on measured efficiency curves from Blackford et al. (1988), there is a modification of the "measured" size distribution in the lower size

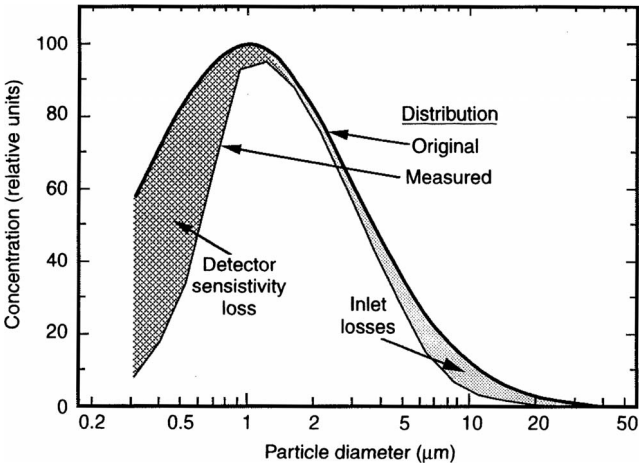

Figure 5-4 Sensor bias data for the aerodynamic particle sizer (APS3300) Taken from Blackford et al. (1988). Adapted from Willeke and Baron (1991).

range due to a poor detector response and at the high end due to particle transport loss at the instrument inlet. Note that neither of these losses change rapidly with particle size, and that the resulting distribution appears nearly lognormal. These distortions of the shape of the distribution may result in incorrect interpretation of the shape of the original aerosol distribution.

Most detectors have such a nonideal response in a certain range of particle size or operating parameters; this factor must be considered when applying any necessary corrections to the measured size distribution.

5.7.3 Coincidence Errors in Detectors

If the detector involves an optical device receiving a light-scattering signal each time a particle passes through the view volume, particle coincidence, that is, simultaneous presence of two or more particles in the view volume, may lead to an erroneous detection of multiple particles as a single particle of larger size. This leads to overestimation of particle size and underestimation of number counts. The coincidence effects become important at high particle number concentrations. Most detectors such as OPCs and CPCs account for coincidence errors at high concentrations through applying appropriate corrections. These errors limit the maximum number concentration a detector can measure.

In a time-of-flight device, such as the APS or the Aerosizer® (Chapter 14), the time of flight of a particle accelerated between two path-intersecting laser beams (separated by a known distance) is a measure of its aerodynamic particle size. In addition to the coincidence errors, these instruments may produce a false background or 'phantom' counts due to presence of more than one particle in the sensing zone at a time. These phantom counts could outnumber the fewer correctly detected particles at the tail of the distribution (Heitbrink, Baron, and Willeke 1991). The phantom counts can be especially important if the distribution is converted to a mass distribution (a few large, phantom particles may outweigh the rest of the distribution) or if the data is used for comparison measurements (Wake 1989), for example, to obtain the ratio of concentrations upstream and downstream of a cyclone.

5.7.4 Corrections for Density and Other Physical Properties

Caution must be exercised to account for difference in equivalent diameters measured by the instruments when using two or more instrument techniques, either over the same size range or to augment the size range. Necessary corrections in density, shape, optical properties, charge levels, and other parameters must be made in order to reduce the data to a consistent size scale.

Different aerosol instruments may be used to measure the same equivalent diameter, say particle aerodynamic diameter (d_a). This can provide some understanding of the biases present in the measurements. However, when the measurements from different instruments, each employing a different measurement technique, are used, it is possible that the size measurements are widely disparate. A comparison of several measurement techniques used on a grinding wheel is shown in Figure 5-5 (O'Brien et al. 1986). Filter samples were analyzed by scanning electron microscope (SEM) and real-time measurements were made with two optical particle counters (Model CI-108, ***CLI***; Model ASAS-X, ***PMS***), a quartz crystal microbalance cascade impactor (Model PC-2, California

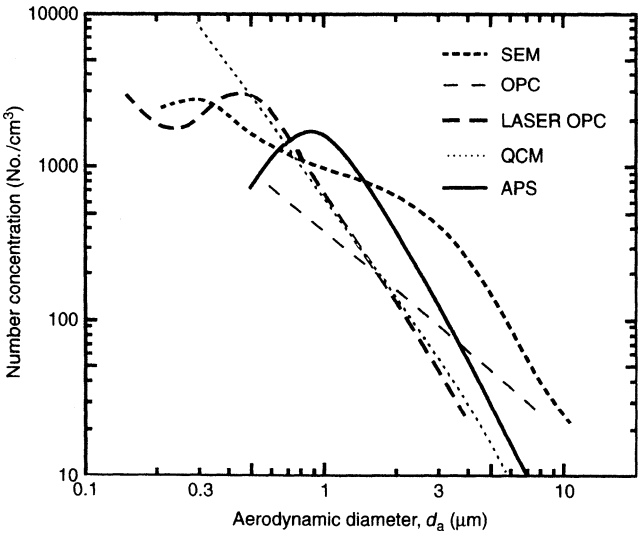

Figure 5-5 Measurement of grinding wheel aerosol using five different measurement techniques including an SEM, two optical particle counters, a quartz crystal microbalance cascade impactor and an APS3300. Adapted from O'Brien et al. (1986).

Measurements, Berkeley; model discontinued) and an APS. Since optical counters measure optical equivalent diameter, and the SEM measurements provide physical size measurements, it was necessary to convert these equivalent diameters to aerodynamic size scale using appropriate correction. With the SEM and optical particle counters, relatively large correction factors based on assumed average particle shape, density, and refractive index may culminate in relatively unsatisfactory results. The aerosol from a grinding wheel was a complex aerosol for such a comparison because of the presence of a number of materials with widely disparate properties.

Appropriate density correction can be applied to convert aerodynamic size to physical size and vice versa. Curve A in Figure 5-6 shows an aerosol size distribution with a median aerodynamic diameter of 5 μm and $\sigma_g = 2$. This aerodynamic diameter can be converted to physical particle diameter by dividing the aerodynamic diameter by the square root of the particle density (see Chapter 2). A shape factor to account for nonspherical shapes also needs to be included in the conversion, but is neglected here. For coal dust, which has a particle density, $\rho_p \approx 1.45$ g/cm^3, the physical diameter (Curve B, Fig. 5-6) is smaller than the aerodynamic diameter.

Curve C in Figure 5-6 represents the measured distribution from an OPC when the actual distribution entering the instrument is given by Curve A. The measured optical size distribution is drastically different from the either the physical or aerodynamic size distribution.

Typically, OPCs, as well as photometers, are calibrated with spherical, nonabsorbing test aerosols such as dioctyl phthalate (DOP) or polystyrene latex spheres (PSL). For example, DOP has a refractive index $m = 1.49$ (no imaginary part or absorptive component). All the light received by these test particles is scattered from the particles. However, if the particles are light absorbing, such as coal dust ($m = 1.54 - 0.5i$, with 0.5 representing the absorptive component of the refractive index), a particle of a given size scatters less light. Therefore, a coal dust particle scatters much less light and appears much smaller than a similar-sized test particle, leading to the bias noted in Curve C (Liu et al. 1974). In addition, the size correction for the absorbing particle, such as coal dust, may be strongly particle-size dependent, leading to further distortion of the measured size distribution. While the distortion and shifting of the size distribution for coal dust is an extreme case, the assumptions involved (spherical shape, refractive index, and density values) illustrate some of the pitfalls of using optical sizing data to determine aerodynamic size.

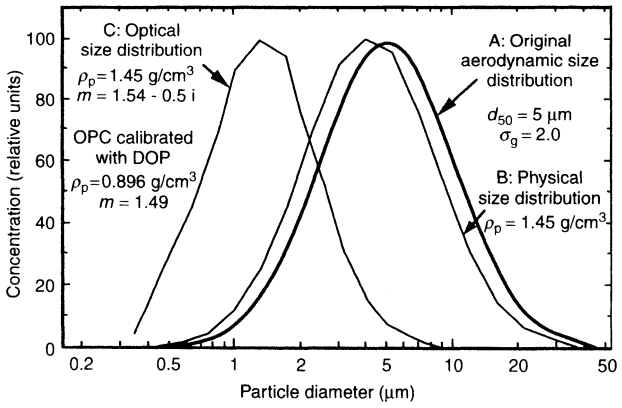

Figure 5-6 Measurement of coal dust using various physical properties of the particles (density, ρ_p, and refractive index, m). Curve A represents the aerodynamic size distribution of a coal dust sample; Curve B represents the physical size distribution of that aerosol (correcting for density); and Curve C represents the measurement of the coal dust by an optical particle counter (OPC) calibrated with monodisperse DOP particles (Liu et al. 1974). Adapted from Willeke and Baron (1991).

5.7.5 Aerosol Sampling Statistics

According to Poisson statistics, the uncertainty in the number count, that is, its standard deviation, can often be assumed to be the square root of the number count. Therefore, in order to reduce the uncertainty, one of the key requirements for any real-time instrument is to sample large number of particles (e.g., to achieve 1% uncertainty, 10,000 particles must be counted). Yet most measurement techniques only sample a small fraction of the population of particles in a given application. Therefore, ensuring that a large enough number of particles is sampled to construct a representative size distribution is essential for any reliable measurement approach.

To illustrate the importance of sampling statistics, Figure 5-7 shows a comparison of two simulated cases, one with a total particle count of 10^6 and the other with a total count of 10^3. Figure 5-7a shows lognormal aerosol size distributions with a number median diameter of 2.5 μm and a geometric standard deviation of 2.0, a relatively large total count of one million particles distributed in 19 size increments over the size range 0.2 to 45 μm. The surface area and the volume distributions are calculated from the number distribution, assuming spherical shape and density value. The representation of the aerosol size distribution by any of the three weightings (count, surface, or volume) results in a smooth curve because a large number of particles were used.

When the sampled number count is reduced to 1000 (Fig. 5-7b), the number distribution curve is still approximately lognormal, though the increased uncertainty due to a smaller total count is apparent. However, the surface area distribution emphasizes the larger particles, of which there are fewer. The uncertainty in particle count for these larger particles is much higher. The volume (or mass) distribution (highlighted by shading) emphasizes even larger particles with even higher magnification of uncertainties, resulting in a poorly determined curve. Conversion of a count distribution to a volume or mass distribution by counting an insufficient

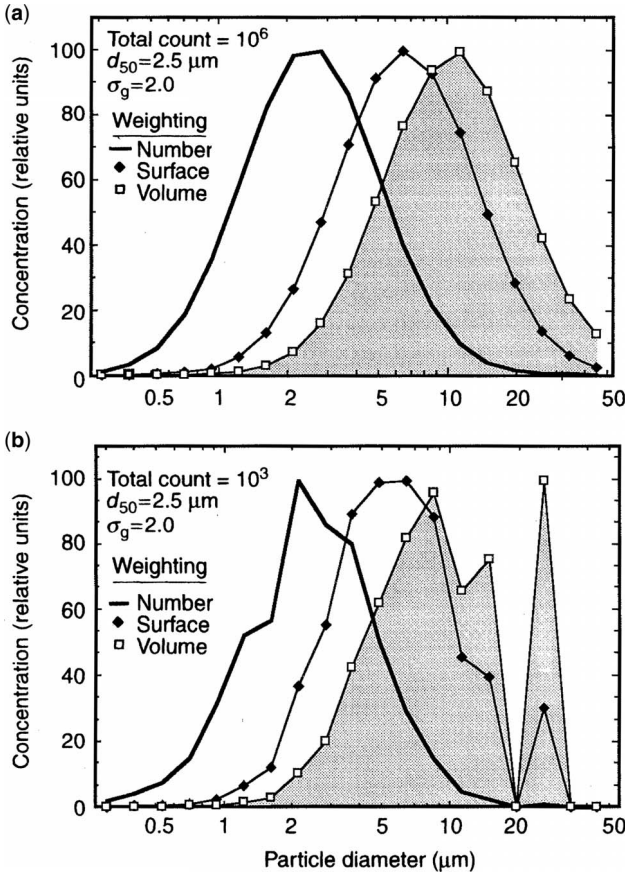

Figure 5-7 Variability in volume, or mass, measurements. Surface area and volume distributions calculated from **(a)** high and **(b)** low particle count are given and the curves are normalized to the same height. The high volume uncertainty at large particle sizes is due to low number count in the tail of the number distribution. Adapted from Willeke and Baron (1991).

number of particles, may, therefore, result in considerable uncertainty. Figure 5-7b illustrates and emphasizes the need for measuring a large number of particles in the particle size range of interest. Several modern real-time aerosol monitors are computer based and offer easy conversion from one weighting to another. Such easy conversion may tempt the user to accept numbers that may have inherent biases and high variability. Note that the variability in mass due to a small number of large particles applies not only to real-time instruments, but also to filter-based gravimetric measurements when small samples are obtained.

5.8 PRESENTATION OF SIZE DISTRIBUTION DATA

There are several ways of presenting measured size distributions, each with advantages and disadvantages (see Chapter 22). Assume that two aerosols are present in the air: aerosol 1 with a geometric mean diameter of 1.5 μm and aerosol 2 with a geometric mean diameter of 10 μm, both with a geometric standard deviation of 2.0. Measurement of the aerosol with a real-time aerosol size spectrometer is simulated to obtain the bimodal size distribution shown in Figure 5-8a.

If this measurement is replotted on a cumulative plot where the value of the ordinate indicates the number of particles less than the given size, the wavy plot of Figure 5-8b is obtained. Starting with the smaller particles, the curve increases with increasing particle size resembling an S-shape. At sizes slightly larger than the mean size of aerosol 1, the

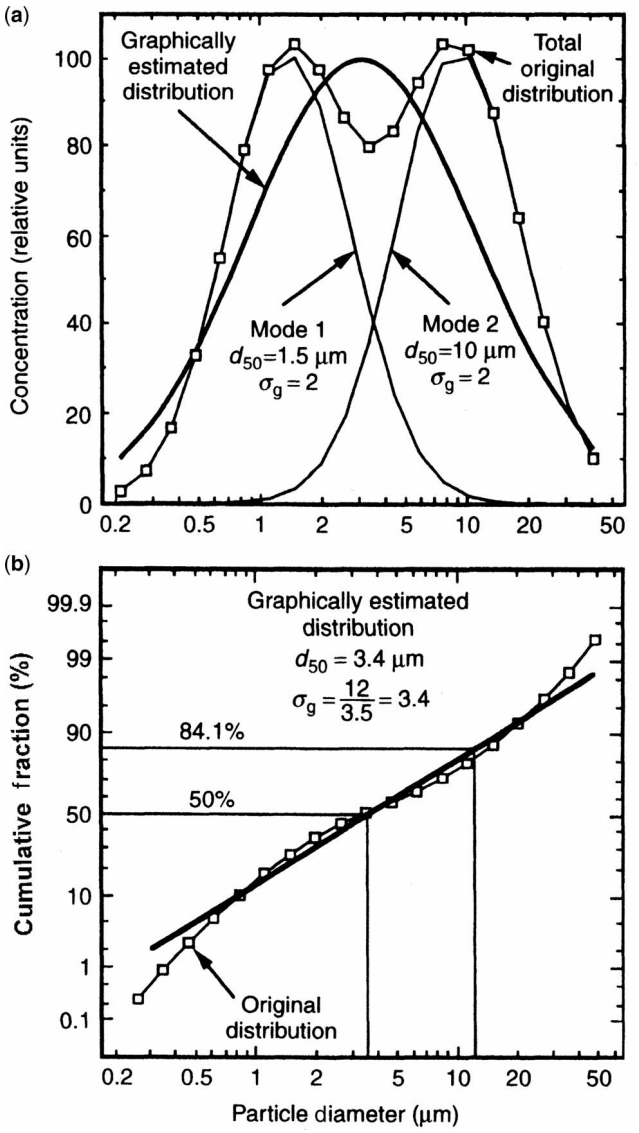

Figure 5-8 Representations of a bimodal size distribution: Histogram versus log probability plot. It is possible to misinterpret the log probability plot of a bimodal distribution as being from a single mode. Adapted from Willeke and Baron (1991).

curve levels off and then increases in slope again as the mean size of aerosol 2 is approached. This type of presentation is common for the results of low resolution instruments such as cascade impactors.

If one does not know that there are two aerosol modes present, one may be tempted to draw a straight line through the cumulative plot, as indicated by the heavy straight line in Figure 5-8b. This is frequently done and justified by attributing the deviation of the data from a straight line to experimental variability. The resulting graphically estimated or "measured" aerosol thus has a geometric mean diameter of about 3.4 μm (corresponding to the minimum between the two aerosols) and a geometric standard deviation of 3.5, indicating a single aerosol distribution much broader than each of the modes in the original bimodal distribution. Potentially valuable information is lost in this representation of the data, because multiple modes usually indicate different sources of aerosol.

Some statistical tests may also indicate that the cumulative data in Figure 5-8b do not fit a single distribution. For instance, the Kolmogorov-Smirnov test (Gibson 1971) would indicate whether the measured distribution fits a single mode distribution and a plot of residuals (the differences between the measured and calculated values) qualitatively indicates whether adjacent measurements in the curve are correlated or whether the data fits the single lognormal distribution model. Chapter 22 discusses such tests in a greater detail.

Both types of representation have advantages and disadvantages. The differential plot gives a better presentation of the distribution shape: modes show up directly and any effect of bias is constrained to a narrow size range and is not propagated throughout the entire size distribution as in the cumulative plot. The cumulative plot provides a better estimate of the median diameter of the aerosol and allows easier presentation of data graphically without using a computer. Frequently, investigation of the data through several display techniques affords a more complete understanding of the physical meaning of the data.

5.9 REFERENCES

Baron, P. A. 1994. Asbestos and other fibers by PCM, Method 7400, Issue 2: 9/15/94. In *NIOSH Manual of Analytical Methods*, 3 ed., P. M. Eller (ed.). (NIOSH) Pub. 84-100. Cincinnati, OH: National Institute for Occupational Safety and Health.

Baron, P. A., and G. J. Deye. 1990. Electrostatic effects in asbestos sampling I: Experimental measurements. *Am. Ind. Hyg. Assoc. J.* 51: 51–62.

Baron, P. A., and K. Willeke. 1986. Respirable droplets from whirlpools: Measurements of size distribution and estimation of disease potential. *Environ. Res.* 39: 8–18.

Blackford, D., A. E. Hansen, D. Y. H. Pui, P. Kinney, and G. P. Ananth. 1988. Details of recent work towards improving the performance of the TSI Aerodynamic Particle Sizer. In *Proceedings of the 2nd Annual Meeting of the Aerosol Society*, March 22–24, Bournemouth, UK.

Buchan, R. M., S. C. Soderholm, and M. J. Tillery. 1986. Aerosol sampling efficiency of 37 mm filter cassettes. *Am. Ind. Hyg. Assoc. J.* 47: 825–831.

Currie, L. A. 1992. In pursuit of accuracy: nomenclature, assumptions and standards. *Pure Appl. Chem.* 64(4): 455–472.

Gibson, J. D. 1971. *Nonparametric Statistical Inference*. New York: McGraw-Hill.

Heitbrink, W. A., P. A. Baron, and K. Willeke. 1991. Coincidence in time-of-flight aerosol spectrometers - phantom particle creation. *Aerosol Science and Technology* 14: 112–126.

Keith, L., W. Crummett, J. Deegan, R. Libby, J. Taylor, and G. Wentler. 1983. Principles of environmental analysis. *Anal. Chem.* 55: 2210–2218.

Liu, B. Y. H., V. A. Marple, K. T. Whitby, and N. J. Barsic. 1974. Size distribution measurement of airborne coal dust by optical particle counters. *Am. Ind. Hyg. Assoc. J.* 8: 443–451.

Liu, B. Y. H., D. Y. H. Pui, and W. Szymanski. 1985. Effects of electric charge on sampling and filtration of aerosols. *Ann. Occup. Hyg.* 29: 251–269.

O'Brien, D. M., P. A. Baron, and K. Willeke. 1986. Size and concentration measurement of an industrial aerosol. *Am. Ind. Hyg. Assoc. J.* 47: 386–392.

Okazaki, K., R. W. Wiener, and K. Willeke. 1987a. Isoaxial aerosol sampling: Non-dimensional representation of overall sampling efficiency. *Environ. Sci. Technol.* 21: 178–182.

Okazaki, K., R. W. Wiener, and K. Willeke. 1987b. Non-isoaxial aerosol sampling: Mechanisms controlling the overall sampling efficiency. *Environ. Sci. Technol.* 21: 183–187.

Taylor, D. G., P. A. Baron, S. A. Shulman, and J. W. Carter. 1984. Identification and counting of asbestos fibers. *Am. Ind. Hyg. Assoc. J.* 45: 84–88.

U.S. Environmental Protection Agency. 2008. Quality Management Tools – Overview. http://www.epa.gov/quality/qatools.html (accessed: March 2011).

Vincent, J. H. (ed.). 1999. *Particle Size-Selective Sampling of Particulate Air Contaminants*. Cincinnati, OH: American Conference of Governmental Industrial Hygienists.

Vincent, J. H. 2007. *Aerosol Sampling: Science, Standards, Instrumentation, and Applications.* New York: John Wiley & Sons.

Wake, D. 1989. Anomalous effects in filter penetration measurements using the aerodynamic particle sizer (APS 3300). *J. Aerosol Sci.* 20: 1–7.

Willeke, K., and P. A. Baron. 1991. Sampling and interpretation errors in aerosol sampling. *Am. Ind. Hyg. Assoc. J.* 51: 160–168.

Williams, K., C. Fairchild, and J. Jaklevic. 1993. Dynamic mass measurement techniques. In *Aerosol Measurement*, K. Willeke and P. Baron (eds.). New York: Van Nostrand Reinhold.

PART II

TECHNIQUES

6

AEROSOL TRANSPORT IN SAMPLING LINES AND INLETS

JOHN E. BROCKMANN

Sandia National Laboratories,[1] *Albuquerque, New Mexico*

6.1 INTRODUCTION

Aerosol measurement frequently requires that an aerosol sample be conveyed to a measurement device. This conveyance is accomplished by withdrawing a sample from its environment and transporting it through sample lines to the device. It is not uncommon for a sample to be transported to a chamber or bag for storage and subsequent measurement. An aerosol sampling system generally consists of

1. a sample inlet, where the aerosol sample is extracted from its ambient environment (the inlet shape and geometry may vary and although this variety is briefly

[1]Sandia is a multiprogram laboratory operated by Sandia Corporation, a Lockheed Martin Company, for the United States Department of Energy under contract DE-AC04-94AL85000.

Aerosol Measurement: Principles, Techniques, and Applications, Third Edition. Edited by P. Kulkarni, P. A. Baron, and K. Willeke

discussed this chapter will focus on sampling through thin-walled tubes),

2. a sample transport system consisting of the necessary plumbing to convey the aerosol sample to the measuring instrument or to a storage chamber (the components, or flow elements, consist of such items as tubes, elbows, and constrictions), and
3. a sample storage volume (although this item is optional and its presence is determined by necessity rather than by choice) that will have an additional sample inlet and transport system to the measuring instrument (the storage volume is usually an inflatable bag that is filled with the aerosol sample over a time scale that is short compared to the time spent measuring the sample).

Figure 6-1 illustrates schematically a sampling system that withdraws an aerosol sample from the environment and transports it through a sample line to a measurement instrument. The inlet efficiency is defined as the fraction of aerosol particles in the environment that are aspirated (drawn) through the inlet plane of the inlet and transmitted through the inlet into the sampling line. Frequently a sample is drawn from a flowing gas stream. The free stream gas velocity is U_0 and the average velocity of gas flow in the inlet, the aspiration or sampling velocity, is U. Very small particles will follow the streamlines and will be aspirated through the inlet plane with nearly 100% efficiency. Large particles are influenced by inertia and are not as responsive to changes in the gas flow. In the limit, with coaxial free stream and sampling velocities, very large particles will approach the inlet plane at the free stream velocity and the efficiency with which these large particles are drawn through the inlet plane is U_0/U. This is defined as the aspiration efficiency. It is then advisable to keep this ratio of free stream gas velocity to sampling gas velocity close to 1 if we want representative sampling. Even if this aspiration efficiency is 100%, larger particles are lost in the inlet. Generally, the further from 100% the aspiration efficiency, the greater the losses of larger particles in the inlet.

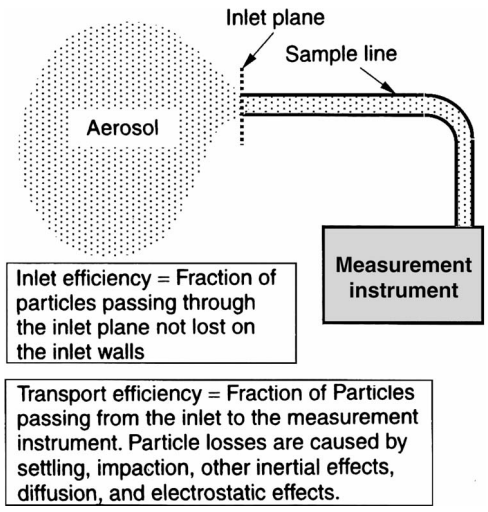

Figure 6-1 Representative sampling of aerosols is critical to making accurate measurements. This schematic diagram illustrates two important aspects of aerosol sampling efficiency; (1) the inlet efficiency, that is, the efficiency with which the aerosol is drawn from the environment in to the transport line; and (2) the transport efficiency, that is, the efficiency with which that aerosol passes through the sampling line (possibly including a temporary storage volume) to the instrument.

It is desirable that the sample is representative of the aerosol in its original environment and is not affected by the sampling process. Such characteristics as particle mass, number concentration, and size distribution should remain unchanged between the point at which the aerosol is sampled and the point where it enters the instrument performing the measurement: This is representative sampling. It is, however, difficult to prevent changes from occurring during aerosol sampling and transport. Particles, because of their inertia, do not always enter the sampling inlet representatively. They can be lost from the sample flow by contact with the walls of the sampling system. Inertial, gravitational, and diffusional forces are among the mechanisms that can act to move the particles toward a wall. Any changes should be assessed quantitatively so that measurements may be corrected. Sampling practices that introduce uncharacterized changes should be avoided.

Many of the mechanisms that inhibit representative sampling depend on the aerosol particle size, so a given sampling system may exhibit representative sampling over some range of particle size but not for particles larger or smaller than that range. Generally speaking, larger particles are more strongly influenced by gravitational and inertial forces and are more difficult to sample representatively; smaller particles with higher diffusion coefficients are more easily lost to the walls of the sampling system by diffusion. If the sampled particles are charged, they can interact with electric fields near and inside the inlet. Use of conductive inlets, sampling lines, and storage containers can often minimize the effects of electrical charge on particles. Employing an aerosol sampling system that samples representatively for the particle size range of interest is of paramount importance. The potential factors that can cause changes in aerosol characteristics during the sampling process or can otherwise contribute to a nonrepresentative sample are:

1. Aspiration efficiency and deposition in the sampling inlet during sample extraction.
2. Deposition during transport through a sampling line or during storage.
3. Extremes (high or low) or inhomogeneity in the ambient aerosol concentration.
4. Agglomeration of particles during transport through the sampling line.

5. Evaporation and/or condensation of aerosol material during transport through the sampling line.
6. Re-entrainment of deposited aerosol material back into the sample flow.
7. High local deposition causing flow restriction or plugging.
8. Inhomogeneous particle concentrations in inlets and transport tubes.

Each of these factors will be addressed in the following sections of this chapter. The first two items are extensively dealt with in the Sections 6.2 and 6.3, respectively. The third, fourth, and fifth items are addressed in the Section 6.4.1. The sixth, seventh, and eighth items are addressed in respective sections of Section 6.4. It is the goal of this chapter to provide useful correlations for transport efficiency to allow simple and straightforward design and evaluation of sampling systems. For those interested in a computational fluid dynamics approach to particle transport and deposition in a more generalized flow, the comprehensive review by Guha (2008) provides a good starting point.

The representative extraction and transport of an aerosol sample is inhibited by loss and deposition mechanisms. The principal driving forces for these mechanisms are gravitational, inertial, and diffusive. The aerodynamic equivalent diameter (Eq. 2-35 in Chapter 2) is appropriate when gravitational or inertial forces drive deposition. Correlations describing this type of deposition are often functions of the particle terminal settling velocity, V_{ts}, the particle Stokes number, Stk, and the flow Reynolds number, Re_f:

$$V_{ts} = \tau g \qquad \text{(Eq. 6-1)}$$

$$Stk = \frac{\tau U}{d} \qquad \text{(Eq. 6-2)}$$

$$Re_f = \frac{\rho_g U d}{\eta} \qquad \text{(Eq. 6-3)}$$

where τ = particle relaxation time (Eq. 2-37 in Chapter 2); g = gravitational acceleration; U = characteristic gas velocity; d = characteristic system dimension; ρ_g = gas density; and η = gas absolute viscosity.

The mobility equivalent, or diffusive equivalent, diameter is appropriate when diffusive forces drive deposition. Correlations describing the diffusive deposition of particles are functions of the particle diffusion coefficient, D:

$$D = kTB \qquad \text{(Eq. 6-4)}$$

where k = Boltzmann's constant; T = gas absolute temperature; and B = particle dynamic mobility (Eq. 2-22 in Chapter 2).

The Stokes number is the ratio of the particle stopping distance (a measure of how quickly a particle can accommodate itself to a flowing gas) to the characteristic dimension of the flow geometry. The Stokes number characterizes the inertial behavior of particles. Particles with large stopping distances have high inertia and large Stokes numbers. Representative sample extraction and transport become more difficult for larger particles because their higher inertia makes them less susceptible to influence by the sample flow.

6.1.1 Calibration

Sampling systems should be calibrated for aerosol sampling and transport efficiency at the gas flows and over the size range of interest. Ideally, a sampling system should be calibrated fully assembled under the conditions in which it will be operating. Often, a calibration of component sections at operational conditions is adequate. Calibration at other than operational conditions may be sufficient if a defensible means, such as models and correlations from the literature, is employed to apply the calibration and predict the performance under operational conditions.

Under some circumstances, a user may not have the means for aerosol calibration. The use of a specified sampling protocol or the use of calibration data found in the literature for some of the commercial samplers or for components in the sampling system may be adequate to ensure that operation will be in a range with acceptable sampling efficiency for the user's application. In this case, at least a flow calibration should be performed.

A system's sampling efficiency can be estimated when the system is composed of components that have well-characterized efficiency data and models available in the literature. A number of these models are reviewed in this chapter. In this case, operation at an estimated sampling efficiency much different from 100% increases the uncertainty in the estimate of the actual sampling efficiency.

6.1.2 Sample Extraction

An aerosol sample is extracted from its environment into an inlet for transport to the measuring instrument. Drawing a representative aerosol sample into an inlet is not trivial. The velocity and direction of the gas from which the sample is being drawn, the orientation of the aerosol sampling probe, the size and geometry of the inlet, the velocity of the sample flow, and the particle size are important factors in how representative an extracted sample is. In extracting a sample, a particle must be sufficiently influenced by the sample gas flow to be drawn into the inlet. The particle must also be transported through the inlet without being deposited in the inlet. Particle inertia and gravitational settling are impediments to representative sample extraction,

and representative sampling is more difficult with increasing aerodynamic particle size.

The aspiration efficiency, η_{asp}, of a given particle size is defined as the concentration of the particles of that size in the gas entering the inlet divided by their concentration in the ambient environment from which the sample is taken. The transmission efficiency, η_{trans}, of a given particle size is defined as the fraction of aspirated particles of that size transmitted through the inlet to the rest of the sampling system. The inlet efficiency, η_{inlet}, is the product of the inlet and transmission efficiencies and is the fraction of the ambient concentration that is delivered to the aerosol transport section of the sampling system by the inlet

$$\eta_{inlet} = \eta_{asp}\eta_{trans} \qquad \text{(Eq. 6-5)}$$

6.1.3 Sample Transport

The transport of the aerosol sample through sample lines from the inlet may occur directly to the measurement instrument or into a temporary storage volume for subsequent transport to instruments via sample lines. These sample lines may contain bends, inclines, contractions, and other flow elements; flow may be laminar or turbulent. The deposition of particles during residence in a bag and during transport will alter the characteristics of the aerosol reaching the measurement instrument. Other phenomena that will change the characteristics of the aerosol in the sample flow are particle growth by agglomeration or condensation, particle evaporation, and re-entrainment of previously deposited material into the sample flow. These phenomena are discussed later; Section 6.3 will address aerosol deposition.

A number of deposition mechanisms may be operating and several can be operating in each flow element. Some are not well characterized and conditions where these are encountered should be avoided whenever possible. Deposition mechanisms can be dependent on the flow regime (laminar or turbulent), the flow rate, the tube size and orientation, temperature gradients, vapor condensation onto the walls of the system, and particle size. Various deposition mechanisms depend on different particle equivalent diameters. Settling and inertial deposition depend on the particle's aerodynamic diameter, while diffusional deposition depends on the particle's diffusive, or mobility, diameter. The transport efficiency for a given particle size, through a given flow element, under the action of a given deposition mechanism, $\eta_{\text{flow element, mechanism}}$, is defined as the fraction of those particles entering the flow element that are not lost by that deposition mechanism during the transit of that flow element. It is defined as a function of particle size for specific deposition mechanisms that are operating in the flow element. The total transport efficiency, $\eta_{transport}$, for a given particle size is the product of the transport efficiencies for each mechanism in each flow element of the sample transport system for that particle size:

$$\eta_{transport} = \prod_{\substack{\text{flow}\\ \text{elements}}} \prod_{\text{mechanisms}} \eta_{\text{flow element, mechanism}} \qquad \text{(Eq. 6-6)}$$

The sampling efficiency, η_{sample}, is the product of the inlet and total transport efficiencies:

$$\eta_{sample} = \eta_{inlet}\eta_{transport} \qquad \text{(Eq. 6-7)}$$

This chapter presents correlations for the transport efficiencies for various mechanisms operating in various flow elements so that the reader can estimate the total transport efficiency for a sampling system.

6.1.4 Other Sampling Issues

There can be times when the sampled aerosol concentration (either mass or number) is too high for the sampling instrument. Under these circumstances, the sample must be diluted with clean gas to bring the concentration within the measurement range of the instrument. Uncertainty in the dilution and sample flows will produce uncertainty in the calculated concentration, which must be addressed. High number concentrations may drive the aerosol to undergo rapid coagulation, which alters the distribution; the number concentration decreases and the mean particle size increases. Dilution of the sample will arrest the coagulation process so that a representative sample can be measured.

The sampled aerosol may be in a condensing or evaporating environment. Condensation or evaporation of material on or from aerosol particles will change the size of the particles and the total suspended mass of aerosol material. To obtain a representative sample from an environment in which material (such as water vapor) is condensing on the particles, the sample may have to be conditioned by dilution or heating. Obtaining a representative sample from an environment in which particle material is evaporating from the particle is more difficult and can be addressed by minimizing the time between sampling and measurement to keep evaporation to a minimum.

In sampling from the ambient atmosphere, from a room, or from a duct, one must be concerned with the homogeneity of the aerosol throughout the volume of gas. A representative sample requires sampling at a sufficient number of points to give an accurate picture of the aerosol throughout the volume of interest (Fissan and Schwientek 1987). In the case of duct sampling, the American National Standards Institute (ANSI) standard NI 3.1 (ANSI 1969) provides agreed-upon sampling locations to obtain a representative sample. In room sampling, convection in the room can cause considerable inhomogeneity in the aerosol. This is especially significant in situations corresponding to very low concentrations, such as in cleanrooms, where long sampling

times are required for meaningful particle-counting statistics to be obtained (Fissan and Schwientek 1987). Sampler placement in this situation may be made on the basis of flow modeling or by the use of tracer smokes or fogs. A further discussion of sampler placement and sample inhomogeneity is given in Chapter 27. Having made the reader aware of the pitfall of inhomogeneity of the aerosol when attempting to obtain a representative sample, it is assumed that this problem has been addressed and, therefore, attention can now be focused on a single sampling point.

6.1.5 Summary

Correlations describing aspiration efficiency, transmission efficiencies, and transport efficiencies will be given in subsequent sections. These correlations can be used to evaluate the performance of an existing sampling system or to aid in the design of a sampling system. Because these correlations are based on assumptions and experiments that are not always the same as the reader's application, they may not be applicable for calculated efficiencies much different from 1. Because the efficiencies are particle-size-dependent, the range of particle sizes over which sampling is representative (sampling efficiency close to 1) can be estimated with a fair degree of confidence using these correlations. In designing a sampling system, parameters such as flow, line size, orientation, and length can be adjusted using the correlations to estimate the efficiency for the particle size range of interest to achieve representative sampling. Of course, the sampling system should be experimentally evaluated whenever possible. At the end of the presentation for each type of efficiency correlation, a short qualitative discussion is given on how the efficiency changes with the dependent parameters. Sampling situations to be avoided and the methods of avoiding them are also discussed.

While some of the phenomena discussed have been extensively investigated and characterized, others have not. It is the purpose of this chapter to provide the reader with some background information on how aerosol sampling can be accurately evaluated and appropriately designed and how sampling pitfalls may be avoided. For additional information on aerosol sampling, the reader is referred to the review paper on sampling of aerosols by Fuchs (1975), to the review on aerosol sampling and transport by Fissan and Schwientek (1987), and to the book by Vincent (1989) on aerosol sampling.

6.2 SAMPLE EXTRACTION

Aerosol sampling arises from a number of requirements. Some of them are:

1. Monitoring the ambient air for pollution.
2. Monitoring air in the workplace for hazardous materials.
3. Monitoring of exhaust stacks and lines in pollution control equipment.
4. Monitoring cleanrooms for particulate contamination.
5. Monitoring manufacturing or industrial processes.
6. Monitoring in experimental research.

In all these applications the first step in obtaining a sample is sample extraction.There are two basic situations in aerosol sampling. They are:

1. Sampling of particles from a quiescent environment.
2. Sampling from a gas flow that carries aerosol particles.

Ambient air sampling must deal with both quiescent sampling and sampling from flowing gas. It often does so by the use of an inlet coupled with an inertial particle size fractionator. The inlet samples representatively for particles smaller than some specified diameter over a specified range of ambient wind velocities and the internal particle size fractionator passes 50% of the particles of that specified diameter. Ambient air sampling is usually performed with commonly available samplers that incorporate an inlet and size fractionator in conjunction with the measurement device, usually a filter or an impactor, located immediately after the size fractionator so that transport of the sampled aerosol and the attendant losses are minimized. Liu and Pui (1981) and Armbruster and Zebel (1985) discuss inlet design and performance for ambient air samplers. These designs are tested in wind tunnels to determine their sampling efficiency as a function of particle size and wind speed. In 1987, the U.S. Environmental Protection Agency (USEPA) set a standard for airborne particulate matter called PM-10 (USEPA 1987). PM-10 required, among other things, samplers to sample 10-mm aerodynamic diameter particles with 50% efficiency. This can be accomplished by employing an inlet with a high inlet efficiency and a fractionator that allows 50% of the 10-μm aerodynamic diameter particles to pass into the rest of the sampler. The PM-10 regulations required a sampler to pass specified tests in a wind tunnel to be officially accepted. The intent was to allow flexibility in sampler design while maintaining a consistency in sampler performance.

While the inlets may perform as required, the internal processes of the samplers, specifically their size fractionators, may cause them to yield results different from those expected from their qualification testing. John, Winklmayr, and Wang (1991) and John and Wang (1991) present a comparison between the Sierra-Andersen® model 321A PM-10 sampler and the Wedding® high-volume PM-10 sampler. They show that how the samplers were loaded and whether or not the fractionators were oiled, produced an effect on the

sampling effectiveness. Deagglomeration and re-entrainment of collected material, caused by bombardment with sampled aerosol particles, was found to produce anomalous results in the Sierra-Andersen sampler. These difficulties with PM-10 samplers appear to be more in the area of instrument response, but they illustrate some of the pitfalls in sampler design.

PM-10 inlets may be too bulky for applications in which an aerosol sample must be extracted from a duct or in which room air must be sampled at a number of locations. Other inlets are required for these applications.

One type of inlet is the blunt sampler. This term encompasses a number of sampler inlets ranging from what could be called thick-walled nozzles to those in which the inlet is small compared to the overall sampler dimension. Vincent, Hutson, and Mark (1982) describe a blunt sampler as one in which the sampler and inlet configuration present a large physical obstruction to the flow. This type of sampling nozzle may be configured as a flat disk with a small centrally located sampling orifice (e.g., Vincent, Emmett, and Mark 1985). Alternatively, the sampling orifice may be in a spherical body or in some body of intermediate shape (Vincent 1984; Vincent and Gibson 1981). Particle deposition on the lip or face of a blunt sampler, particle bounce at the inlet, and re-entrainment of material into the inlet make blunt samplers difficult to characterize for larger particles. There may be difficulty in obtaining representative sampling of larger particles as well.

Another inlet type is the thin-walled nozzle. This nozzle is an idealized sampling nozzle that does not disturb ambient flow and has no rebound of particles from the leading edge into the nozzle. Sampling with a thin-walled nozzle has received more extensive study than sampling with a blunt sampler or a thick-walled nozzle. For practical usage, a nozzle can be regarded as "thin-walled" when the ratio of its external to internal diameter is less than 1.1 (Belyaev and Levin 1972). This chapter deals with sample extraction employing thin-walled nozzles.

Sampling situations in which the flow velocities vary present a problem. Generally, the sampling velocity is not a variable quantity. A variation in the sample flow rates introduces variable transmission efficiency through the sampling lines that can effectively result in nonrepresentative sampling. In fact, most instrumentation has a measurement response that is dependent on flow rate and, consequently, operates at a fixed flow rate. Exceptions are the instruments that perform a total integral collection, such as filters. These instruments can be positioned close to the inlet, minimizing the transport distances and losses, making them relatively independent of sample flow rate. This situation still requires some type of integral flow measurement should a variation of sample flow occur.

Still, sample flow rate may vary because a sampler is turned on and then off. If the sampling velocity is constant during the period of time in which the sampler is on, and the sampler is on for a long period of time compared to the sampled gas residence time in the sampler's inlet and sampling lines (at least a factor of 10 greater), then the dead volume of gas in the inlet and lines is cleared and is small compared to the total volume of gas sampled. The assumption of constant sampling velocity is valid.

Ambient free stream gas velocity variations may be beyond the control of the user because of flow adjustments or conditions in the duct from which the sample is being drawn. This situation is commonly encountered. Under these conditions, one may sample at a constant sample flow rate over a range of free stream flows and note the largest particle size for which representative sampling still occurs over this range. The measurements made with this sampling system would need to disregard particles larger than this noted size, since their sampling efficiency would be effectively unknown. This is a similar approach to that used in ambient sampling but may not be optimized for large particles. One may develop an inlet along the lines of an ambient air sampler to optimize performance for larger particles over a wide range of free stream velocities. This has been done by McFarland et al. (1988), who present a shrouded aerosol sampling probe that representatively samples $\sim$10-μm and smaller particles from duct flow ranging from 2 to 4 m/s.

An alternative approach to the problem of varying free stream flows is to vary the sample flow so that representative sampling is maintained over the range of free stream flow variation. This entails variable sample flow and should only be used under conditions in which the particle loss in sampling lines and the instrument response do not depend strongly on sample flow rate. Null-type nozzles, in which pressure measurements responding to the flow inside and outside of the nozzle are balanced at a null condition so that the sampling and free stream velocities are matched (Orr and Keng 1976; Paulus and Thron 1976), can be used to obtain representative sampling. This is an active system in which the sample flow is adjusted to obtain the null condition. The null condition may, because of local fluctuation in the flow, not reflect equality in the sample and free stream velocities. Kurz and Ramey (1988) suggest an active sampling nozzle that employs a flow sensor and flow controller to maintain representative sampling conditions over a range of duct velocities.

There are specific sampling protocols given by the USEPA for source sampling of particles in stacks (USEPA 1974) when the sampling data are required to verify or test compliance with rules. Sample trains and procedures are specified. The reader is referred to appropriate USEPA documentation for this type of sampling.

This chapter concentrates on aerosol sampling through thin-walled nozzles and the transport of the sampled aerosol through sampling lines to the instrument.

6.2.1 Efficiency

Withdrawal of an aerosol sample from its environment into the sampling system requires making a particle enter the sampling inlet and conveying it to the transport portion of the system. The efficiency with which this is accomplished is called the inlet efficiency. There are two components to the inlet efficiency, η_{asp}, and η_{trans} of Equation 6-5. These efficiencies are dependent on the ambient gas velocity, U_0; the inlet geometry, size, and position; the sampling gas velocity, U; and the particle's aerodynamic diameter, d_a.

In efficiently extracting a sample, the sampling gas velocity must be low enough so that the sampled particle can accommodate itself to the sampling gas flow within a distance comparable to the inlet diameter. This is an inertial condition. The sampling gas velocity must also be high enough so that the sampled particle does not settle appreciably in the time that sampling occurs. This is a gravitational settling condition (Davies 1968).

In sampling from a flowing gas with a nozzle, it is implicitly assumed that the flow velocities are large compared to the settling velocity of the particles being sampled, that is, that the gravitational-settling condition is met. Grinshpun et al. (1990) point out that in low velocity sampling, the aspiration efficiency will depend on the ratio of the settling velocity to the ambient gas velocity. It is prudent to determine this ratio for the particle size of interest to ensure that the gravitational-settling condition is met.

A nozzle sampling from still air or from flowing gas may be used in various orientations with respect to gravity and the ambient gas stream flow direction. A nozzle is said to face in the direction opposite to the inlet sample flow direction. Thus, a nozzle facing upwards draws the sample downwards and a nozzle facing the gas flow draws a sample in the same direction as the gas flow. A nozzle facing the gas flow where the direction of the sample flow is aligned with that of the gas flow is said to be sampling isoaxially. Anisoaxial, or non-isoaxial, sampling occurs when the gas flow and sample flow directions are not parallel.

Sampling is said to be isokinetic when it is isoaxial and the mean sample flow velocity through the face of the inlet is equal to the gas flow velocity. Strictly speaking, the term isokinetic applies only to laminar flow in the ambient free stream. The more general term, iso-mean-velocity, is applicable to both laminar and turbulent flow conditions in the free stream. Convention, however, applies the term isokinetic to both flow regimes. This chapter employs conventional terminology, but the reader should be aware of the distinction. Sampling with a sampling velocity not equal to the gas velocity is aniso-kinetic (aniso-mean-velocity) sampling. When the sampling velocity is higher than the gas velocity, the sampling is super-isokinetic (super-iso-mean-velocity) and when the sampling velocity is lower than the gas velocity, the sampling is sub-isokinetic (sub-iso-mean-velocity).

Figure 6-2 is a schematic diagram of isoaxial sampling with a thin-walled nozzle for isokinetic ($U = U_0$), sub-isokinetic ($U < U_0$), and super-isokinetic ($U > U_0$) flow conditions. The limiting streamline represents the boundary between gas that enters the inlet and gas that does not. Gas is always sampled representatively and particles that do not deviate from the gas streamlines will also be sampled representatively. Particles with sufficient inertia to deviate from the streamlines may not be sampled representatively. The figures are, strictly speaking, for laminar flow in the ambient gas stream. This condition is not always encountered. Turbulent flow in the ambient gas stream introduces a lateral component to the gas velocity that in turn influences the particle motion. However, these figures are qualitatively correct in their depiction of flow and particle transport to and through the inlet for both laminar and turbulent flow conditions.

Figure 6-2a shows isokinetic sampling, in which the limiting streamline flows directly into the nozzle without deviation. In this case, the aspiration efficiency is 1 (100%). Transmission losses arise from gravitational settling, inside the nozzle (Okazaki, Wiener, and Willeke 1987b). Losses in the inlet can also be caused by free stream turbulence (Wiener, Okazaki, and Willeke 1988), in which the particles' lateral motion caused by turbulence causes them to impact the internal wall of the inlet.

Figure 6-2b shows sub-isokinetic sampling, in which the limiting streamline must diverge from the ambient free stream flow into the nozzle. Particles with sufficient inertia that lie outside the limiting streamline can cross the limiting streamline to be aspirated by the nozzle. In this case the aspiration efficiency is 1 or more for all particles, increasing from 1 to U_0/U for larger particles. Transmission losses arise from gravitational settling in the nozzle (Okazaki et al. 1987b), from free stream turbulence effects (Wiener et al. 1988), and from inertial impaction on the inner wall of the nozzle by particles with velocity vectors toward the wall caused by the expanding streamlines (Liu et al. 1989).

Figure 6-2c shows super-isokinetic sampling in which the limiting streamline must converge from the ambient free stream flow into the nozzle. Particles with sufficient inertia that lie within the limiting streamline can cross the limiting streamline and not be aspirated by the nozzle. In this case the aspiration efficiency is 1 or less for all particles, decreasing from 1 to a limit of U_0/U for larger particles. Transmission losses arise from gravitational settling in the nozzle (Okazaki et al. 1987b), from free stream turbulence effects (Wiener et al. 1988), and from turbulent deposition of particles in the vena contracta formed in super-isokinetic sampling (Hangal and Willeke 1990b).

Figure 6-3 is a schematic diagram of anisokinetic sampling for flow conditions where $U_0 = U$, $U_0 > U$, and $U_0 < U$. The angle θ is the angle between the direction of the